

POLITECNICO DI MILANO



Facoltà di ingegneria dei sistemi

Corso di laurea in ingegneria fisica

Corso di studi in nanotecnologie e tecnologie fisiche

**SILICON NITRIDE MEMBRANES
NANOSTENCILS FOR PATTERNING AND
CONTACTING OF GRAPHENE**

Tesi di laurea di: Eleonora ZAMBURLINI matr. 751197

Relatore: Prof. Peter BØGGILD, Prof. Roman SORDAN

Co-relatore: Phd. Filippo PIZZOCCHERO, Post doc. Alexey
SAVENKO

Anno Accademico: 2011-2012



Technical University of Denmark

Alla mia famiglia: Daniela, Paolo e Beatrice:
senza il loro supporto non avrei portato a
termine nemmeno la metà del lavoro.

Index

Introduzione	7
I. Scopo del progetto: obiettivi e analisi	7
II. Panoramica del progetto:	12
III. Conclusioni	12
Abstract	15
Preface	16
Chapter 1 Introduction	17
1.1 Introduction on graphene	17
1.2 Application of graphene in nanotechnology	21
1.3 Introduction to graphene milling	23
1.1 Aim of the project:	24
1.4.1. <i>Goals, investigation and key questions</i>	24
1.4.2. <i>Project overview</i>	29
Chapter 2 Theory background and fabrication techniques	31
4.1. Focused Ion Beam Milling	31
2.1.1. <i>Theory on focused ion beam</i>	31
2.1.2. <i>Applications of focused ion beam</i>	33
2.2. Theory of milling processes	40
2.2.1. <i>Milling of silicon nitride membranes</i>	42
Chapter 3 Membranes fabrication	44
3.1 Cleanroom techniques: standard process overview and reasons for membranes fabrication	44
3.2. Membranes design	48
3.3. Characterization and results	49
Chapter 4 Devices fabrication	53
4.1. Introduction to nanostencil	53
4.2. Milling of the Si₃N₄ membranes	55
4.2.1. <i>Issues and stress points: empirical studies on membranes stress and comparison between different kind of membranes</i>	60
4.2.2. <i>Results and discussion</i>	68
4.3. Milling of graphene and graphite	71
4.3.1. <i>Design and requirements</i>	73
4.3.2. <i>Results and discussion</i>	75
4.4. Contact deposition on graphene	76
4.5. Contact pad fabrication and alignment	77
4.5.1. <i>Devices for improvement of contacts and contact pads</i>	78
Chapter 5 Measurements and characterizations	80
5.1. Raman spectroscopy	80
5.1.1. <i>Measurements procedure and set up</i>	80
5.1.2. <i>Measurements with Raman spectroscopy technique</i>	80
5.2. Electrical measurements	83
5.2.2. <i>Procedure and set up</i>	83
5.3. Contamination measurements	84

5.3.2. <i>Overview of XPS techniques</i>	84
5.3.2. <i>Measurements with XPS technique</i>	85
5.3.3. <i>Conclusions</i>	89
Chapter 6 Conclusions and discussion	90
6.1. Outlook	91
Bibliography	92
Appendix 1 Details of process for Si₃N₄ membranes fabrication	95
Appendix 2 XPS measurments for cutted graphene	98

Index of figures

Figure 1 schema per la fabbricazione di patterns Hall bar su flakes di grafene, utilizzando Si_3N_4 membranes come maschere protettive.....	8
Figure 2 Membrane ordered from Protochips, with scheme of dimensions.....	9
Figure 3 Schema del processo di milling (figura in alto) e del risultato desiderato (in basso) per la deposizione di contatti four point probe su grafene	11
Figure 4 graphene structure	18
Figure 5 graphene structure and reciprocal lattice; the six points of the hexagonal reciprocal lattice are the "Dirac points"	19
Figure 6 Graphene band structure in comparison of a normal semiconductor band structure. The peculiar band structure of graphene is responsible of its unique properties ⁴⁹	19
Figure 7 process of mechanical exfoliation of graphene	21
Figure 8 Direct milling of graphene through Si_3N_4 membrane to fabricate Hall bar patterns .	24
Figure 9 scheme of process of pattern transfer with stenciling mask (a) and final sample (b) with metal contact on graphene flake.....	26
Figure 11 FIB schematic setup.....	32
Figure 13 scheme of gas assisted FIB deposition process	36
Figure 16 Membrane ordered from Protochips, with scheme of dimensions.....	44
Figure 18 schematic drawing of the sample after lithography	47
Figure 19 schematic drawing of the sample after RIE etching and resist removal	47
Figure 20 final sample	48
Figure 21 scheme of the lithography mask for Si_3N_4 membranes fabrication (left figure) and zoom of the membrane chip design (right figure).....	49
Figure 22 Failures in membranes fabrication: a) misalignment of the mask with the crystal orientations of the sample and subsequent overetching and destruction of the sample b) pinholes in the structure caused by particles contamination during the nitride deposition c) too short time in the KOH bath cause underetching: the structure is not defined in the Si wafer.	50
Figure 23 successfully fabricated membranes; they can be divided by mechanical pressure.	51
Figure 25 cross-section sputter for gold deposition.....	55

Figure 26 Simple pattern trials. fig a) cross of respectively 4X1, 3x1, 2x1 and 1x1 μm bars crossed with 90°angle, bars of 4x1, 3x1, 2x1 and 1x1 μm , squares 4x3, 3x3, 2x2, 1x1 μm and circle with 4, 3, 2 and 1 μm diameters. b) Squares and circles.....	56
Figure 27 single line and two point probe contact mask.....	57
Figure 28 comb fingers pattern for stencilling masks fabrication.....	57
Figure 29 typical breaking points during milling of Si_3N_4 membranes, comb finger pattern...	65
Figure 30 typical breaking points during milling of Si_3N_4 membranes, single line milling	65
Figure 31 typical cracking of the Si_3N_4 membranes along the stress points.	68
Figure 32 Two examples of total collapsing of membranes	68
Figure 33 single milled lines of 80 μm	69
Figure 34 Comb finger lines pattern milled according to the specifications above.....	69
Figure 35 Comb finger pattern on a 150nm membrane fabricated in Danchip. We can see that the cracking is happening on the typical lines studied above; nevertheless the stencil mask is still working for our purpose.	70
Figure 36 Comb finger pattern milled on 400 nm membranes. Also here a small crack is visible, but not influencing the contact deposition.	70
Figure 37 scheme of alignment technique using alignment marks (Red) for the milling of Hall bar patterns.....	72
Figure 38 gluing of Si_3N_4 membrane with IPA. The cracking caused by the attachment is visible.....	73
Figure 41 Scheme of the design for contact pads	77
Figure 42 contact connection mask: the mask is the dark blue drawing. The dimensions are adapted to overlap the contact pattern of few micrometers	78
Figure 43 Blue pattern: simplified contact pattern; orange pattern: contact pads	79
Figure 44 Raman spectra of good quality single layer graphene ⁶¹	81
Figure 45 Raman spectra of multilayer graphene ⁶¹	82
Figure 46 Raman spectroscopy of graphene from our laboratories.....	82
Figure 47 Scheme of a four probes system set up.....	83

Introduzione

Questa tesi prende in considerazione alcuni importanti tasselli emersi nella ricerca scientifica degli ultimi anni riguardo al grafene, un materiale altamente innovativo che, grazie alle sue particolari proprietà, quali l'alta conducibilità e il carattere bidimensionale, si sta diffondendo a grande velocità nel settore dell'elettronica integrata e del fotovoltaico.

Inoltre, l'uso della tecnologia Focused Ion Beam per la fabbricazione di maschere per la deposizione di contatti offre numerosi vantaggi e potrà essere utilizzata in futuro, per il milling di flakes, consentendo così la creazione di contatti elettrici direttamente su grafene, con forma e contorni precisi e con minima contaminazione.

Il lavoro qui presentato vuole essere una guida per future ricerche sulla fabbricazione di contatti di grafene, in particolare utilizzando la tecnologia del Focused Ion Beam (FIB).

Sarà quindi studiato un metodo per la deposizione di contatti metallici su grafene, utilizzando stenciling masks ricavate da membrane di Si_3N_4 , fabbricate direttamente nella cleanroom Danchip, e sfruttando la tecnica del nanostencil.

Si ricaverà poi dagli esperimenti un'analisi approfondita del comportamento di queste membrane quando sottoposte all'azione del FIB, ricavandone così stress e punti di rottura.

L'ottimizzazione del processo di fabbricazione sia di membrane sia di maschere nanostencil e il design di patterns è parte integrante del progetto, e i dati così ricavati potranno essere impiegati nelle future ricerche su contatti di grafene realizzati tramite FIB.

I. Scopo del progetto: obiettivi e analisi

Contatti di grafene sono già stati fabbricati in vari laboratori, incluso il DTU nanotech, usando tecniche diverse.

Nel nostro laboratorio, ad esempio, la tecnica standard utilizzata consiste in un processo litografico, che sarà illustrato in dettaglio nel capitolo 3.

Tuttavia, questo procedimento presenta limitazioni riguardanti la contaminazione del campione, poiché prevede un diretto contatto con resist chimici. Questo potrebbe ridurre la conduttività e la qualità dei contatti fabbricati.

Nonostante siano stati raggiunti ottimi risultati con questo metodo, usando il FIB milling potrebbe essere possibile ridurre le contaminazioni, che a quel punto avrebbero origine solamente dal flusso di ioni altamente energetici che potrebbero rimanere intrappolati nel

campione, e potenzialmente ottenere di conseguenza una minore resistività, e quindi, una migliore efficienza del contatto.

L'idea iniziale del progetto, era di ottenere un contatto di grafene della forma Hall bar, ottenuto tagliando il flake con la tecnologia del FIB come mostrato in Figure 1 e utilizzando una membrana di Si_3N_4 per protezione e per ridurre la rideposizione.

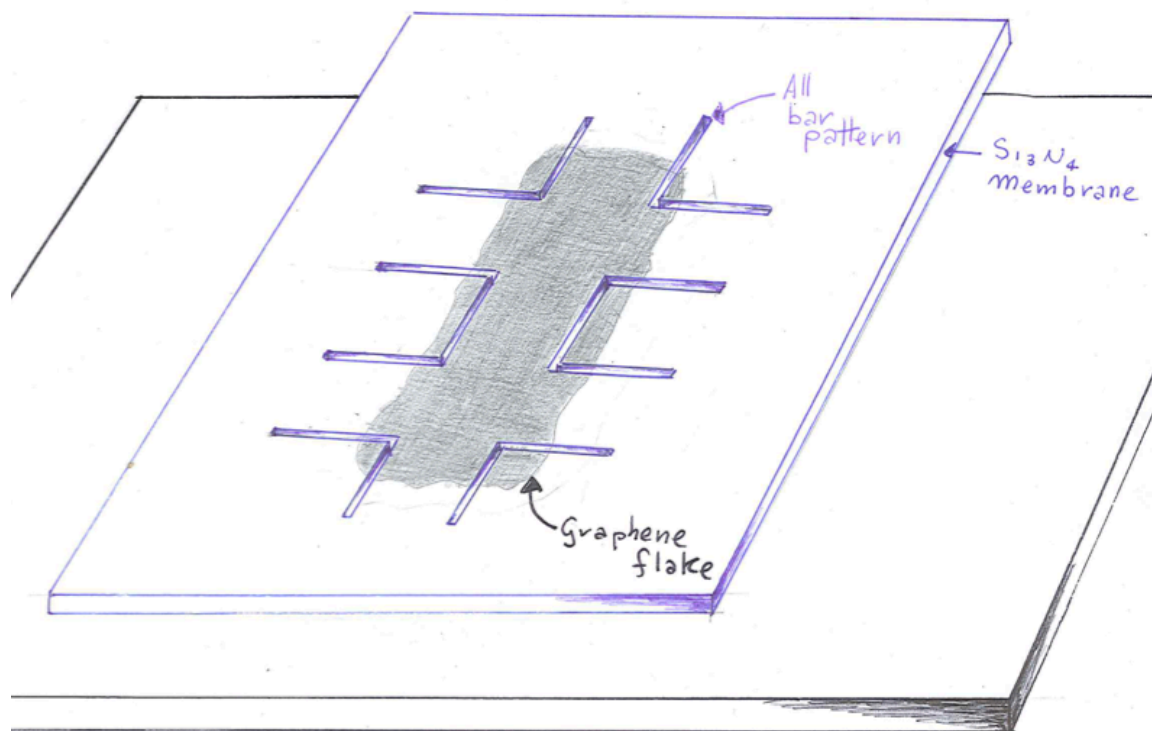


Figure 1 schema per la fabbricazione di patterns Hall bar su flakes di grafene, utilizzando Si_3N_4 membranes come maschere protettive.

In questo modo, con misurazioni elettromagnetiche, si potrebbe caratterizzare il contatto, e verificarne l'effettivo miglioramento della qualità rispetto ai precedenti contatti ottenuti mediante litografia.

Uno dei punti chiave di questo progetto è quindi l'uso di membrane di Si_3N_4 come stencilling masks e come schermo protettivo sul grafene durante il milling.

All'inizio del lavoro, queste membrane sono state ordinate da un fornitore esterno, Protochip, con dimensioni predefinite di 200nm di spessore, e window size 1x1 mm. (Figure 2).

Procedendo con gli esperimenti, sono emerse alcune limitazioni sull'utilizzo di queste membrane:

- Il supporto attorno alla membrana è di dimensioni molto ridotte, (meno di un cm^2), e questo comporta serie difficoltà nel maneggio e nell'allineamento della membrana con altri campioni.
- Inoltre, l'operazione di fissaggio del chip della membrana ai campioni di grafene risulta alquanto difficoltoso a causa delle dimensioni ridotte.

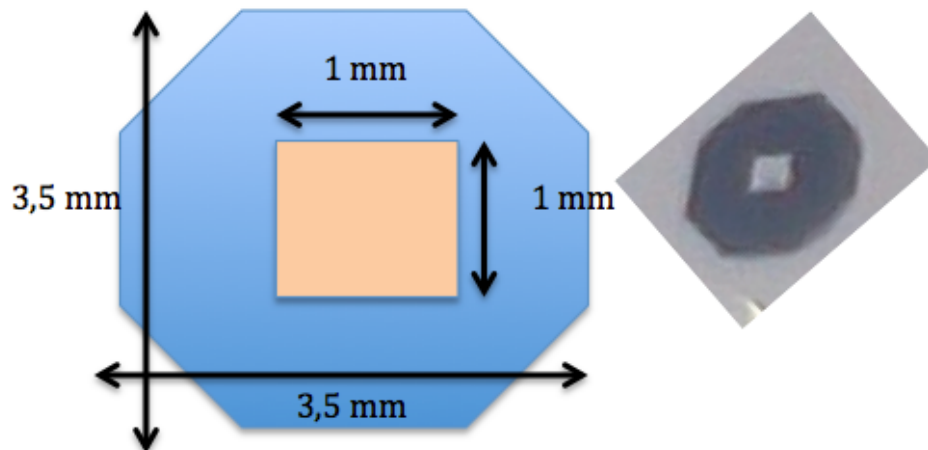


Figure 2 Membrane ordered from Protochips, with scheme of dimensions

- Le dimensioni predefinite di spessore, non più di 200nm, limitano le possibilità di milling con FIB, perché le membrane tendono a rompersi o crollare completamente per certi parametri del processo.

Un set di membrane di Si_3N_4 , con spessore variabile e un supporto di dimensioni maggiori sarebbe vantaggioso per gli esperimenti successivi; per questo che è stato deciso di fabbricare le membrane nella cleanroom Danchip, con un processo di litografia standard che consente di controllare lo spessore delle membrane, e garantisce uno strato di nitrato a low stress. Per la litografia è stata usata una maschera per produrre campioni TEM, mostrata nel capitolo 3, e che quindi prevede un supporto di circa 1 cm^2 , che è risultato più adatto agli scopi di questo lavoro perché maneggevole e pratico.

La fabbricazione di membrane dello spessore di 400nm e 150 nm è stata portata a termine con successo, e, dagli esperimenti effettuati in seguito sullo stress e sui punti di rottura, è risultato che queste membrane, oltre ad essere più facili da maneggiare, sono effettivamente più resistenti allo stress indotto dal FIB milling, ed è quindi possibile disegnare su di esse una maggiore varietà di patterns, anche a correnti relativamente elevate, senza osservare rotture o flessioni.

Il processo utilizzato è anch'esso descritto in dettaglio nel capitolo 3; si tratta di un processo di litografia standard, seguito da KOH etching. Le tavole dello schema di processo sono visibili in appendice 1.

In seguito, queste membrane sono state utilizzate per la fabbricazione di stenciling masks.

La tecnica della litografia nanostencil è un metodo usato per trasferire patterns da una maschera perforata a un substrato sottostante. Una membrana perforata di spessore nell'ordine dei nanometri (nanostencil) protegge il substrato dal flusso di materiale, durante la deposizione. In sostanza, la membrana agisce come una "shadow mask", schermando durante la deposizione e trasferendo il pattern desiderato sul substrato sottostante. Nel nostro caso, il materiale depositato è metallico, ad esempio oro o argento, e il risultato è un pattern di contatti trasferito su campioni di grafene.

Molti sono i vantaggi di questa tecnica, ad esempio, la superficie del campione rimane pulita e priva di contaminazioni, poiché è protetta dalla stenciling mask; inoltre non dovrà essere effettuata alcuna rimozione di materiale con solventi chimici dopo la deposizione, e questo consente di utilizzare nanostenciling anche su campioni fragili, che non sopravvivrebbero invece a un processo di litografia.

La fabbricazione delle stenciling mask, come già accennato, verrà effettuata in questo progetto tramite Focused Ion Beam milling. Una descrizione dettagliata della teoria riguardante questa tecnica è presentata nel capitolo 2.

La tecnologia del milling ha il grande vantaggio di consentire una modifica diretta della superficie del campione, diversamente dalla nanolitografia, dove è necessario l'utilizzo di resist e maschere.

Il processo di milling, i parametri e il confronto tra i diversi tipi di membrane utilizzate sono illustrati nel capitolo 4, dove sono anche riportati i dati sul danneggiamento durante il milling e sui possibili pattern riprodotti, che mostrano la maggiore resistenza delle membrane prodotte in Danchip rispetto alle altre. I pattern trasferiti sulle membrane sono tali da consentire la deposizione di contatti metallici su grafene. Un disegno esplicativo del risultato desiderato è mostrato in Figure 3.

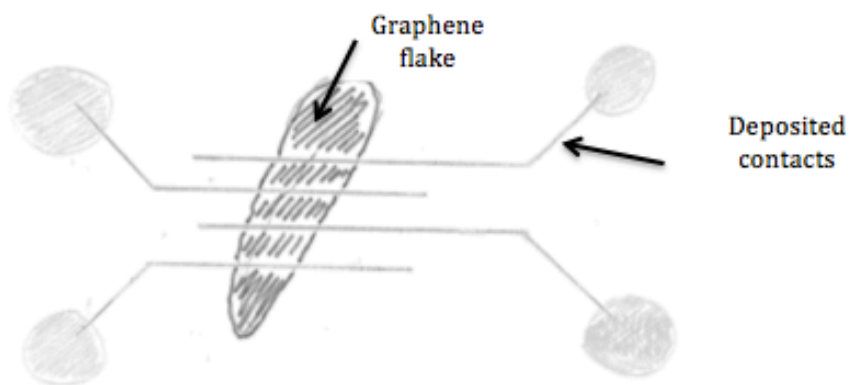
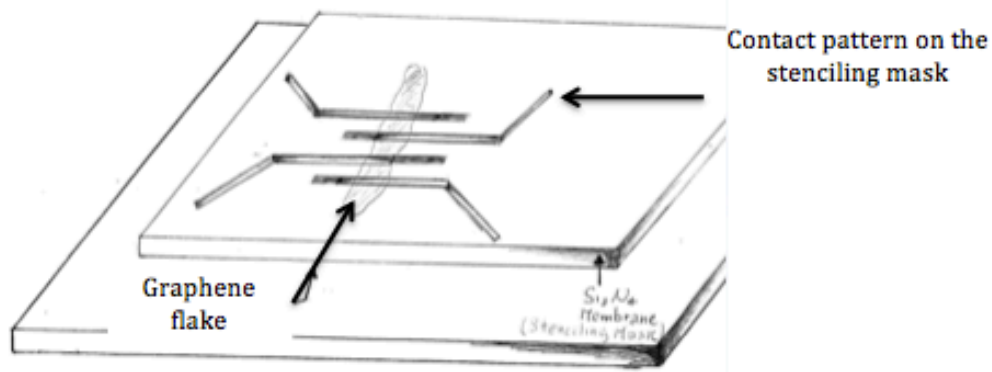


Figure 3 Schema del processo di milling (figura in alto) e del risultato desiderato (in basso) per la deposizione di contatti four point probe su grafene

La fabbricazione di maschere per la deposizione di two point probe measurements e four point probe measurements è stata eseguita con successo.

L'ideale sviluppo successivo prevede la creazione di contatti direttamente su flakes di grafene, con uno schema Hall bar, mostrato in precedenza.

Notevoli difficoltà si sono presentate nel momento dell'allineamento e fissaggio delle membrane, dovute soprattutto alle ridotte dimensioni dei flakes. Diversi tipi di fissaggio sono stati testati, e in seguito la deposizione di metallo è stata effettuata in cleanroom, utilizzando oro, argento e platino.

Misure relative al pattern transfert e alla precisione di allineamento sono state effettuate e presentate nel capitolo 5, insieme a un'analisi della contaminazione dei campioni, dovuta al contatto membrana-campione e al FIB.

Sono state effettuate anche alcune prove di milling direttamente su flakes di grafene.

I contact pads sono stati fabbricati su PMMA, utilizzando un nanodrill. Anche in questo caso l'allineamento risulta complicato.

I campioni di grafene, ottenuti per mechanical exfoliation, sono stati analizzati con una spettroscopia Raman, per verificarne la qualità, identificando i single layers, double layers e multilayers.

II. Panoramica del progetto:

Il progetto è strutturato come segue: dopo un'introduzione al problema e un overview dell'attuale stato della ricerca (capitolo 1), il capitolo 2 illustra le basi teoriche riguardanti la tecnologia del FIB e milling di membrane.

Il capitolo 3 riguarda la fabbricazione di membrane, descrivendo più in dettaglio i motivi che hanno spinto a produrre membrane direttamente nel nostro laboratorio piuttosto che utilizzare quelle prodotte da una compagnia esterna. Inoltre il processo di fabbricazione è presentato nei suoi vari passaggi, concludendo con la visione dei risultati ottenuti.

Il capitolo 4 contiene uno studio approfondito del comportamento delle membrane durante il milling, i processi di fabbricazione di nanostenciling masks, con parametri e confronti dei diversi tipi di membrane, e i risultati ottenuti. È visibile uno studio empirico sullo stress e sui patterns che è possibile trasferire sulle diverse membrane.

Inoltre, è presente una panoramica del processo di allineamento e fissaggio delle membrane ai campioni, il procedimento di deposizione dei contatti metallici sul substrato, la tecnica usata per la creazione di contact pads, e un accenno al milling diretto di flakes di grafene.

Il capitolo 5 riguarda la caratterizzazione dei campioni risultanti, con misurazioni di contaminazione ottenute con XPS, una panoramica della tecnica di Raman spectroscopy utilizzata per caratterizzare i flakes di grafene, e le misurazioni elettriche ottenute dai contatti depositati.

Nel capitolo 6 saranno presentati le conclusioni e i risultati ottenuti, suggerendo possibili sviluppi futuri per il milling di grafene.

III. Conclusioni

Lo scopo ultimo di questo progetto è fornire delle linee guida per il futuro sviluppo di contatti di grafene fabbricati con la tecnologia del focused ion beam.

A questo proposito è stata eseguita la fabbricazione di stenciling mask su membrane di Si_3N_4 , ricavandone dati empirici sullo stress e i punti di rottura, e adoperandole per depositare contatti su sample di grafene.

Studiando l'ottimizzazione dei parametri di milling e il metodo di processo che dia i migliori risultati, sia nella produzione di stenciling masks che nel milling diretto di grafene flakes, si sono ricavati dati che potranno poi essere utilizzati nelle future fabbricazioni.

I risultati principali ottenuti sono quindi:

- La fabbricazione di membrane che meglio si adattino agli scopi di questo progetto, e che quindi siano facili da maneggiare e resistenti sia al processo di milling che al trattamento in laboratorio.
- L'analisi empirica dello stress indotto nelle membrane dal FIB milling, il paragone tra le membrane prodotte nel nostro laboratorio e quelle ordinate dal produttore esterno, in modo da ottenere un set di parametri che consentano il processo di fabbricazione di stenciling masks in maniera ottimale.
- La deposizione di contatti metallici mediante stenciling masks, passando attraverso l'implementazione di un metodo efficace per l'allineamento e il fissaggio delle membrane al substrato. L'osservazione dei contatti depositati in termini di forma e rispetto delle dimensioni prestabilite. Il design e la fabbricazione di contact pads adatti allo scopo di questo progetto.

L'obiettivo della caratterizzazione dei contatti non è stato completamente raggiunto, a causa dell'ostacolo dell'allineamento dei contatti e dei contact pads sui contatti depositati.

Infatti, nonostante i risultati siano stati migliori utilizzando le membrane fabbricate in Danchip, il preciso allineamento manuale dei pattern di contatto con i flakes di grafene risulta particolarmente difficile; inoltre, al momento del fissaggio, anche il minimo spostamento della stenciling mask causa il disallineamento dei campioni.

L'allineamento dei contact pads risulta oltretutto difficile a causa delle grandi dimensioni dei pads rispetto al pattern dei contatti.

Soluzioni per risolvere questi problemi, che comportano l'utilizzo di stenciling masks aggiuntive, sono presentate nel paragrafo 4.5.1.

1. Futuri sviluppi

Sebbene in questo progetto non si sia arrivati all'attuale fabbricazione dei contatti direttamente su flakes di grafene, si sono effettuati studi per esplorare la fattibilità di una fabbricazione di questo tipo e analizzare i problemi e le soluzioni per renderlo possibile, iniziando a ricavare una completa panoramica del comportamento delle membrane di Si_3N_4 prodotte in laboratorio, analizzando i requisiti necessari affinché siano adatte ai futuri

sviluppi della ricerca; in questo modo, utilizzando i risultati qui ottenuti e implementando un metodo per superare l'ostacolo dell'allineamento ottimale, sarà possibile procedere con successo su questa strada.

L'utilizzo di appropriati alignment marks, per esempio, ha facilitato l'allineamento manuale dei campioni. In futuro, l'utilizzo di bracci meccanici controllati con leve esterne potrebbe rendere l'allineamento più semplice ed efficace.

Inoltre, l'utilizzo di un collante adeguato consentirebbe il fissaggio senza disallineamenti della membrana.

Alcune prove sono comunque state effettuate, rivelando la concreta possibilità di portare a termine questi esperimenti. I risultati ottenuti consentiranno in future di implementare un metodo facilmente attuabile ed efficace per la fabbricazione di contatti di grafene.

Abstract

Negli ultimi anni, grazie alle sue straordinarie proprietà, quali ad esempio la mobilità dei portatori, nell'ordine di centinaia di migliaia di cm^2/Vs e la trasparenza alla radiazione visibile, il grafene è stato valutato come uno dei più promettenti candidati per l'implemento di dispositivi di nano-elettronica ed elettronica ultraveloce, quali transistors e sensori.

Inoltre, le proprietà ottiche di questo materiale lo rendono particolarmente adatto all'implementazione di dispositivi opto-elettronici, in particolare nel settore delle nanotechnologie e del fotovoltaico, grazie al suo carattere bidimensionale e alle ridotte dimensioni, nell'ordine di decine di micrometri.

Prendendo in considerazione i risultati emersi dalle recenti ricerche, questo lavoro vuole essere una guida per il futuro sviluppo di contatti di grafene, utilizzando la tecnologia del Focused Ion Beam (FIB), che offre numerosi vantaggi e potrà essere utilizzata per il milling diretto di flakes, senza l'uso di resist e solventi chimici.

In questa tesi è stato studiato un metodo per la deposizione di contatti metallici su grafene, utilizzando stenciling mask fabbricate sfruttando la tecnica del Focused Ion Beam su membrane di Si_3N_4 , e utilizzando la tecnica del nanostencil.

Per aprire la strada alla produzione di questo tipo di grafene devices, verranno fabbricate membrane di Si_3N_4 direttamente nella cleanroom della Technical University of Denmark, e verrà investigato lo stress intrinseco e indotto dal FIB durante la fabbricazione delle stenciling masks.

Allineando e fissando le membrane a substrati di grafene, sarà possibile trasferire i pattern metallici, e quindi i contatti, sui flakes, per poi studiarne le caratteristiche.

Preface

This thesis is carried out at Department of Micro and Nanotechnology (DTU Nanotech) at the Technical University of Denmark.

It is the Master thesis that conclude the course of study in Physic and Nanotechnology for the achievement of Master of Science degree in engineering.

The thesis has been supervised by the professor Peter Bøggild and co-supervised by the Postdoc Alexey Savenko and the PhD student Filippo Pizzocchero

The project corresponds to 35 ECTS point and has lasted from 1st of September 2008 to 31st of August 2009.

I would like to thank my supervisors for guidance and helpful discussions throughout the project, and in general all the Nanointegration group at DTU Nanotech for helpful suggestion and ready technical assistance when needed.

Eleonora Zamburlini

*DTU Nanotech – Department of Micro and Nanotechnology Technical
University of Denmark*

15 November 2012

Chapter 1 Introduction

This thesis wants to be a guideline for future research on fabrication of graphene contacts, therefore, a study on the possibility of fabricate a device of metal contact on graphene flakes, passing through analysis of silicon nitride membranes behaviour during nanostenciling fabrications, and processes of fabrication of the membranes themselves.

Due to its peculiar properties, the use of graphene in devices such as low cost solar cells and high frequency operating transistors has seen a wide spread during recent years.

Moreover, the use of Focused Ion Beam technology, in order to create stencilling masks on Silicon Nitride membranes and, in the future, to directly mill the flakes in desired shapes may improve the quality of the devices in terms of contamination and precision of milling patterns.

Thus, this work is about fabrication of Si_3N_4 membranes and nanostenciling masks to contact graphene. Studies and optimization of the process have been done in order to clear the way for the future research on graphene contacts fabrication using focused ion beam.

1.1 Introduction on graphene

We should start by talking about graphite, that is an allotrope of carbon, and unlike diamonds, it is an electrical conductor, a semimetal. Graphite has a layered, planar structure. In each layer, the carbon atoms are arranged in a hexagonal lattice with separation of 0.142 nm, and the distance between planes is 0.335 nm.⁶²

The layers are held together by Van Der Waals interaction, with energy of approximately 42,6 meV per atoms, such a relatively low energy allows to separate the graphite layer in the parallel direction to the crystalline plane.^{16 17}

Graphene is a monolayer of carbon atoms, organized in a hexagonal structure, as shown in Figure 4. It is a 2 dimensional material, but can be rolled into a nanotube and folded in a spherical structure called buckyball. Each of these structures has different and unique properties, and they are widely exploited and investigated in the forefront nanotechnology.³ The carbon atoms constituting graphene are hybridized sp_2 , which means that the s orbital will hybridize and mix with 2 of the three available p orbitals.

It has been demonstrated that, due to its structure and geometry, graphene has a very special band structure, which determines its peculiar properties.

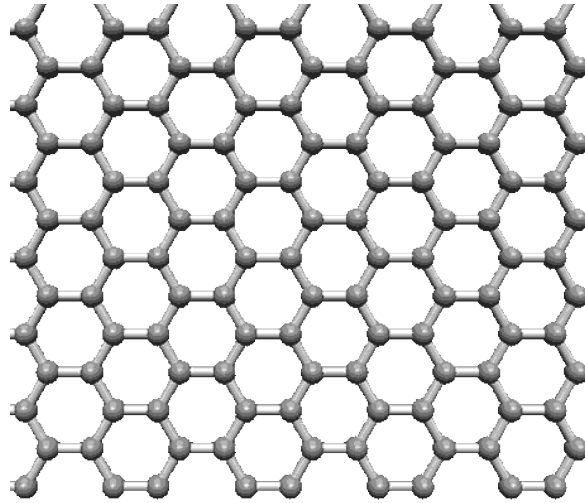


Figure 4 graphene structure

In fact, the band structure is formed in a way that at the “Dirac points”, corresponding to the six corner of the hexagonal structure in the reciprocal lattice (see fig. 2), the valence and the conductive band are in contact, and graphene turn out to be the only discovered semimetal acting like a zero band gap semiconductor.

It has been discovered studying the electronic structure of graphene, that the E-k relation is linear for low energies near the six corners of the two-dimensional hexagonal Brillouin zone, (see Figure 5) and this leads to a relativistic effect: zero effective mass for electrons and holes. In fact, using quantum mechanics it can be shown that for an electron in an external electric field E , the effective mass can be calculated as:

$$m_e = \hbar^2 * \frac{d^2\mathcal{E}}{dk^2}$$

Therefore, since the linear dispersion is zero at the edge of the Brillouin zone, the effective mass for carriers is also zero.

Due to this linear, or more precisely conical, dispersion relation near the Dirac points, electrons and holes at low energies, show a relativistic behaviour, described by the Dirac equation for particles that have spin equal to $\frac{1}{2}$.^{18 19}

This is a peculiar and unique characteristic of graphene, as it is the connection between quantum electrodynamics and solid-state physic, and this very special feature is responsible for many of the electronic properties.¹

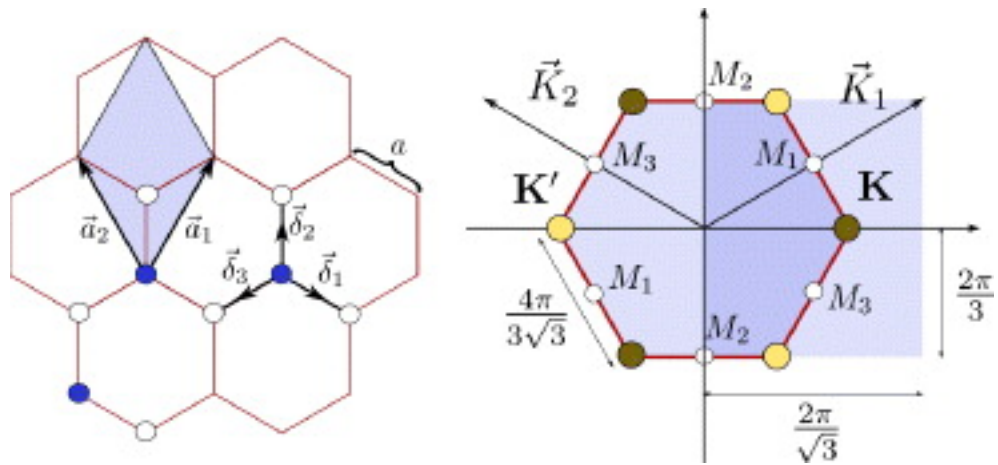


Figure 5 graphene structure and reciprocal lattice; the six points of the hexagonal reciprocal lattice are the "Dirac points"

Graphene was first discovered in 2004, two Russian scientists *Andre Geim and Kostya Novoselov* demonstrated that it was possible to isolate the thinnest material possible: a monolayer of carbon atoms, ordered in a hexagonal structure.¹

This astonishing material turned out to be stronger than steel, a better conductor than copper, and having heat conductance in a range of 4 to 5 x 10³ W/mK, higher than any other material ever observed. Furthermore is transparent to light, but somehow so dense that even the Helium atoms cannot pass through it.

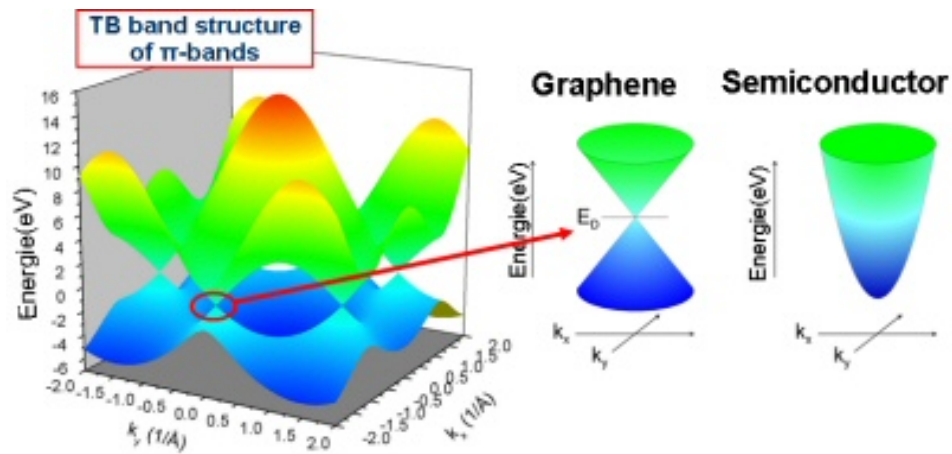


Figure 6 Graphene band structure in comparison of a normal semiconductor band structure. The peculiar band structure of graphene is responsible of its unique properties⁴⁹

Since this new graphene has properties that overcome all the materials that have previously been used, it has been rated as one of the element that will change radically the world of electronic and photonic.

A great interest in graphene has been in electronic field: many are the applications of this material, which have been investigated since its discovery. An example is the fabrication of

FET's (Field effect transistors), for which graphene is particularly suitable, due to its high electronic quality.

The first top-gated FET, with an on-off ratio of <2 , was demonstrated by researchers of AMICA and RWTH Aachen University in 2007.⁵

The main problem to overcome in developing this technology is the fact that current graphene transistors show a very poor on-off ratio. The research have tried to find creative solutions, and many step forward have been made in the last 10 years; for example in 2009, researchers at the LNESS laboratory in Como, from Politecnico di Milano demonstrated four different types of logic gates. Each gate was constituted from a single graphene transistor.⁸

In the same year, the Massachusetts Institute of Technology researchers built a frequency multiplier that is an experimental graphene chip, capable of registering an incoming electrical signal of a certain frequency and producing an output signal that is a multiple of that frequency.⁹

These discoveries, of course, open up a range of new applications, in fact, in 2010, researchers at IBM have been able to create a graphene transistor that exceed the speed of a Si transistor of the same length, that is, for the first time ever a graphene device can be use as a conceivable replacement for silicon.^{11 12 13} This is just giving a slight idea on how graphene can be striking in future researches.

Another fundamental point of the research is to integrate the graphene electronic devices in conventional nanocircuits. For example, in June 2011, IBM research group announced that they had created the first graphene-based integrated circuit that was a broadband radio mixer.¹⁵ This device was able to handle frequencies up to 10 GHz, and its performance was unaffected by temperatures up to 127 degrees Celsius.¹⁵

All this above were just basic examples on graphene researches, that shown the potentials of this materials and the outstanding usefulness it can have once it will be possible to understand and exploit all its properties, and knowledge on managing and treating this materials. Nevertheless those enormous step forward in developing graphene devices for various applications show that graphene is extremely interesting and exciting for innovative electronic devices.

The methods of preparation of graphene can be different:

The most efficient way to achieve a high number of single layer flakes of graphene is the mechanical exfoliation technique. It is starting with highly oriented pyrolytic graphite (HOPG), which is sandwiched between sticky tapes. Then the tapes are peeled and one can

see that the graphite is sliced into two parts thus each part has to be thinner than the original one.⁶³

Repeating the process many times, thin flakes can be produced and transferred to silicon substrate. Single layer flakes can be identified by optical microscopy and can be verified by Raman measurements or by AFM.⁶³

The other way to produce graphene is to grow it on a surface using CVD, MBE or SiC reduction. These methods not provide currently single layer graphene but a few layers instead. The clear advantage is that one can cover an entire wafer with graphene such way. CVD or MBE technique is often done using metal 3 substrates (Ru, Ni) due to the underlying hexagonal lattice that initiates graphene formation.⁶³

These thin films cannot be used directly in electronic applications due to the conducting substrate however it is possible to transfer the graphene on them to other substrates like silicon.⁶³

In our case, graphene was fabricated via mechanical exfoliation (Figure 7): adhesive tape is used to repeatedly split graphite crystals into increasingly thinner sheets. The optically transparent mono and multilayer flakes of graphene are then transferred on a suitable insulating substrate.

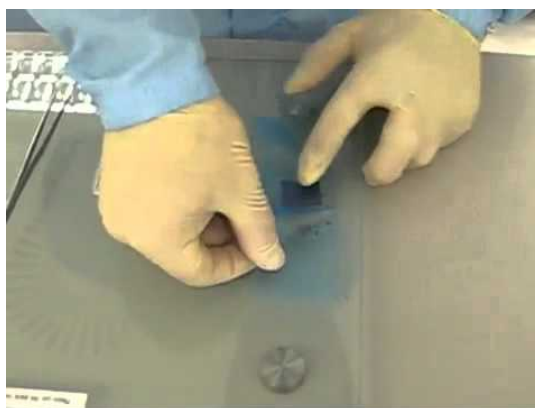


Figure 7 process of mechanical exfoliation of graphene

This is so far the most efficient way to achieve monolayer graphene flakes with electrical and mechanical properties that can be exploited for further experiments.¹

1.2 Application of graphene in nanotechnology

As we have seen before, graphene is very attractive, because of its outstanding electrical properties, is bidimensional character and its transparency to light radiation.¹

Furthermore, the combination of its mechanical properties and electrical characteristics make graphene very suitable for flexible electronic devices.¹

The properties of saturable absorption can be extremely important for laser and ultrafast optics applications. This material can also be used as electrode in devices for renewable energy such as hydrogen cells and lithium batteries.³

Finally, the exceptionally high ratio between surface and volume can be exploited in the construction of sensors for gas detectors. The capability of graphene to resolve also single gas molecules has in fact already been demonstrated by Schedin⁵, and regardless the difficulties in the fabrication process, this may be a huge step forward in sensors technologies.

As to quote a nice example of graphene usage in nanotechnology, it has been demonstrated the possibility to use graphene for graphene nanoribbons (GNR) to fabricate memory cells based on nondestructive storage mechanism. The memory devices are fabricated by Ar ion beam etching of graphene monolayer using V₂O₅ nanofibers as masks. The resulted memory cell has shown good durability and stability, without any degradation or failure on over 10⁷ cycles.⁴

The GNR based memory cell can operate under ambient condition with signal swiching in the range of KHz. In the future, very fast memory with clock frequencies that overcomes the conventional dynamic random access memories may be achievable with this technique, using GNR with well-defined crystallographic orientation.⁴

The devices fabricated with focused ion beam

In this project, a focused ion beam microscope has been used to fabricate

- Stencilling masks: a sheets of material, in our case Silicon nitride, perforated using FIB to create a pattern trough which metal can be deposited to create the printed pattern on the surface below. These stencilling masks have been exploited to deposit metal contacts on graphene flakes.
- A study has been made to clear the road to the fabrication of graphene contacts, cutting the graphene with the energetic ions beam trough a protective Si₃N₄ membrane, and contact the edges with an adequate contact pad made by PMMA.

The reason for using FIB for the fabrication process is mainly linked to contamination issue of the previously used method. The standard method for creating the devices is lithography, method that involves the usage of chemical resist, which, as a result, leave organic contaminations (resist residuals) on the sample, lowering the electrical quality of graphene.⁶⁴

Organic contaminants, in fact, cause film interface defects, SiC formation, and an increase in contact resistance. It can also cause a reduction of charge carriers mobility and shift of charge neutrality point.⁶⁴ Other than that if any residues, or even water are on the surface, or under graphene, they can interact with the surface and steal or donate charges, to affect the electronic properties, changing the conductance, the position of charge neutrality point and affect the mobility.⁶⁷ It has been shown, in fact, that by using vacuum annealing, it is possible to remove residuals for example from PMMA coming from CVD transfer of graphene, and that leads to mobility two times higher than the one measured in the presence of residuals.⁶⁸ It is reasonable to think that, if it is possible to reduce the residuals and contaminations due to transfer of graphene and photolithography, better electronic properties can be achieved.

Moreover, with FIB it is possible to obtain a variety of patterns with very precise dimensions and shapes, without the necessity of a photolithographic mask.

The disadvantages of the FIB, nevertheless, are, for example, the high probability of breaking the Si₃N₄ membranes, depending on the intrinsic stress of every single membrane and on the milling parameters, and the possibility of redeposition of Ga ions and therefore contamination of the sample.

A detailed study of the milling techniques of Si₃N₄ membranes, in order to give guidelines for optimal fabrication of graphene stencil devices, has been performed in this work.

1.3 Introduction to graphene milling

Due to its material stability and strength, absence of defects, and unique electronic band-structure, graphene holds considerable promise for a number of applications. Moreover, the possibility of patterning graphene in the nanoscale opens a variety of possibility in electronics, such as fabrication of high-speed transistors.

Unlike other existing nano structures, patterned graphene can form complex extended geometries and can be readily contacted electrically.⁴⁶

This is basically the idea we would like to suggest with this project: the possibility to pattern directly graphene using focused ion beam, to create a geometry that is suitable for being connected with electrical contact. The obtained devices will have all the electronic properties of graphene, and moreover it will be transparent, so that it may be possible to integrate it in optoelectronic circuits.

Different methods have been used to pattern graphene, including electron beam lithography in conjunction with reactive ion etching^{54 55} and direct etching with an electron beam in a transmission electron microscope (TEM)⁵⁶. Both methods are suitable to produce patterns in the tens of nanometer range. The former is limited by uncontrolled under-etching by the oxygen plasma; the latter relies on transferring graphene flakes onto TEM grids, which is not suitable for larger-scale fabrication of devices.⁴⁶

The method we analyse here consists in patterning graphene by using FIB. The graphene will be patterned through a Si_3N_4 membrane; the presence of the membrane on top of the flakes should limit the redeposition and creation of defects and contamination.

The basic idea is to align the Si_3N_4 membrane to the graphene flake, and then mill through it, as shown in Figure 8.

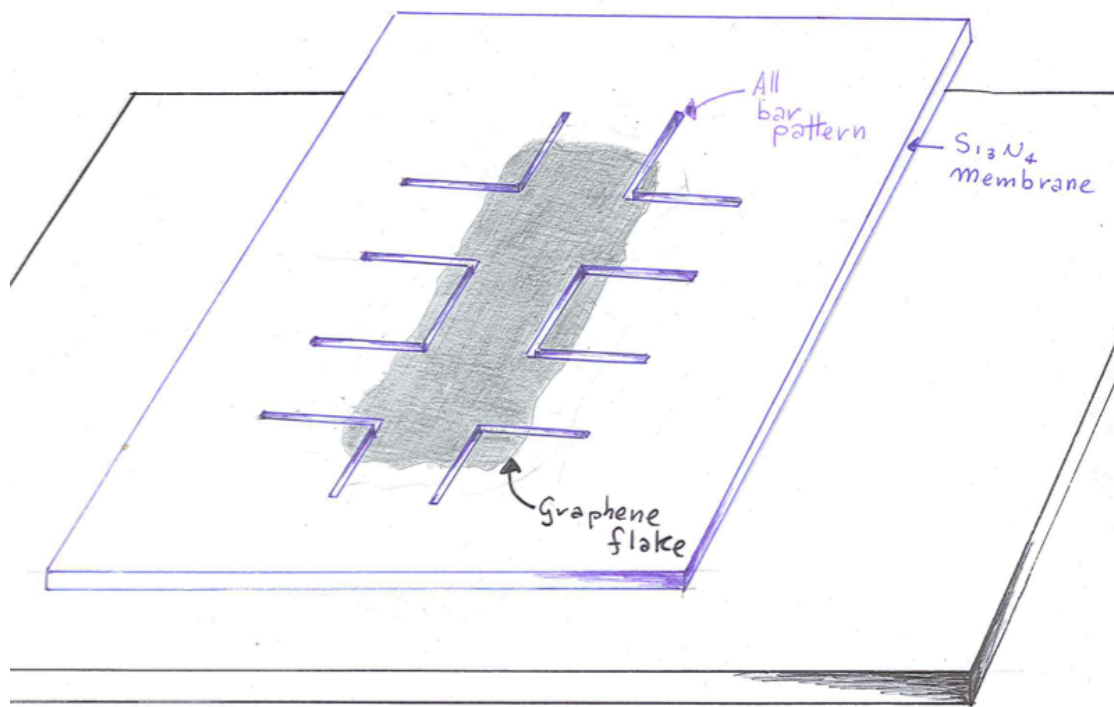


Figure 8 Direct milling of graphene through Si_3N_4 membrane to fabricate Hall bar patterns

An Hall bar geometry is obtained on the flake, and, by depositing metal as shown, the flake can be used as an electrical contact, and can be characterized in its electronic properties.

1.1 Aim of the project:

1.4.1. Goals, investigation and key questions

Contacts to graphene devices have already been fabricated, using a variety of techniques.

The standard technique that is used in our laboratory consists in a UVL or EBL lithography process that will be explained further.

This technique, as I said above, presents limitations regarding the contamination of graphene; the contact fabricated this way, in fact, have been in contact with chemical resist, and this lower the conductivity and the quality of the contact. Although highly impressive results have been achieved by photolithography, the fabrication of graphene contact with FIB milling will, in our opinion, lead to a lower resistance, and therefore in better working devices.

In this project, we want to test the possibility of using FIB techniques to fabricate graphene contacts, by getting an overview of the properties of Si_3N_4 membranes, investigating which requirements they have to fulfil in order to be suitable for this kind of fabrication.

Furthermore, we will create stencilling masks on this kind of membranes, with different shapes and designs, and use them to deposited metal contacts on graphene flakes, to tests both the suitability of Si_3N_4 membranes for this purpose and the quality of the contacts deposited in this way.

A scheme of the procedure, and an ideal resulting device, is shown below. (Figure 9)

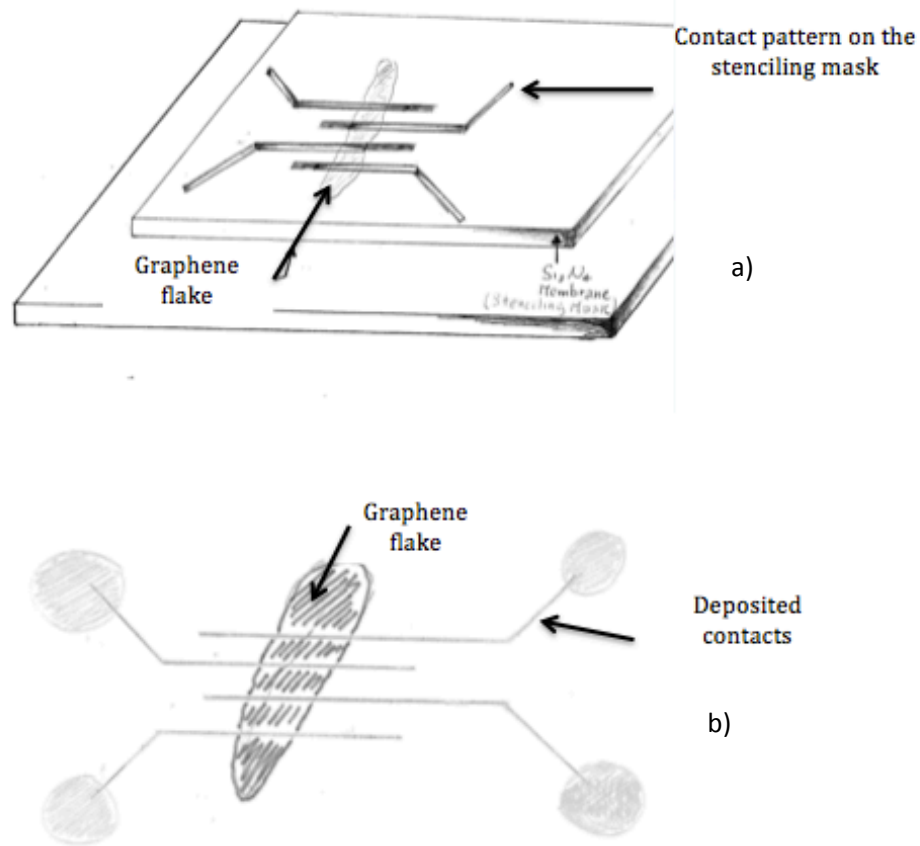


Figure 9 scheme of process of pattern transfer with stenciling mask (a) and final sample (b) with metal contact on graphene flake.

The technology widely used for this project is milling by Focused Ion beam (FIB). Basically it is possible to mill pattern in the scale of micrometers and nanometers by bombarding the samples with high-energy ions of, in our case, Gallium. More on this technique will be said further in the report, but the key concept is that, by using FIB, stenciling masks constituted by Si_3N_4 membranes will be fabricated, and then they will be used for depositing metal contacts on graphene and graphite.

The following step will be to fabricate graphene contacts with direct milling using FIB through a Si_3N_4 membrane, as described above. This should prevent the redeposition from the focused ions, and provide an operating device with low contamination and well-defined edges, important for lowering the dispersion and for the reproducibility of the process.

During the outgoing of the process, we had reasons to believe it was better to fabricate our own Si_3N_4 membranes rather to use the one we ordered from an outside company (Protochips), since having membranes with higher thickness and wider holder was better for the purpose of this project. Therefore, a fabrication process has been optimized, and an

empirical study on the quality of the fabricated membranes compared to the previous one has been performed

The optimal result will be to achieve final contacts, using stencilling masks created by milling the membranes we have fabricated in the cleanroom; Trials of contact deposition will be performed both on insulating substrate and on graphene flakes; it will be therefore possible to verify the possibility to use this method, achieving good alignment, and well defined contact patterns.

Before this, an investigation of the stress of the membranes will be carry on, since it is necessary to test the quality of both types of membranes to establish if the one we fabricated are actually more suitable for our purposes.

This project aim to be a guideline for future graphene contacts fabrication with FIB techniques, giving data on the membranes that can be used, the milling parameters and the different methods for alignments and attachments, concluding with an analysis of the contacts fabricated with the stencilling masks.

In summary, this project is about:

- Fabrication of Si_3N_4 membranes that are
 - Easy to handle, especially compared to the one ordered from external suppliers (Protochips).
 - With the thickness of low stress nitride that we can chose during the fabrication process.
 - More resistant to ion beam milling, with the possibility to mill the pattern we need for the stencilling mask fabrication and for future fabrication of graphene contacts.

- An analysis of the membrane stress, comparing the membranes from Protochips with the fabricated one, to have a clear overview of the reason of membrane breaking, milling parameters, data on stress point, critical patterns and limit currents.

- Contact deposition trough membranes
 - Verify if it is possible to deposited contacts on SiO_2 substrate

- Implement an aligning method of the stencilling masks on graphene flakes, and a way to attach them to the sample.
- Verify that the contacts well defined in shape, with dimensions that respect the specifications, with no broadening or deformations
- Is it possible to achieve contact pads masks that suits the pattern, and deposited contact pads suitable for electrical measurements

1.4.2. *Project overview*

In chapter 2, the theory behind the techniques used is presented, giving particular relevance to FIB and milling process of silicon nitride.

In chapter 3, a study of the Si_3N_4 membranes used for the stencilling masks fabrication will be lead on. As I said before, some of them were ordered from our commercial suppliers Protochips, while others were fabricated in the Danchip at DTU.

A critical observation of the initial membranes has been carried on, and starting from their disadvantages, new membranes with better specifications, such as larger support and thicker Silicon Nitride layer have been fabricated.

In chapter 4, experiments in milling different sizes and shapes of patterns performed with both type of membranes will be presented. The key issue is to find systematic condition for milling without breaking and bending, and to create masks that can be used for some metal depositions without degradation.

The stress of the membrane, as well as the limiting features of the pattern that can be milled, has been investigated and modelled, in order to have an overview of the techniques that has to be used to create the stencilling masks for the deposition of the contacts; Empirical data have been collected based on milling experiments, in order to optimize the milling parameters to create the patterns we need.

Then, issues and solution proposal for alignment of membranes to graphene samples and attachments have been presented. The different trials and errors will be analysed, and the final solutions will be shown.

Ideas and improvements for the future step, that is the direct milling of graphene contact in a Hall bars shape, using Si_3N_4 membranes, as a protective layer against redeposition and spreading of the milling, will be explored.

There will also be a description of how metal contacts have been deposited on SiO_2 substrate, defining and designing contact pad masks of PMMA to fabricate contact pads suitable for four point probe electrical measurements.

In chapter 5, the set up for the electrical measurements and the results from the sample we obtained is presented, together with the investigations on contamination detection.

Measurements of the dispersion during contact deposition depending on the position of the stencilling mask, and contact measurements have been carried on, confronting different metal combinations.

Subsequently, graphene and graphite flakes have been identified using optical microscope and Raman spectroscopy, and the contact has been deposited on them.

This should give a complete overview of the advantages of these techniques in respect of the old fashion way of fabrication, and it should clear the way for future graphene contact fabrication and further applications and usage of the devices in nanointegration and optoelectronic.

In chapter 6 a discussion of the global results of the projects will be presented, and conclusions will be drawn out from the work done, presenting also some ideas for future developments.

Chapter 2 Theory background and fabrication techniques

4.1. Focused Ion Beam Milling

2.1.1. Theory on focused ion beam

Focused ion beam, is a technique for site-specific analysis, deposition, and ablation of materials.

It is basically consisting of a bombardment of high-energy ions on the sample, which can lead to different results, depending on what is needed. It can be used for imaging, etching or deposition.

The focused Ion beam microscope that has been used in this project is a combined FIB-SEM instrument, which means a set up that includes a Scanning Electron Microscope (SEM), for an accurate analysis of the etching or deposition process.²⁰

In the DTU CEN there are two focused ion Beam microscopes, Quanta 3D and Helios, the last one with a better resolution.

SET UP

The set up of a focused ion beam instrument is consisting in a vacuum system and a chamber, an Ion beam source and column, a sample stage, detectors and gas system. Of course all of this is connected to a PC that can control the process. A picture of a focused ion beam is shown in fig. 5, while a scheme of the set up can be seen in fig. 6.

In our case, the PC program can show the inside of the chamber with a camera, and the images from ion beam and from electrons.

In a combined system like the one in fig. 6, the ion beam column is typically tilted to a certain angle compare to the electron column.

The Ion beam source is, in the case of Helium ions, a tip, that can release high brightness He ions, that are then accelerated trough the column with a potential of 1–50 keV, and focused onto the sample with an electrostatic lens, and directed to the sample, mounted on a stage in the observation chamber.

The sample stage is in generally able to 5 degree of movement (X,Y,Z tilt and rotation), and that is

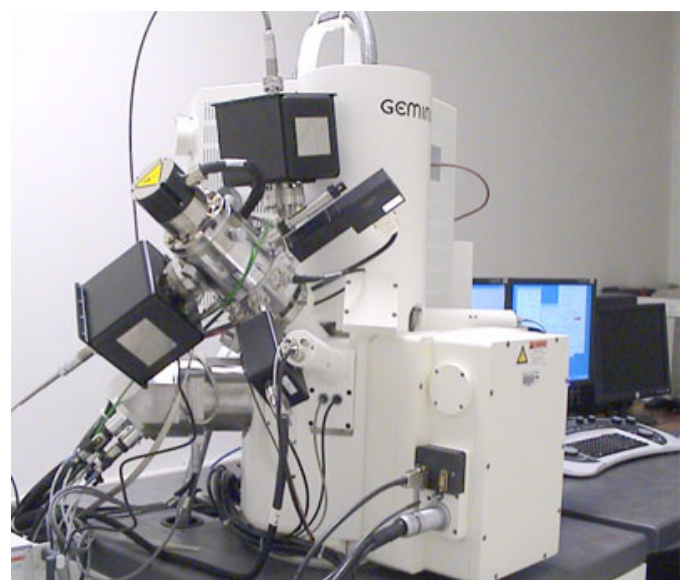


Figure 10 FIB set up as the one we have in CEN

because, if the ion beam device combined with a SEM microscope, a tilt of the stage is necessary to combine this two devices, is necessary to find an eucentric position, where the SEM and the FIB will see the same feature even if the SEM will be tilted compared to the sample.

Other ions are also used for FIB, such as Gallium, iridium or gold. In our case the use of helium ions guarantee a low damage of the sample.

We can see an image of the set up in Figure 11.

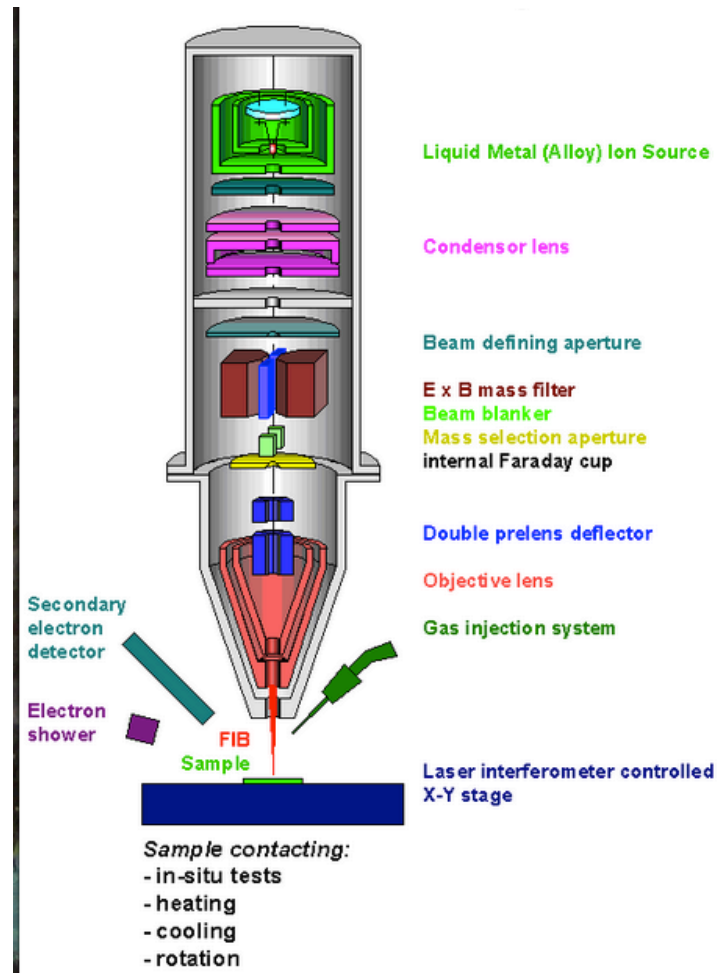


Figure 11 FIB schematic setup

PHYSICAL PRINCIPLE

The ability to mill, image and deposition materials on the sample using the FIB is all linked to the nature of the ion beam – solid interactions.

In our case, we are interested in the milling, that takes place due to a pure energy transfer process: the kinetic energy of the coming ions are transferred to the atoms in the sample, that are scattered away by momentum transfer

A portion of the ejected atoms may be collected and analysed for imaging and mass analysis.²¹

Also inelastic interactions will occur due to the ion bombardment, and that result in a production of photons, plasmons, and the emission of secondary electrons. Observing these secondary emissions, it is possible to get additional information about the sample, because the incoming ions that get trapped in the sample surface will create a positive charge that can trap the secondary electrons, so that a shaded area will be created in the observed region of the FIB, and will be seen as a darker contrast in the SEM imaging screen.²²

For the milling process, we are basically dealing with a scattering process. Sputtering can be considered as a statistical phenomena caused by surface erosion on an atomic scale. We can define the sputtering yield as number of ejected particles per incident ion; it can be quantified as:

$$Y = \frac{\# EjectedAtoms}{incidentIon}$$

for a typical FIB process we have a sputtering yield between $10^{-1} < Y < 10^2$.

The sputtered particles are emitted at energies around 2 eV and their energies follow a cosine distribution for normal incident ions.²²

The emitted particles can of course both be redeposit or cause secondary interactions with other atoms on the surface of the sample.

2.1.2. *Applications of focused ion beam*

A crucial goal of nanotechnology is the modification of surfaces, and this, for sample in the range of micro and nano meter can be tricky.

The FIB allows manipulation of small samples, defining complex patterns in the nano scale, moreover as a microscope, it can be exploit for imaging and observation of small samples.

FIB enables various materials to be deposited on samples, and it also allows very precise etching; this technique are widely used for mask repair, circuits modification, fabrication of contacts in semiconductors, tips for atomic force microscope and TEM samples.

The three main functions of FIB, etching, imaging and deposition, are all very used for nanotechnology applications. The main and well-known function of FIB is that of a scanning ion microscope. The secondary electrons exited by the ion beam are collected and analysed, and this is called SIM (scanning ion microscope) imaging.

This type of microscope is very useful because it can show the channelling contrast (contrast mechanism which discriminates between crystallographic orientations⁶⁵) more strongly than the SEM, and an observation of the crystal grain of metals is possible. Nowadays the resolution of SIM can be less than 5 nm.

The second function of FIB microscope is, of course etching. If the FIB irradiates over an area, several nanometers of materials can be removed without the use of a mask, and with a non-invasive process, that doesn't damage the sample too much and doesn't cause an excessive heating.

Moreover, with the simultaneous observation of the process using the microscope function, high precision in the etching of areas can be obtained.

The last application of this kind of microscope is the deposition of different kinds of materials on a selected sample.

In this section we will go deeper in the details of the theory and the basic concept of the main functions of the focused ion beam, examine the details of the different processes and the eventual improvement that has been done during the years.

Gas assisted focused ion beam etching

Using FIB, it is possible to precisely mill away materials from a localized area, and therefore to modify and create nano structures, prepare masks and transmission electron microscope (TEM) samples. The process is done by bombarding the selected structure with the ions, in a chamber filled with a reactive neutral gas through a fine tube, to enhance the etching rate and reduce the amount of redeposit materials.

The gas chemically reacts with the sample to produce volatile compounds that can be removed easily by the vacuum system.

However, as with any physical process, the etching will change the characteristic of the sample, at least in its top layer. With a 30kV gallium ion beam, for example, the top 30nm of material is implanted with gallium, and the atomic structure will be altered. These damages are very visible in TEM sample prepared via FIB, notwithstanding the eventual damage minimizing procedures that may be applied.

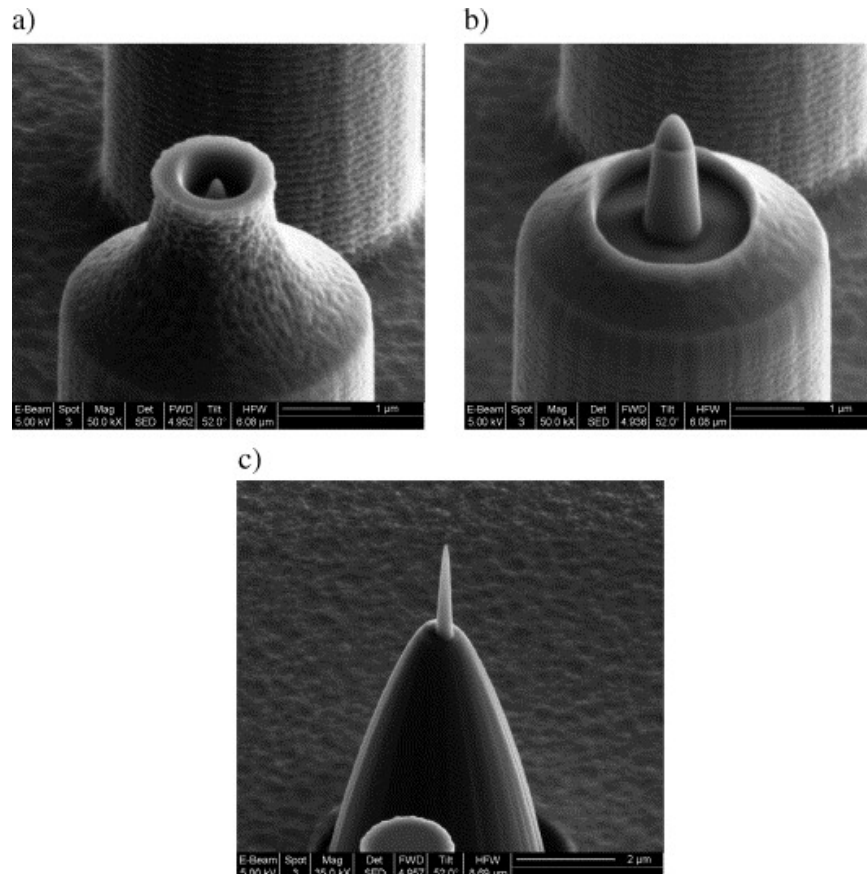


Figure 12 SEM micrographs of the FIB etching of the structures in Fig. 2a. (a) Initial etching around the tip; (b) intermediate step; (c) nanotip obtained after a complete etching.⁴⁸

Gas assisted FIB deposition

This technique is a direct deposition that is done using only FIB and the assisting gas. This deposition will take part in a very localized area, only where the controlled focused ion beam is scanning.

Basic steps of the process are:

- The gas is injected in the chamber by a fine tube, inserted close to the surface. The gas will be adsorbed on the surface of the sample.

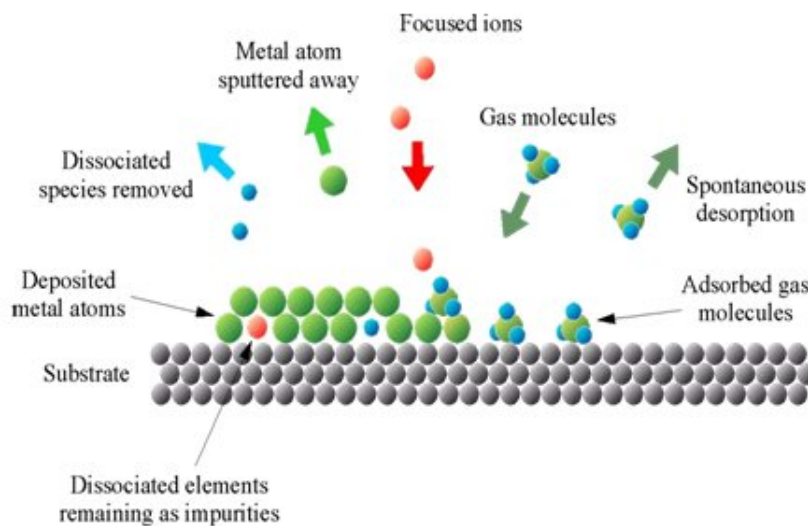
- The adsorbed gas molecules will be decomposed to form volatile and non-volatile compounds by the incident ions, only in the restricted region where the ion beam is scanning. At the same time, the surface of the sample will be etched by the incident ions.
- The non-volatile products remain on the surface producing a deposited layer, while the volatile compounds will be taken away from the vacuum system.

A schematic drawn of the process is reported in Figure 13.

Optimizing the deposition parameter, such as properties of precursor gas, gas flux, ion beam current and so on, it is possible to obtain very fine and precise deposited structure on the sample.

The precursor gasses can be many; in the first experiment conducted on the focused ion beam deposition the trimethyl aluminum (TMA) $\text{Al}_2(\text{CH}_3)_3$ was used to assist the deposition on metal organic material.

Nowadays, dozen of different precursors have been successfully used in FIB induced deposition of metal, insulator and carbon. The critical point is to correctly calibrate the proper amount of gas precursor in a local area; this parameter can be adjusted by relocating the nozzle and by controlling the temperature of the gas crucible.



1. Adsorption of the precursor molecules on the substrate
2. Ion beam induced dissociation of the gas molecules
3. Deposition of the material atoms and removal of the organic ligands

Figure 13 scheme of gas assisted FIB deposition process

Imaging using electrons and ion beams

Traditionally, Scanning electron microscopes (SEM), transmission electron microscopes (TEM) and scanning TEM (STEM) have been used for observation of micro devices and materials. In recent year, gallium FIB has been used for preparing the sample for these microscopes. In this case FIB works both as a milling beam and a probe for scanning ion microscope (SIM).²⁸

The resolution of SIM has gradually been improved, to reach the present value of 5nm, and it has been used instead of SEM when there is no special need for high image resolution.

However, the properties of the images in SEM and in SIM are somewhat different.

Comparison between SIM and SEM imaging

In the image below (Figure 14), we can see a comparison of two identical features observed with SIM and SEM. First of all black and white contrast is opposite between the two microscopes, and the grain contrast can be observed clearly in SIM.³⁴

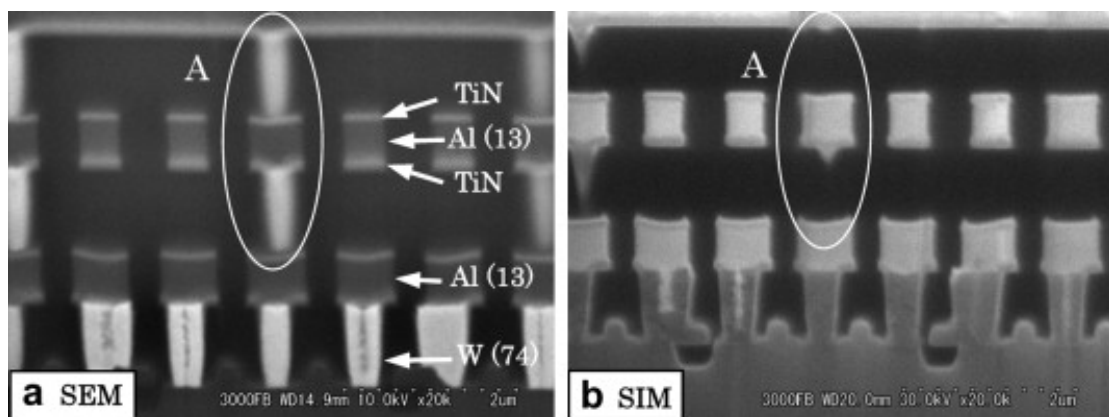


Figure 14 comparison between SEM (a) and SIM (b) imaging of the same sample

Resolution and surface detection:

- SIM imaging is more sensitive to the surface than SEM, because of the higher dimensions of the ions compared to the electron, so that they don't penetrate deep in the sample, but they give better information on the surface layers.
- In comparison, SEM imaging gives more information on the bulk structure of the sample.

Secondary electron behavior

Greater utilization of SIM images depends on understanding the secondary electron behavior under ion impact.^{31 32 33}

To understand deeper the theory behind the ion beam imaging, a small overview of the penetration behavior of the energetic ions has to be introduced.

Interaction between ions and materials is fairly complex: before being scattered out of the surface, an energetic ion may experience a large number of elastic and inelastic scattering events, producing all sort of secondary interactions, such as secondary electrons emission, auger electrons, photons and phonons and so on.³⁰

The range of this interaction varies according to the energy of the incident ions and the type of target material. It has been demonstrated that, for ion energy of 30keV, the interaction range is around 6 μm for a Si sample, and its reduced to 0.05 μm for energies of 1,5 keV.²⁹

- SIM

Bombardment of a solid surface by ions will cause secondary electron emission, due to the many secondary interaction processes.

After the SE are created, they can evolve with two processes: the first one is called potential emission, and kinetic emission.²⁵

The first one happens when the energy transfer from the incoming ions to the solid is more than twice the work function of the material. In this case the electrons may proceed through resonance neutralization and auger de-excitation or neutralization. However, for the Ga ions, this never happens because the ionization potential, around 6eV, is not twice the work function, that for metals is around 4-5 eV.^{25 27}

The second effect, kinetic emission, is the one happening for the Ga ion beam. SE are emitted in the solid with direct transfer of kinetic energy from the ions. If they are located near the surface, they may be emitted (if the transferred energy is enough to overcome the surface barrier). In general, the secondary electrons are created in the volume of the solid interacting with the ions. They subsequently migrate to the surface, and then, if their kinetic energy is higher than the surface barrier, they are emitted. The secondary electrons from the ion bombardment are therefore only different from the electron induced ones for the production stage.

Secondary electrons from SIM have considerably higher energy compared to the one from SEM; that is due, of course, to the difference in mass between ions and electrons.²⁵ In fact, when the initial impact takes place, the velocity of the electrons is 2 or 3 times higher than the one from ions. This causes a major difference in the free paths for excitation of an electron by primary ions or electrons. The maximum SE yield happens for primary ions it happens at hundreds of keV.

- SEM

For electron bombardment, the emitted electron can be divided in “true” secondary electrons, created during the secondary interaction of the processes, with energies below 50 eV, and the backscattered electrons (BSE), with higher energy.²⁵

Following the discussion above, the maximum SE yield happens for primary electron energies below 1keV.

As a result, we can say that, at energies of tent of keV, the SE yield becomes smaller with the increasing of impact energy for electron bombardment, and it goes the opposite way for ion bombardment.^{25 27}

The discussion about SE is important when talking about imaging, because it gives rise to the differences in contrast and sensibility to the surface between SIM and SEM images.²⁴

An example of application of FIB together with the modern SEM/STEM/TEM technology is the microscopy of FIB cross-sectioned specimens.²³

A focused ion beam has been used to prepare specimens with thickness of 0.1 μm for TEM. It is actually difficult to fabricate this kind of specimens, because of the defects present on the surface, which are hard to detect. With the FIB, however, it is possible to sputter away the failure in the TEM specimen preparation. A simultaneous observation with SEM of the failures and removal with FIB microscope can prepare very accurate TEM sample.²³

Backscattering

The phenomena of backscattering have also been accounted in the study of imaging.

- SEM

In general, if the sample is constituted by atoms with higher mass, the backscattering yields η for a scanning electron microscope is also higher.

- SIM

For ions, nevertheless, the backscattering yield is fairly low, way lower than electrons, for example, for Ga ions on Si target backscattering have never been shown. That is due, to the bigger mass of ions compared to the electrons.²⁸

Total path length

The total path length is defined as an accumulated path length along each zigzag trajectory of the electrons or ions stopped in the sample.

- SEM

There is little difference among the electrons, since their loss of energy during the collision with the material atoms are low, considering that

$$\frac{M_{target-atoms}}{M_{electrons}} \gg 1$$

Nevertheless, they are slowed down and deviated due to secondary effects (scattering with other electrons in the sample, generation of secondary interactions particles such as plasmons, photons and phonons).

- SIM

For ions, conversely, the large mass implies that the larger the ion deflection angle, the larger the energy loss. Thus the ion range after scattering becomes short on average. If the energy transferred from the ion to the target atom exceeds the threshold energy, the atoms in the target will get displaced, causing second interactions that lead to lattice damages and sputtering.²⁸

2.2. Theory of milling processes

The goal of nanofabrication is to build nanoscale structure, in the range of 0.1 to 100 nm, in large quantities and potentially low costs. The FIB milling has become very popular for this application. It has in fact many advantages compare to other energetic particle beams in nano fabrication, for example ions are heavier than electrons, and they can strike target with higher energy and relatively short wavelength, to transfer patterns on hard materials, such as metals, with less forward and backscattering.²⁸

On the other hand, the interaction between the ions and the material has to be considered carefully.

Two basic schemes of fabrication, projection printing and direct writing, are used to fabricate nanostructures with this techniques. In the first one, a collimated bean of ions passes trough a stencilling mask, and the image of the mask is projected on the substrate using electrostatic lens systems. In the direct printing, on the other hand, a small spot of the focused beam is used to directly pattern the surface, without any masks.²⁸

Milling is a sub process in the direct writing category, and it will be analysed further. It is in fact the process used for the fabrication of the stencilling masks.

The milling process is a pure physical interaction between the energetic ions and the target material, and it is a combination of physical sputtering, material redeposition and amorphization. Without any doubt, the most important of this interaction is the sputtering, in which the energy transferred from the ions to the targeted substrate is high enough

leading to a collision cascade involving substrate atoms on or near the surface to cause material removal.²⁸

The FIB is using liquid metal ion sources (LMIS), which produce a beam of heavy ions that can be focused into fine spots (10nm) with adequate current densities for direct writing. The metal sources currently used in FIB technology are many, for example Al, As, Au, Ga, Ge, Fe and others. In our case, a gallium source is present.³⁵

Once the focused ions hit the substrate, as said above, the kinetic energy transfer from the ions to the atoms in the material is happening, and eventually this energy allows the atoms to escape the surface barrier and being ejected from the target, in a typical sputtering process.

An idea of the efficiency of the process is given by the sputtering yield.

It is possible to predict the sputter yield with software, using models such as the Monte Carlo one, and they can provide a distribution of the ions and the kinetic phenomena associated with the ion's energy loss. They can also predict information about target damage and phonon production, ionizations and other secondary effects.²⁸

The sputter yield is found to be dependent on the incident angle of the ions, and the target material. In general we can say that heavier ions sources or lower surface binding energy of the atoms in the target can produce high sputter yield.^{36 37}

Moreover, the sputter yield level off or decrease for ion energies higher than 100keV, where the implantation becomes dominant, and ions penetrate too deep in the target and get trapped in the lattice.^{36 37}

In an ideal milling, only the sputtering interaction is present. Unfortunately, other interactions like material redeposition and amorphization gives problems in obtaining a precise mill pattern.²⁸

Since the ejected atoms, released in gas form, are not in their thermodynamic equilibrium, they tend to condensate back into the solid phase upon collision with any other thing nearby.²⁸

Therefore, for example in trench milling, the collisions with the sidewalls of the channel will make the atoms redeposited on these walls.

The redeposition depends not only from the scanned area, but also from the geometry of the milled pattern.²⁸

In case of a too low energy of the incident ions, amorphization may occur instead, where the incident ions are buried in the target material and may also displace the target atoms from their lattice site, creating mismatch.^{38 39}

Milling, if well performed, can produce very precise nanostructures.

Another key issue while milling nanostructures is the heating of the target.

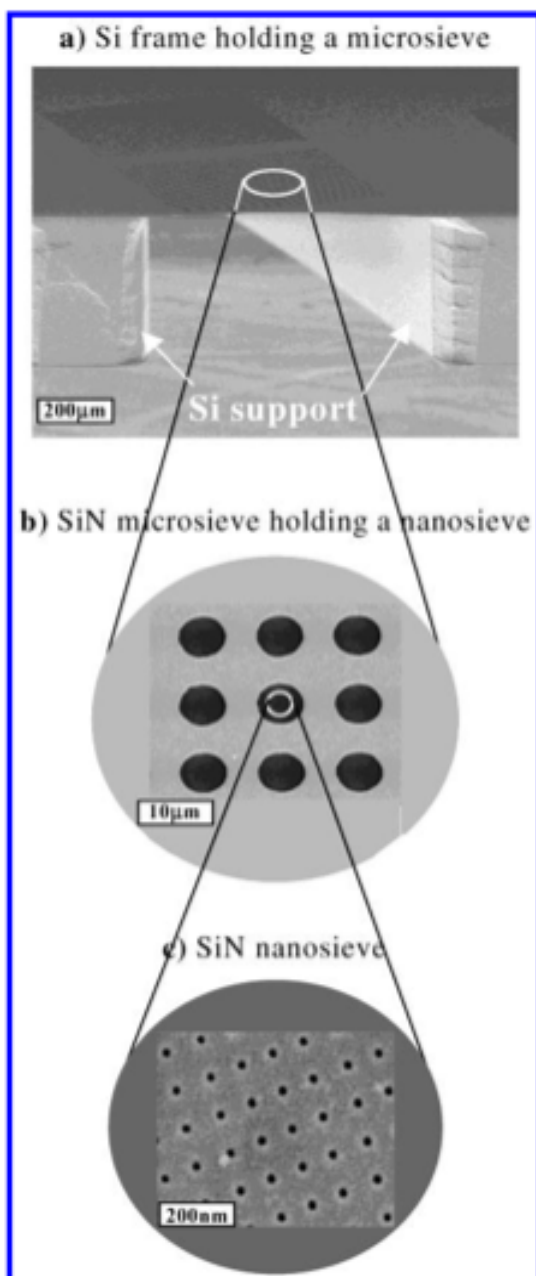
The bombardment of the sample with a high-energy ion beam is causing, of course, heating in the target material, due to the kinetic energy transfer.

According to the literature, this heating can cause defects in the crystalline structure of the material and heat spikes.²⁸

The right way to estimate, in a pessimistic view, how much heat we will have on the sample is to suppose that all the energy of the ion beam is converted in heat.

So the heat can be relevant depending on the mass of the ions, the density of the target, the milling pattern and, of course, and the incident energy.

2.2.1. Milling of silicon nitride membranes



A topic of particular interest for this project is the milling of nano patterns on silicon nitride membranes. Experiments on these devices have already been carried on widely in different labs.

In the literature we can find reports where milled patterns by scanning ion microscope are investigated by atomic force microscopy and the key parameters, such as the relation between the ion doses and milling depth is measured.⁴⁰

We have, for example, for helium ion microscope, that milling depth varies linearly with beam dose, resulting in a straightforward method of controlling local film thickness.⁴⁰

A potential application of this milling control is local thickness manipulation of freestanding membranes.⁴⁰

One of the applications for such an array is that fluid can be filtered against larger particles with a relatively high flux in comparison with an array of nanochannels.

The low stress silicon nitride (Si_3N_4) membrane are chosen for several reasons, such as the availability of Si_3N_4 membranes after standard microsystem

Figure 15 SEM overview with a close-ups for the nano sieve membranes⁴³

processing such as KOH etching of a silicon support and the thermal stability and chemical inertness of Si_3N_4 material. So far, electron beam lithography followed by reactive ion etching (RIE) or FIB etching have been used to create pores in the Si_3N_4 membrane. Because the suspended Si_3N_4 membrane should survive handling during the fabrication process and application, its thickness should be made adequate; however, thicker membranes limit the capability of direct drilling nanopores with FIB.^{41 42 43}

The membranes thickness has to be a good compromise, in order to favorite a precise drilling without sacrificing the strength and perforated area.^{41 42 43}

The successful fabrication of strong Si_3N_4 nanosieve membranes with a small and uniform pore size has been documented. The essence of the method is the micromachining of an ultrathin nanosieve within a thin supporting microsieve using FIB with the smallest possible beam current to drill the holes. In this way, uniform pores as small as 25 nm were drilled.^{41 42 43}

As said in the papers, the key point of the milling of Si_3N_4 membranes is to achieve the right thickness of the membranes, so that it is possible to mill precise and small patterns without breaking and bending the membranes.⁴⁴

For doing this, a good investigation of the parameters of milling has to be carried on. For example, working on the beam current of the ion beam, is possible to optimize the process. The parameters and the pattern combination used for our process will be presented and analyzed in the chapter regarding the fabrication.⁴⁴

For now we can just affirm that Irradiation of a silicon nitride membrane with a focused gallium ion beam may lead to cracking and bending of the membrane, especially near the stress points, typically corners and longer feature of the patterns.⁴⁴

This bending, nevertheless, can be used in fabrication of nanopores and atomic force tips.

Chapter 3 Membranes fabrication

3.1 Cleanroom techniques: standard process overview and reasons for membranes fabrication

One of the key points of the process was the usage of Si_3N_4 membranes as stencilling masks and to screen the graphene flakes during milling.

In the beginning, these membranes were ordered from the external company Protochips, and they can be pursued with a maximum thickness of 200nm, with a window size of 1x1 mm. (Figure 16)

This membranes, however, presents some issues for the purpose of our process:

- The holder around the actual Si_3N_4 window has dimensions of is too small, and implies substantial difficulties in handling and aligning the membranes with the graphene flakes.
- Furthermore, the attachment of the membrane to the graphene sample is tricky, again because of the size of the handler

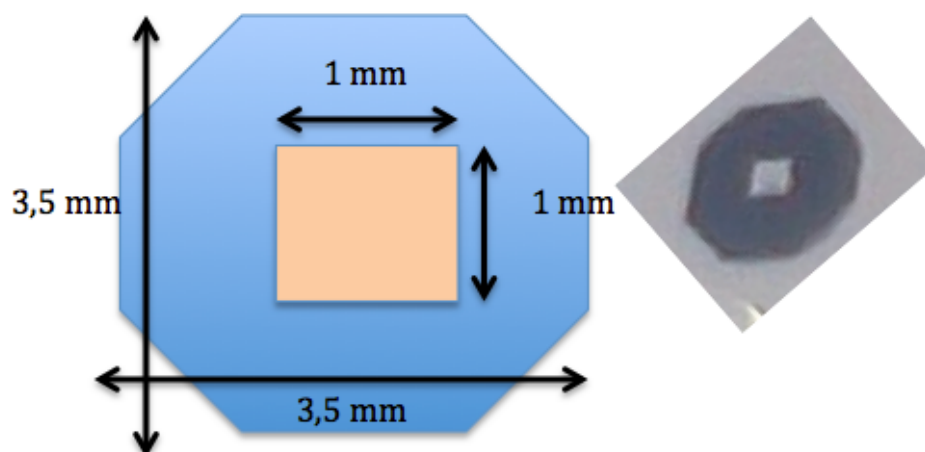


Figure 16 Membrane ordered from Protochips, with scheme of dimensions

- The fixed thickness of 200 nm limits the milling possibilities, since only some pattern structure can be milled on them without experiencing bending and breaking of the membranes.
- This membranes may be bended or curved from the fabrication, and can therefore have an internal stress that is specific for each sample, and hard to

predict. This factors limit the working environment, in terms of the kind of patterns that is possible to draw without damaging the membranes.

More suitable membranes made of low stress Si_3N_4 , with variable thickness of the nitride layer, and larger frame holder would be best suited to the process.

For that reason, it has been decided to design a fabrication process in the cleanroom, in order to have 400nm thickness membranes with an holder of 1cm^2 approximately, that should be easier to handle while aligning the graphene.

Furthermore, production of membranes of 150nm thickness have been carried on, in order to confront the properties of this kind of devices with the old membranes, and see if the quality of our low stress nitride is better. If it is, in the future, will be more profitable to produce out silicon nitride membranes, every time we need low stress devices.

The main goals of our the fabrication are:

- To product low stress membranes, that can be milled with a standard set of parameters with a percentage of success of more than 75%.
- Having samples with larger holder, that will facilitate the alignment and the attachment to the graphene wafers.
- Obtaining higher thickness, but having membranes that are still transparent enough to ensure the possibility of a good alignment with graphene flakes.
- The devices should be stronger and more stable than the previous ones, to prevent destructions during, for example, handling with tweezers.

In this way we hope to be able to determine standard parameters for the milling process, and to be able to pattern the predetermined designs with a high ratio of success. Furthermore, more stable membranes will allow the usage of the devices for more than one contact deposition.

The cleanroom process fabrication is pretty standard, and it is following the preselected cleanroom recipes. The global overview of the standard recipe is reported in appendix, but some steps are presented below, to give an idea of the fabrication process.

Of course, this original recipe was performed some times before having a satisfied result, since the process parameters has to be optimized.

Some of the issues and optimizations are presented below, while the global process recipe is shown in appendix 1

The low stress nitride furnace

First of all, a layer of low stress Si_3N_4 has to be deposited on the double polished Si wafers.

LPCVD nitride can easily be deposited in a reproducible, very pure and uniform way. This leads to layers with good electric features, very good coverage of edges, high thermal stability and low etches rates. However, high temperatures are necessary for deposition and reaction rate is slower.

Parameters:

Table 1 deposition time for Si_3N_4 deposition

	400 nm	150 nm
Time of deposition	2h 30 min	1h

For the 400 nm, however, two depositions of 1 hour and 15 minutes each are needed in order to let the nitride relax in between.

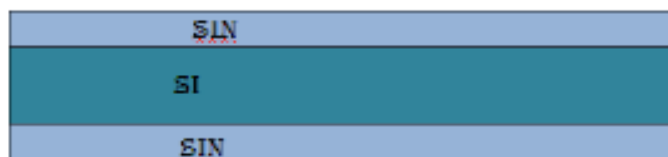


Figure 17 schematic drawing of the sample after processing in the SiN furnace

Lithography process

The starting point is spinning the AZ5214E resist on our samples, with the standard recipe for 1,5 μm thickness resists in the SSE spinner in the cleanroom.

Exposure process has been performed with KSaligner, with an exposure time of 10s. The outline of the mask use is shown, and it is the masks for fabrication of TEM samples.

Developing of the resist has been done using standard recipe in the wet bench.

A final cleaning with the plasma Asher for 2 minutes has been performed.

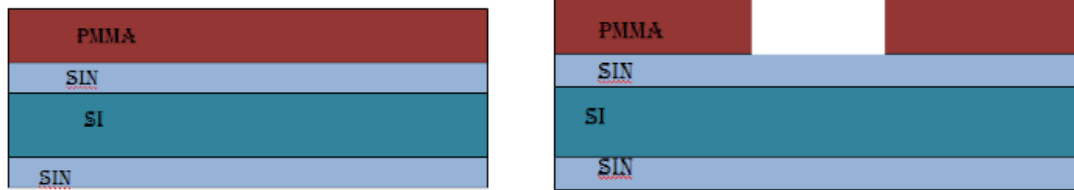


Figure 18 schematic drawing of the sample after lithography

RIE etching

Reactive-ion etching (RIE) uses chemically reactive plasma, generated under vacuum by an EM field, to remove material deposited on wafers.

The High-energy ions from the plasma interact with the wafer surface and etch away the materials.

Table 2 etch time for RIE etching, depending on the thickness of nitride layer

	400 nm	150 nm
Etch time for Si ₃ N ₄ etching	17 min	10 min

A standard recipe for Si₃N₄ etching has been used

Cleaning procedure before KOH etching

A critical passage in the process was to find an optimal cleaning, to completely remove the residues of chemical resist before KOH etching. In fact, if any resist is left on the wafer, it will contaminate the KOH bath.

From the literature and 4 different trials, we have got an optimal cleaning procedure:

- 40 minutes in plasma Asher
- Standard cleaning in the 7up bath.



Figure 19 schematic drawing of the sample after RIE etching and resist removal

KOH etching

This is probably the most critical step of the whole fabrication process.

Thirty seconds exposure in BHF prior the etching are also suggested to achieve sharper pattern edges.

Then, to calculate the right time for the etching, measurements of the etched Si have been performed periodically during the etch:

Table 3 Etch time and depth for KOH etching of Si

Time (h:m)	Measured etch step
2:00	170 μm
4:00	350 μm
5:00	440 μm
6:00	520 μm
6:30	Complete etch

A calculated time of 6h and 30 min is needed to etch completely trough the Si layer of 567 μm .

With a final rinse in water and spin dry the samples are ready to use.

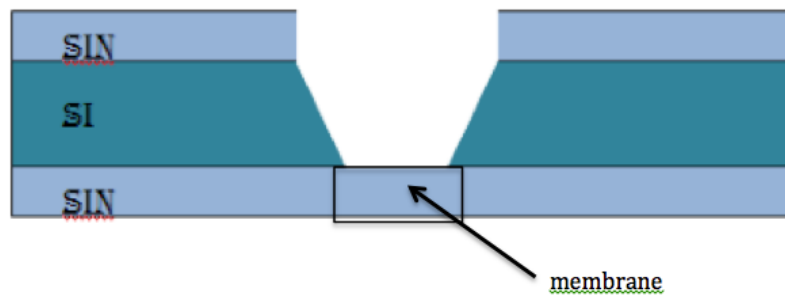


Figure 20 final sample

3.2. Membranes design

For imprinting the design of the membranes shape on the Si_3N_4 wafer, we have used photolithography. The mask used in this process already a mask in use in our research group, to fabricate TEM grids.

The mask design is shown in Figure 21.

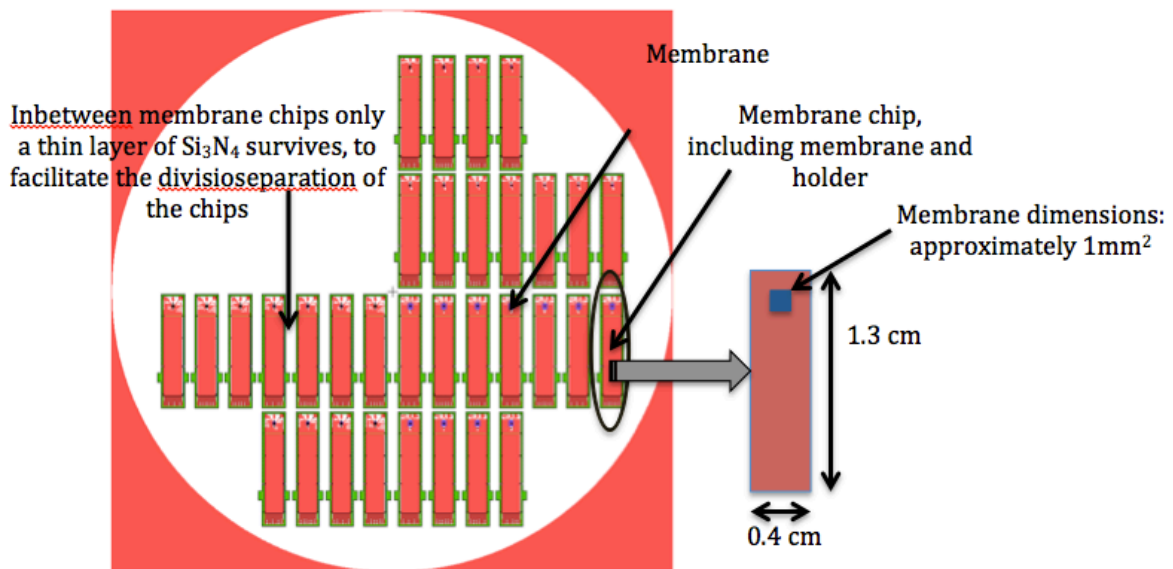


Figure 21 scheme of the lithography mask for Si_3N_4 membranes fabrication (left figure) and zoom of the membrane chip design (right figure)

As it shown, it is possible to get more than 20 working membranes from the same wafer, and this is very practical in term of manufacturing.

The samples are fabricated in a way that, in-between membrane chips, only a thin layer of Si_3N_4 survive, and that makes very easy to split the membranes, just by applying a mechanical stress with tweezers.

3.3. Characterization and results

Some trials have to be made before optimizing the process and obtaining some working devices, working mainly on the fabrication issues described above in section 3.1.

Basically the critical steps are the deposition with the LPCVD furnace and the KOH etching.

In Figure 22 is possible to see how a bad nitride deposition, with particles contamination, can cause pinholes in the final structure, once the KOH is performed

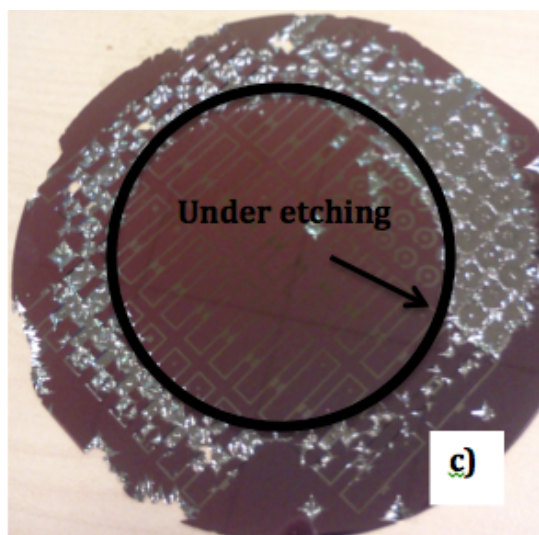
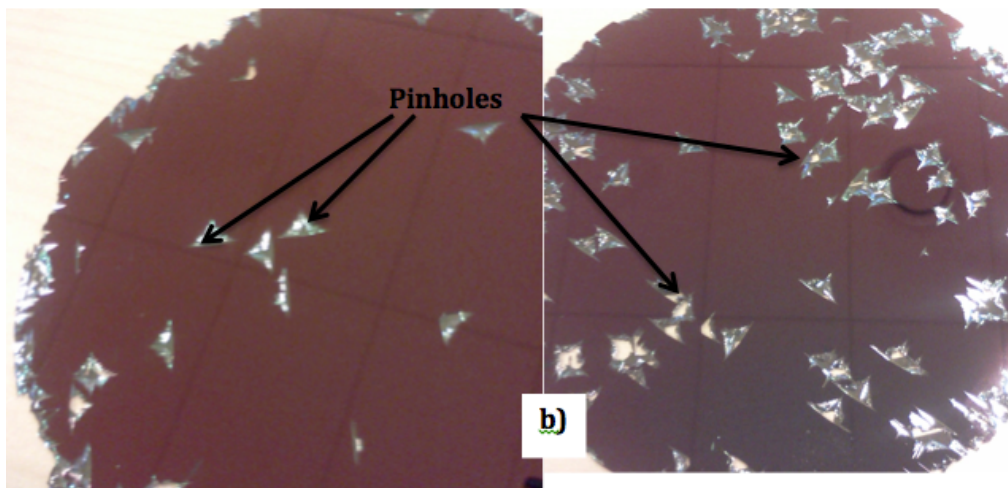
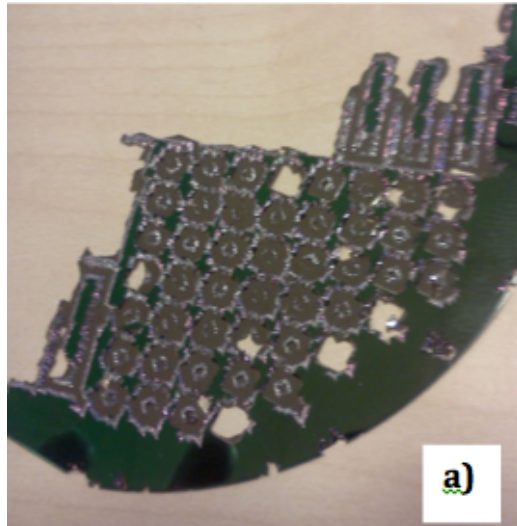


Figure 22 Failures in membranes fabrication: a) misalignment of the mask with the crystal orientations of the sample and subsequent overetching and destruction of the sample b) pinholes in the structure caused by particles contamination during the nitride deposition c) too short time in the KOH bath cause underetching: the structure is not defined in the Si wafer.

Finally, I have succeeded in fabricated two different kinds of membranes using two different LPCVD furnaces for the initial layers of Si_3N_4 . The initial project was for fabrication of

respectively 150 nm and 400 nm thicknesses; measuring the effective thickness with the filmtek, we have achieved values of 220nm and 409 nm.

A wafer of membranes can be seen in Figure 23.

The final chips can be separated mechanically by gently bending the wafer or using tweezers.

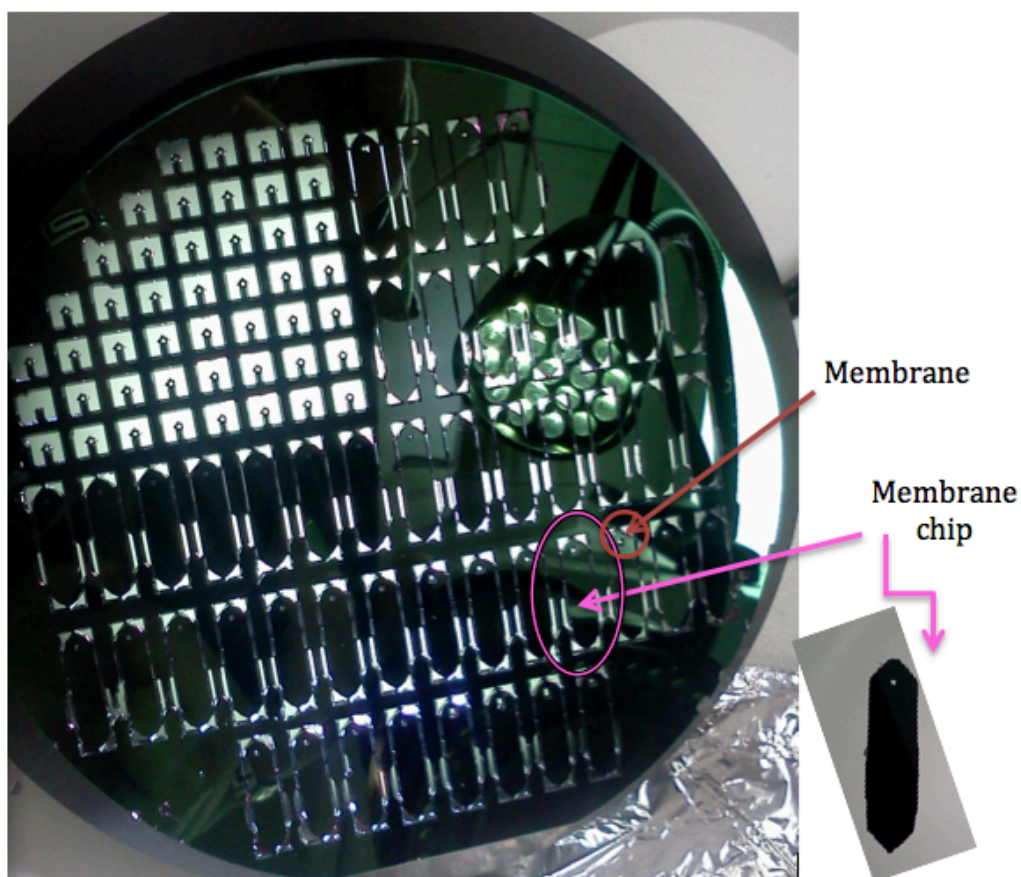


Figure 23 successfully fabricated membranes; they can be divided by mechanical pressure.

We get that approximately 9 membranes out of 10 on the chip are suitable to be used for the fabrication of the stenciling masks, since anyway some of them may be not totally open or transparent, so not suitable for our purpose, due to fabrication errors.

Nevertheless, issues with cracking and breaking is still present; we can however get some conclusions by the experiments:

- Handling this type of membranes is way easier. In fact, even the thinner membranes, of only 150 nm thick, are not getting broken during handling, even if they fall or the tweezers touches them.
- The bigger holder facilitates the managing, the alignment and the attachment of the new membranes on the graphene samples. The same membrane, on which a stencil pattern has been milled, can also be used repetitively to deposit contacts.

- It is proved in literature that the smaller the membrane windows, the higher the strength of the membrane.⁶⁶ Since this new devices have a windows size that is slightly smaller than the previous one, they should be more stable and harder to break or crack.
- In observation with tilted SEM, it is possible to see that the membranes are flat: no deformation could be detected. Therefore they suit our purpose better than the older membranes, where it was possible sometimes to see, even without tilting the sample, some bending in the membrane window. The flatness of the membrane is in fact important during the contact deposition: in order to have an uniform pattern transfer, the stenciling mask and the sample should be closer, and at the same distance all over the deposition area.⁶⁶
- Nevertheless, sometimes the newly fabricated membranes, especially the one with 400nm thickness, are not transparent enough, and this makes difficult to individuate the graphene flake under them, and raise issues with the alignment.

In conclusion, however, we may say that the fabrication of homemade membranes it is worthy, since it gives us the possibility to control the thickness of membranes, and to handle them easier. They are therefore more suitable for the purpose of this project.

Chapter 4 Devices fabrication

4.1. Introduction to nanostencil

Nanostenciling lithography is a pattern method that uses perforated membranes (nanostencil) to shield substrate from material flux during deposition on a substrate. Practically, the stenciling mask is working as a shadow mask, shielding during deposition of structures, in our case metal contacts on graphene devices. The structures created with this method can be in the 10-100 nm scale.⁴⁴

Fundamental requirements for this process are a small distance between the stenciling mask and the sample, a reduced thickness of membranes and large distance to the evaporation source. In this way, the deposited pattern will resemble the perforation on the membrane.⁶⁶

The advantages of this technique are many, for example that the surface of the sample stays clean, since is shielded by the membrane, and no materials has to be removed after deposition.⁶⁶ Therefore, fragile samples, that would not survive a lithography process, can also be patterned. Furthermore, a great deal of possibilities will arise if the normal nanostencils is combined with the use of different evaporation sources, with movement of the sample during deposition or with microactuator shutters (active nanostencils).⁶⁶

In this project, the fabrication of stenciling mask is performed using focused ion beam technology, already described in chapter 2.

The main advantage for nanofabrication of using focused ion beam is that gives the possibility to modify directly the structure surfaces, while in nanolithography the use of a mask is needed. Besides, the fabrication of real-time 3D device prototyping has become possible. Also, the possibility of combine focused ion beam and electron beam optics allows a real time observation and analysis of the milling process, and therefore a more precise control of the structures compare with lithography.⁵⁰

The standard lithography process use in our nanointegration group for graphene contacts fabrication, in fact, consists in a step process as shown in Figure 24.

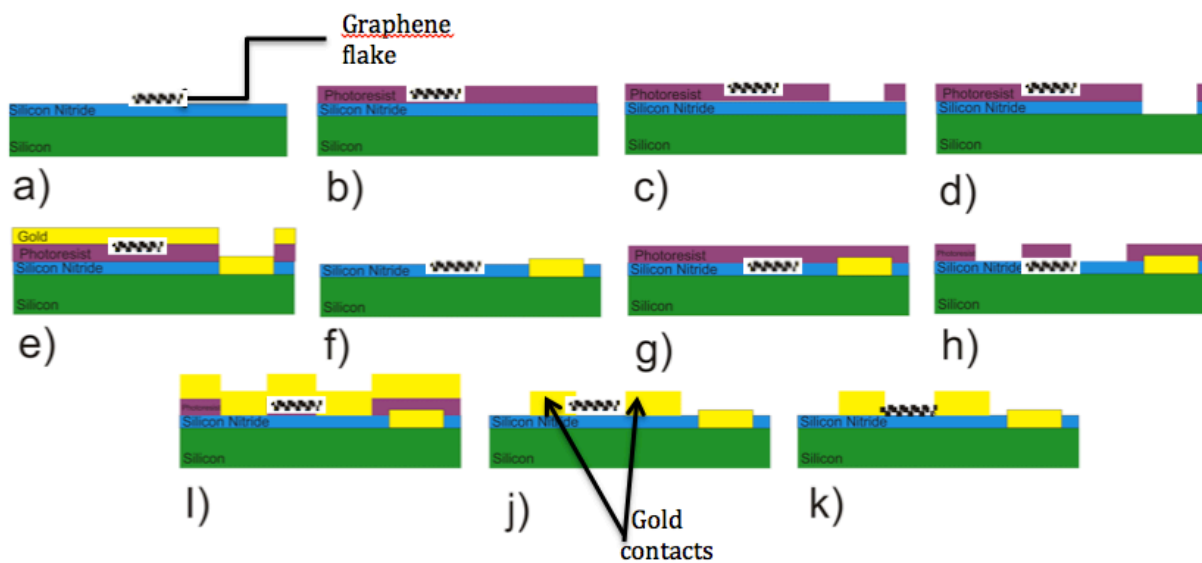


Figure 24 steps for fabrication of graphene contacts with lithography⁶⁷

The basic steps are

- a): Silicon/silicon nitride substrate is cleaned.
- b): Layer of Photoresist applied.
- c): Photoresist is patterned.
- d): Silicon nitride is dry-etched.
- e): NiCr/Gold evaporation.
- f): Removal of photoresist, then we have the ground contact
- g): Layer of photoresist applied.
- h): Patterning of photoresist.
- i): NiCr/Gold evaporation.
- j): Removal of photo resist.
- k): Completed substrate with gated and non-gated electrical contacts.⁶⁷

The main disadvantage of this process is that the graphene on which the contact is fabricated will be spread with the chemical resist, that may contaminated it and compromise the electronic properties. Some disadvantages of the standard method have already been described in the section above.

With nanostenciling lithography, on the other hand, is not necessary to use photoresists, and a non-contact fabrication is possible. That limits the contamination and makes this method applicable to surfaces that are mechanically unstable, like membranes or cantilevers.

The only font of contamination in this case may be the Ga ions that could get trapped in the graphene structure.

The disadvantages of this technique are due to the fact that the structure deposited through the nanostenciling mask depends on the aperture size and the gap between mask and substrate. During the evaporation of the material, some effects can occur that will affect the gap, and modified the shape of the deposited pattern. One effect is for example the clogging, where the opening in the mask will slowly be reduced and eventually closed by the evaporated material.

Moreover, the residual stress in the evaporation material can affect the membrane, causing deformation that will change the distance between the mask and the substrate, influencing the resulting pattern.

4.2. Milling of the Si_3N_4 membranes

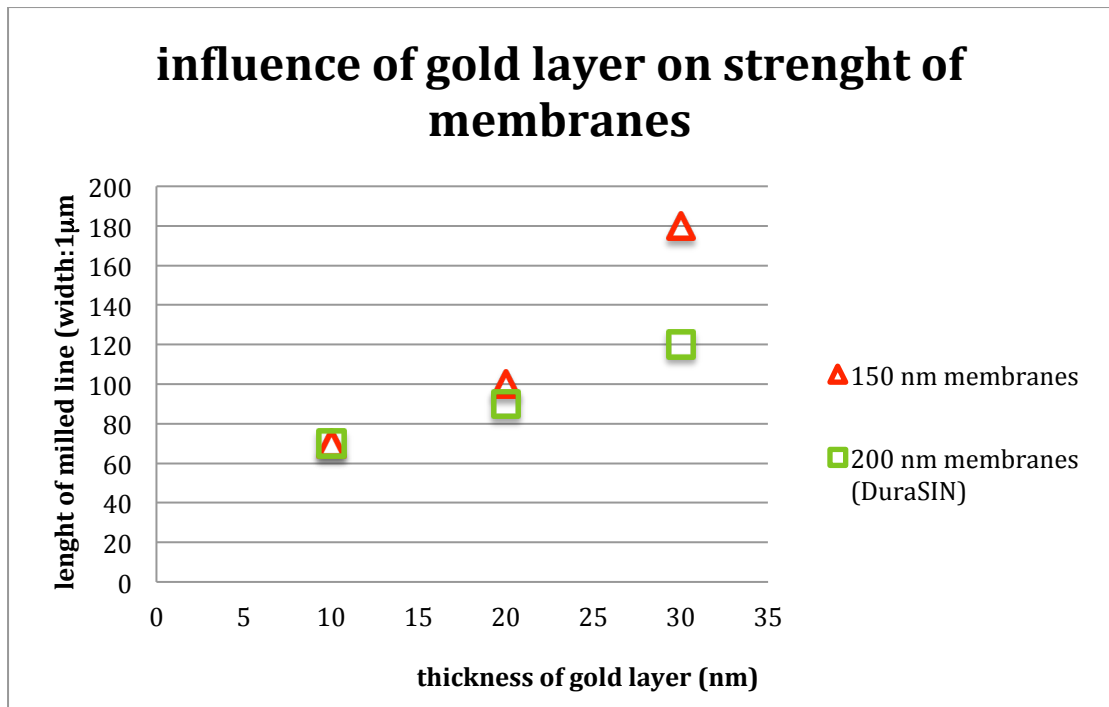
For the milling of the membranes, the Focused Ion Beam microscope Quanta 3D from the Centre for electron Nanoscopy in DTU has been used. This microscope consists in a typical combination of an ion beam microscope and an electron microscope for the real time observation of the process.

Before the milling, the Si_3N_4 membrane has been covered with a thin layer of gold, using the sputtering machine shown in fig. 20, in order to make them more stable, and get rid of charging. The thickness of the gold film is between 10 and 20 nm.



Figure 25 cressintong sputter for gold deposition

The gold layer is influencing the milling, in fact is increasing the strength of the membranes. Some data are presented below:



As it is possible to see, especially for the membranes fabricated in our laboratory, the gold layer is very important, and it can increase considerably the milling possibilities. Nevertheless, a too thick gold layer may compromise the transparency, and rend the alignment very difficult.

In the beginning, some experiments have been carried on to calibrate the microscope parameters suitable for our experiment and to better choose the pattern to mill on the membranes.

Simple features have been milled with different currents, and they are reported in Figure 26.

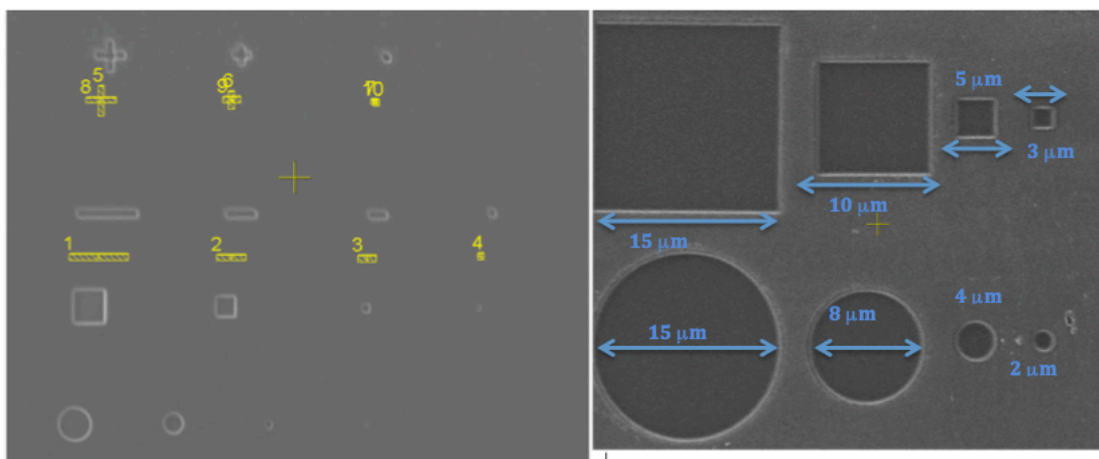


Figure 26 Simple pattern trials. fig a) cross of respectively 4x1, 3x1, 2x1 and 1x1 μm bars crossed with 90°angle, bars of 4x1, 3x1, 2x1 and 1x1 μm, squares 4x3, 3x3, 2x2, 1x1 μm and circle with 4, 3, 2 and 1 μm diameters. b) Squares and circles

Subsequently, the patterns for the actual milling of the stencilling mask have been drawn.

The patterns are shown below

Pattern for single metal line deposition (a) and two point probe contacts deposition

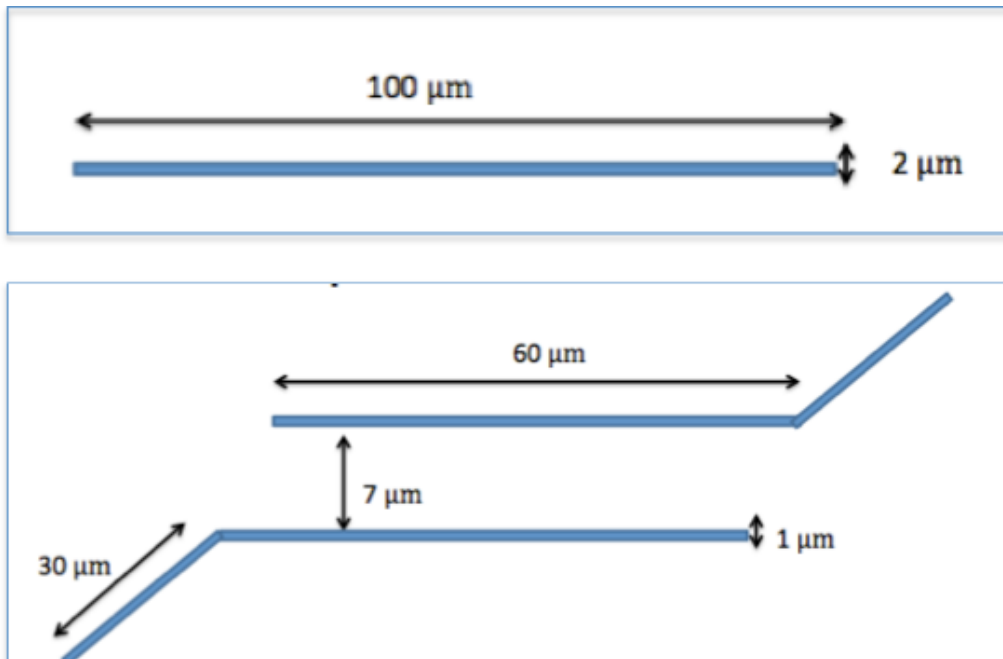


Figure 27 single line and two point probe contact mask

Pattern for four point probe contacts deposition

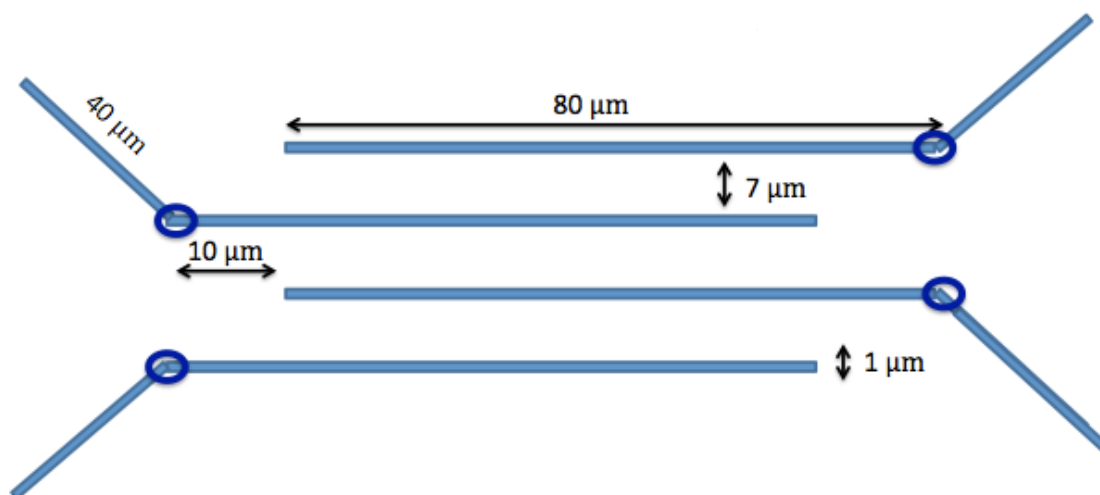


Figure 28 comb fingers pattern for stenciling masks fabrication

The requirements for the patterns for stenciling masks are:

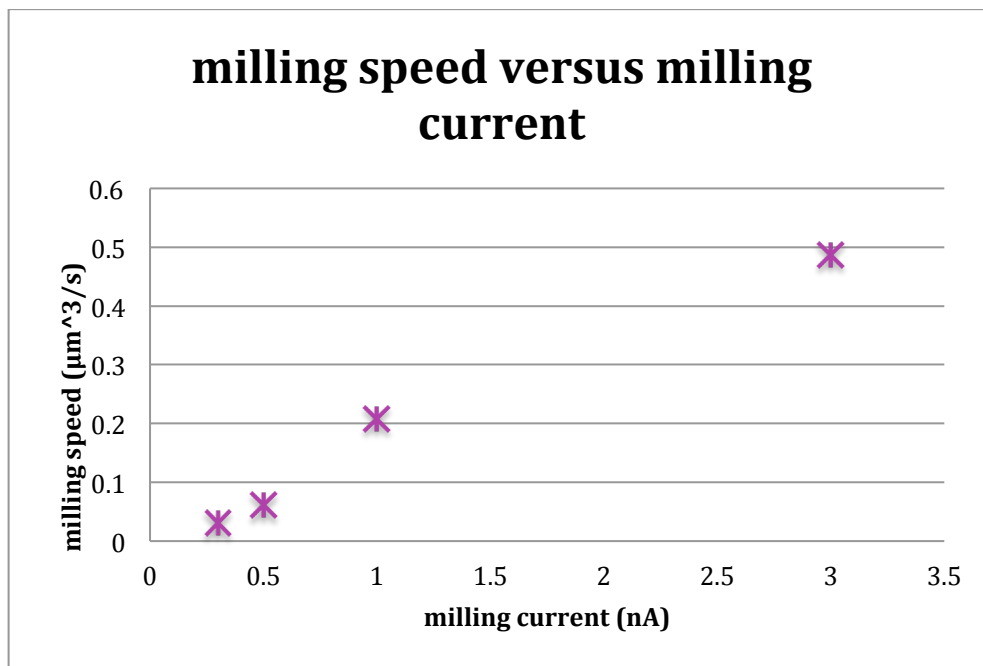
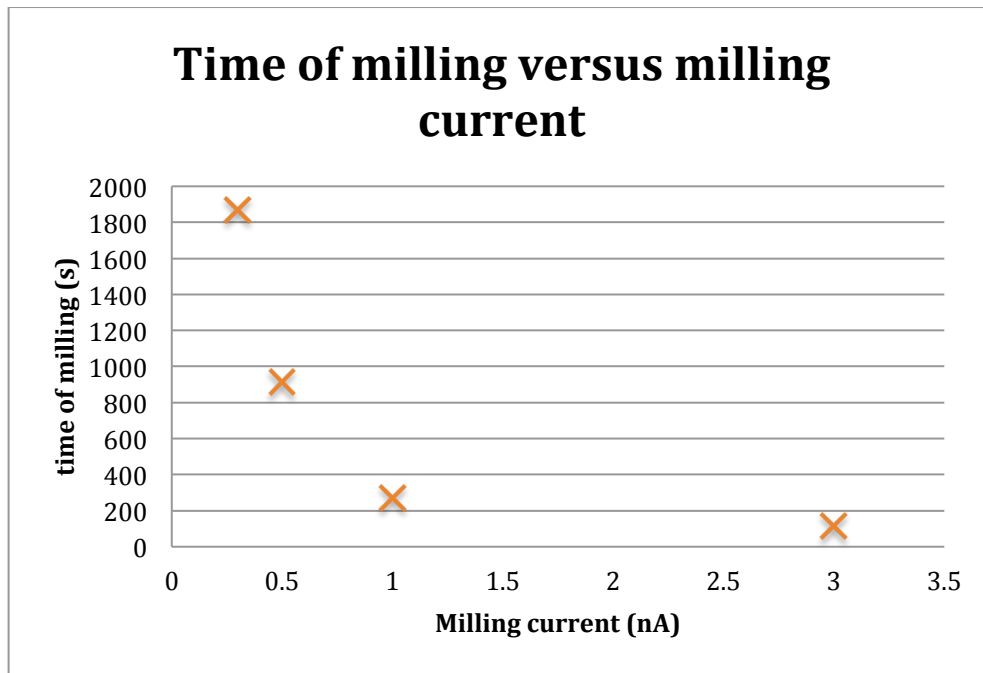
- **Size:** they should be small enough in the vertical direction, in order to not overcome the graphene flakes size. Typical flake sizes are between 20 and 40 μm .
- **Shape:** the milled lines should be narrow and sharp, to allow precise metal contacts on the flakes
- **Critical features:** The tilted lines should be long enough to permit the overlap of a contact pad mask, but their length is limited by the focused ion beam milling, in the sense that lines longer than 40 μm tend to cause breaking and collapsing of membranes.
- **Milling current:** it has been varied between 0.5nA and 2 nA; It has been shown that the long lines, if milled one by one, can be milled with no breaking at 1 nA, while it is necessary to mill the tilted features at 0.5 nA. The circular points of stress relieve have diameter of 3 μm , and they can be milled at 2nA.

In order to have a better understanding of the milling process, the milling speed to remove material has also been investigated.

In the graph below, both the time of milling and the milling speed are shown, in relation with the milling current.

Table 4 time of milling and milling speed for different milling currents

<i>Milling with 10nm gold layer</i>		
<i>Line: length 70 μm, width 1μm</i>		
<i>Milling depth 800 μm</i>		
<i>Total material milled:</i>		<i>56 μm^3</i>
<i>Milling current (nA)</i>	<i>Milling time</i>	<i>Milling speed ($\mu\text{m}^3/\text{s}$)</i>
0.3	0:31:10	0.029
0.5	0:15:12	0.061
1	0:04:30	0.207
3	0:01:55	0.486



As we can see, the milling speed tend to increase when the current increase. That means, higher current allows a faster removal of material, so it can be advantageous for a quicker process. Nevertheless, faster milling can lead to more defects and there is the risk of more contamination, since higher energetic ions will remain trapped easier in the material.²⁸

It has been shown from our experience that the milling speed does not vary significantly for different pattern.

4.2.1. Issues and stress points: empirical studies on membranes stress and comparison between different kind of membranes

Since the milling process is the key point of the process, an careful observation of the stress of the membranes, and of the differences between the membrane pursued from Protochips and the fabricated one has to be done, in order to have a clear overview of our possibilities and to chose the best pat for future fabrications.

Some milling trials have been performed on both membranes, milling the patterns that will be useful for the future development of this work, trying to push them to the limit break point and studying the way in which breaking and cracking occurs.

Proceeding empirically to achieve data on the membrane usage possibilities, we have collected quite a few results, some of which are presented below:

MILLING TEST ON 200 nm PROTOCHIPS MEMBRANES:

- Milling of long, thin lines:
 - Lines width: 1 μ m
 - Gold layer deposited on top: 10nm

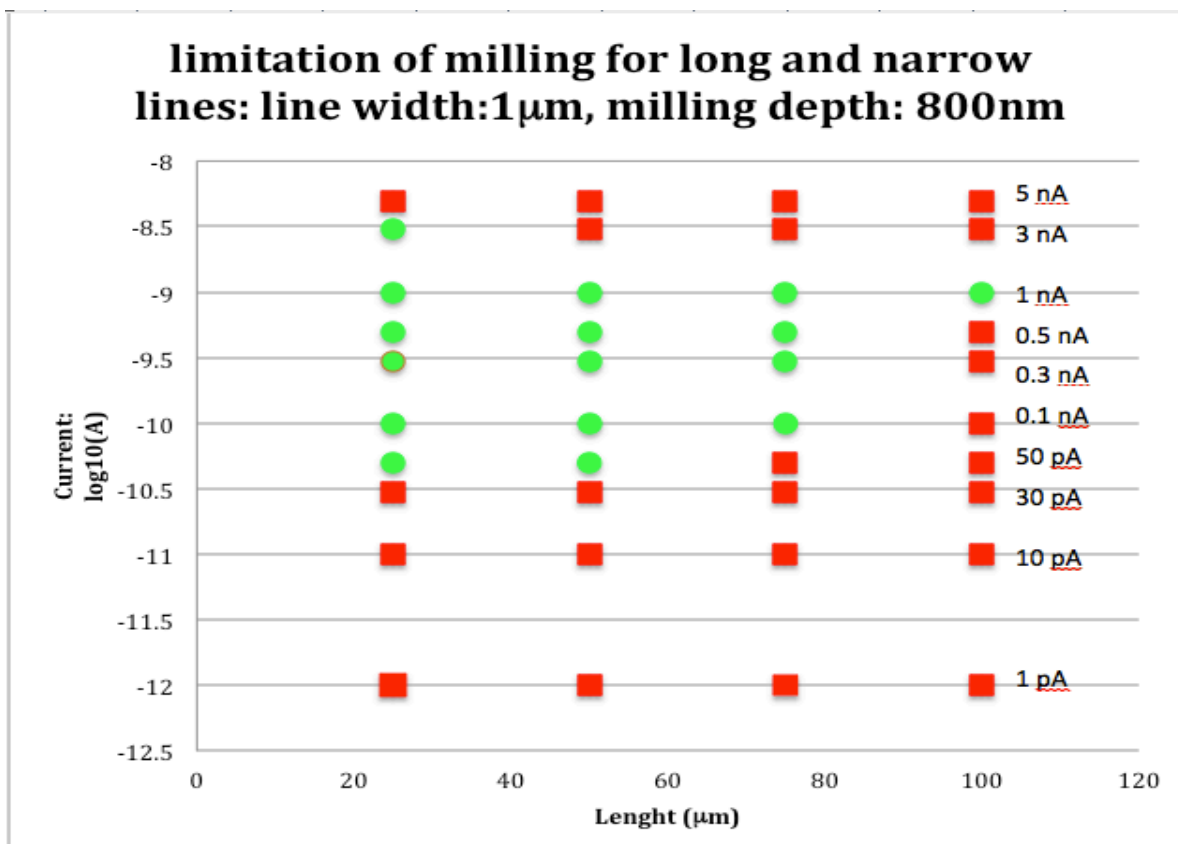


Table 5 data on milling of thin lines, milling depth set to 800 nm, 200nm membranes

Line length	Milling current	Result	
20-30	1pA-30 pA	Fail	Not milled trough
	50pA-3nA	Succeed	Milled
	More than 3nA	Fail	Breaking
40-60	1pA-30pA	Fail	Not milled trough
	50pA-1nA	Succeed	Milled
	More than 1nA	Fail	Breaking
70-80	Less than 0.1 nA	Fail	Not possible (too small pattern for too small current)
	0.1nA-0.5nA	Succeed	Milled
	More than 0.5nA	Fail	Breaking
90-130	Less than 1nA	Fail	Not possible (too small for too small current)
	1nA	Succeed	Milled 50% times, otherwise breaking
	More than 1nA	Fail	Breaking

Overview of critical dimensions for simple features (Protochips membranes)

Table 6 overview of critical dimension patterns on 200 nm membranes

Old membranes Milling extreme possibilities (tested with quanta 3D)	
Smaller hole diameter:	400nm
Longest 1µm thick lines:	130 µm if parallel to border
	40 µm if tilted
Thinner line	400 nm
Smaller distance between long lines:	3 µm
Critical corners:	30° (with stress relive circles of 3µm diameters)
Higher "safe" current:	0.5 nA for most of the patterns
	1nA for small and simple features (circles and short lines)

As it is possible to see, the fragility and the unpredictable behavior of the Si₃N₄ membranes represent a major issue, since they make the process not reliable to reproduce using standard parameters.

Furthermore, as said before, these membranes have quite small supports, of approximately half a centimeter, that makes the handling and the aligning of the devices with graphene flakes quite tricky and hard to perform.

Tests on the stress of the new membranes has been performed, with the same procedures used for the old membranes, and it has been shown that it is actually possible to obtain better results from the stress tests:

MILLING TEST ON 150 nm MEMBRANES:

- Milling of long, thin lines:
 - Lines width: $1\mu\text{m}$
 - Gold layer deposited on top: 10nm

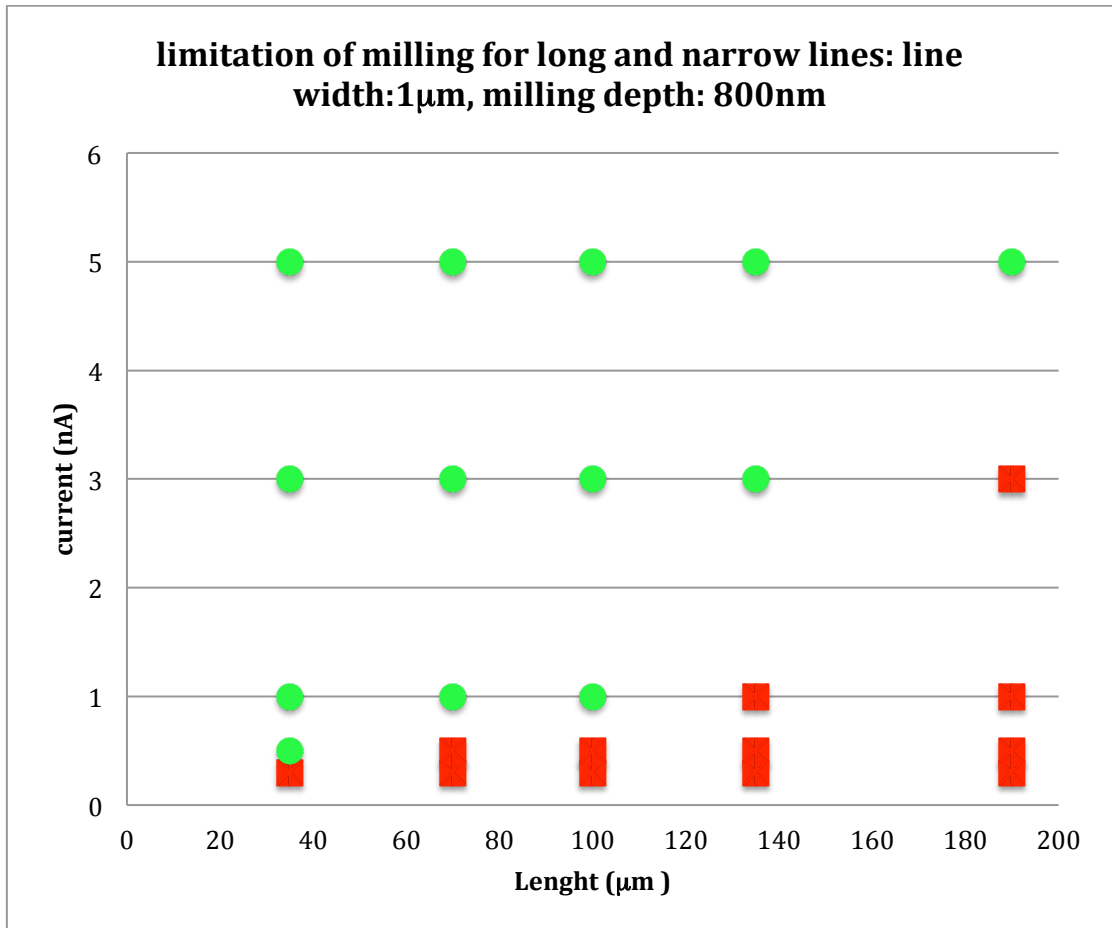


Table 7 data on milling of thin lines, milling depth set to 800 nm, 150nm membranes

Line length	Milling current	Result	
20-50	≤ 0.3nA	Fail	Not possible (too small pattern for too small current)
	50pA-3nA	Succeed	Milled
50-90	≤ 0.3nA	Fail	Not possible (too small pattern for too small current)
	50pA-1nA	Succeed	Milled
70-80	≤ 1nA	Fail	Not possible (too small pattern for too small current)
	0.1nA-0.5nA	Succeed	Milled
90-130	≤ 3nA	Fail	Not possible (too small for too small current)
	5 nA	Succeed	Milled 50% times, otherwise breaking

Overview of critical dimensions for simple features (Cleanroom membranes)

Table 8 overview of critical dimension patterns on 150 nm membranes

New fabricated membranes Milling extreme possibilities (tested with quanta 3D)	
Smaller hole diameter:	200nm
Longest 1µm thick lines:	190 µm if parallel to border
	70 µm if tilted
Thinner line	300 nm
Smaller distance between long lines:	3 µm
Critical corners:	45° (without stress relief circles)
Higher "safe" current:	1 nA for critical patterns and corners,
	3nA for non critical patterns
	5nA for small and simple features (circles and short lines)

The results for 400 nm membranes are practically the same as the one for 150 nm, except:

- The set milling depth for the process has to be increased up to 1000-1200 nm to be sure to get completely through the Si₃N₄ layer.
- Higher current can be used, without risk of breaking, for short line. Using 3nA or 5nA to mill lines up to 60 µm, no breaking is shown in 90% of the cases.

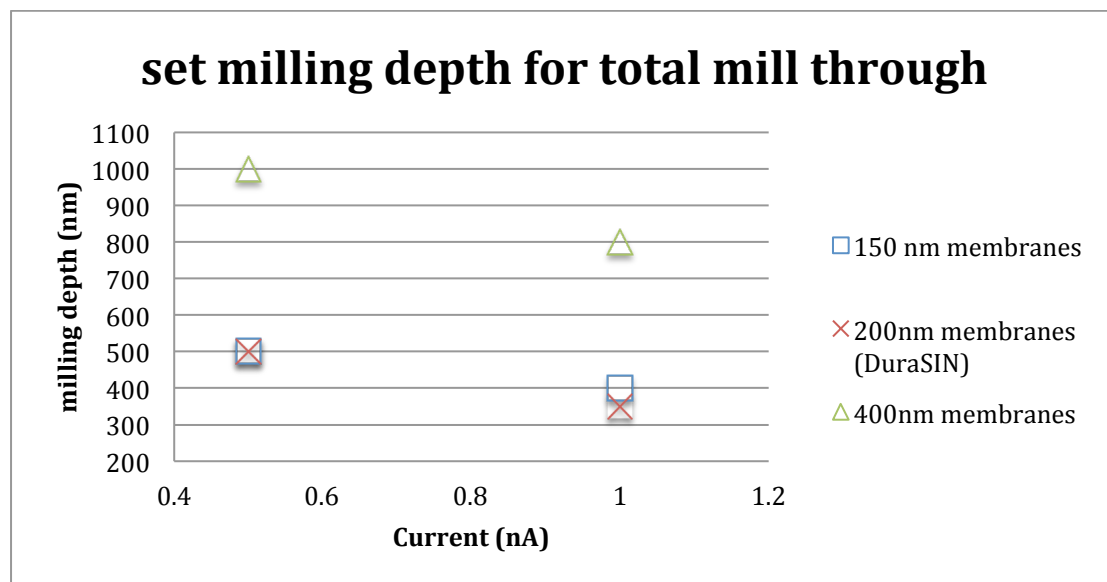
In fact, in order to obtain a stencilling mask, the Si₃N₄ layer needs to be totally milled trough.

The milling depth that has to be set in the instrument to achieve a completely mill through the membrane is in fact an issue that has been investigated.

With the Protochips membranes, a nominal milling depth of approximately two times the thickness of the membranes (400nm) was necessary to pass through the Si_3N_4 . With the newly fabricated membranes, however, it is sometimes necessary to use a milling depth that is way bigger than the actual thickness.

Data from experiments to find the parameters that ensure a total milling through the membrane to create apertures are shown below:

Since we have set the currents of 0.5nA and 1 nA as optimal currents, that guarantee a high percentage of success of milling without breaking of most of the patterns, and guarantee the possibility of mill pattern of sizes that are suitable for our project in a reasonable time, the data for the milling depth that has to be set in the instrument have been collected for them.



It is substantially coming out from the empirical procedure, that at least a milling depth that is double the actual thickness of the membranes has to be set to obtain a complete mill through the membranes.

During the milling, some issues arise; there are conditions of milling that tends to crack the membrane, and it is necessary to study compromises in order to optimize the process

- The milling current has to be as low as possible to avoid breaking. Nevertheless, it is not possible to mill small features with too low current, or, in order to perform that, is necessary to increase the magnification, and it is not possible with lines longer than 80 μm , because the milled pattern has to be in the area of focus. The

parameter reported above are a good compromise for a good milling without breaking the membranes.

A study on the stress of the membranes is shown below

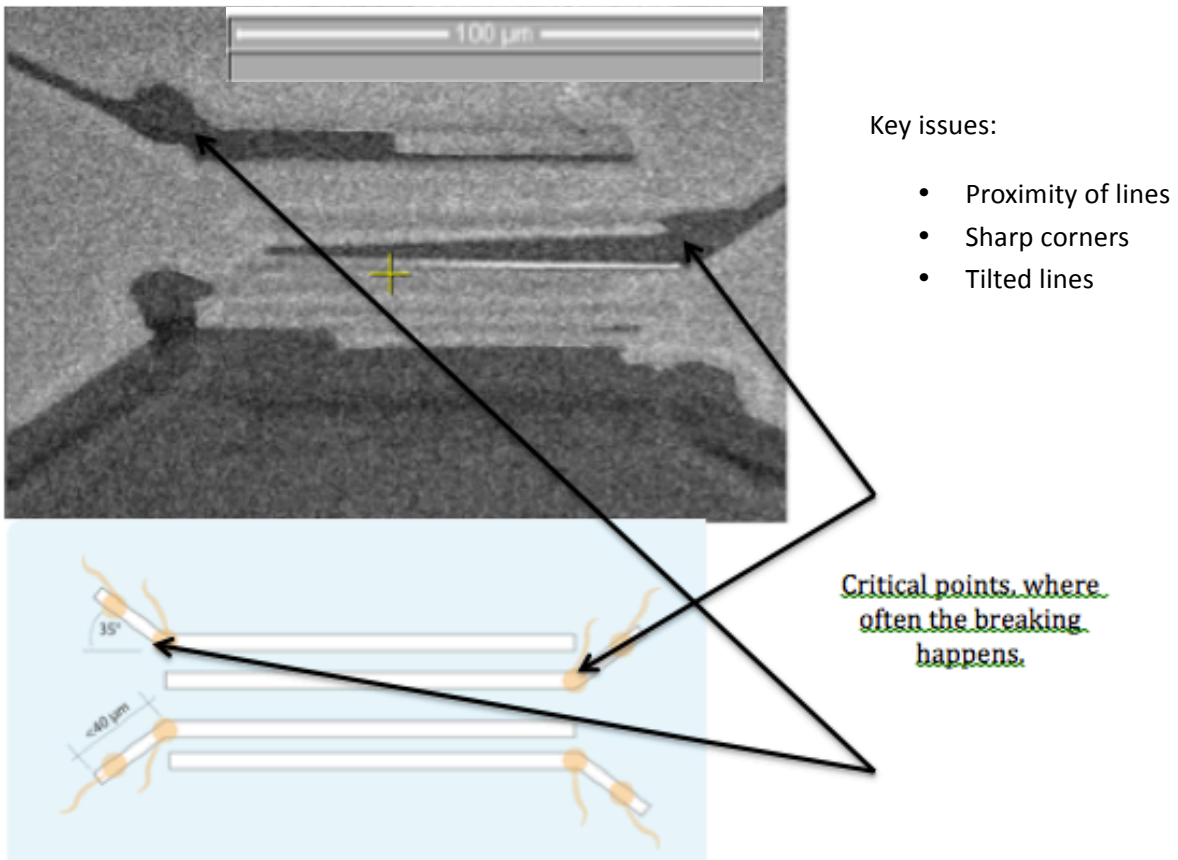
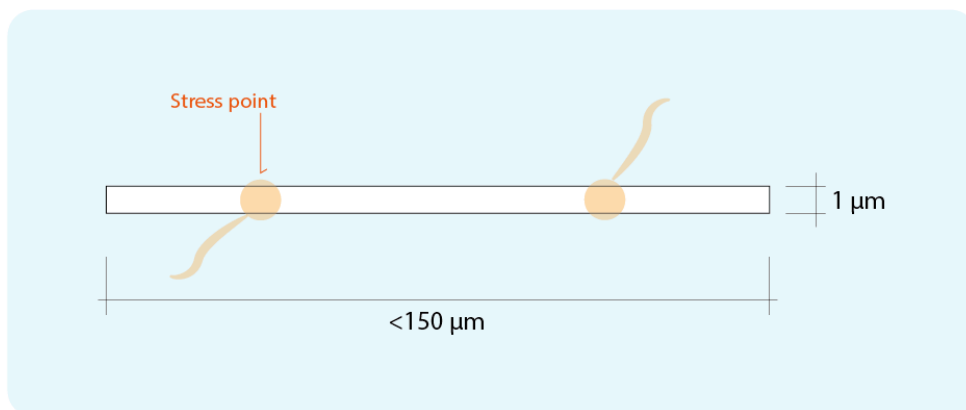


Figure 29 typical breaking points during milling of Si_3N_4 membranes, comb finger pattern

Pattern 1



Key Issues
- Long lines
- Thickness

Figure 30 typical breaking points during milling of Si_3N_4 membranes, single line milling

If we compare the two kinds of membranes, we can state that

- The membranes fabricated in the cleanroom have lower stress, and therefore they are more resistant to breaking and cracking. Milling with higher current, such as 1nA or even 3 nA for non-critical patterns, like for example the circles, is possible.
- Nevertheless, when breaking occurs, it happens in the same lines as the old membranes. This prove the fact that there are effectively some critical points and milling patterns, that tests the strength of the membranes; they are also weaker lines along which the membranes get cracked if the breaking occurs.
This suggest that the breaking, in case it happens on the predicted lines, is not due to the internal stress of the membranes, but to the induced stress from the focus ion beam milling.

Other critical milling issues:

- The change of milling current can cause a slight misalignment of the pattern. It is therefore necessary to check and re align the draw pattern to the milled one each time the current is varied.
- The ion bombardment can cause bending of the membrane, even is no actual cracking is observed. A bending can interfere with the contact deposition, causing the shape of the deposited contact to be different from the designed one. It is crucial that the contact lines are not varying as much as they finally get in touch with one another.

The thin layer of gold deposited on the membranes before the deposition increase the membrane strength, and therefore is reducing this phenomenon.

Also mill the patter with the membranes upside down, so that both the metal layer and the substrate will support them during the process, is a good technique to prevent bending.

- The bombardment of the sample with a high-energy ion beam is causing, of course, the heating of the target material, which, according to the literature, can cause defects in the crystalline structure of the material and heat spikes.^{51 52}

The right way to estimate, in a pessimistic view, how much heat we will have on the sample is to suppose that all the energy of the ion beam is converted in heat. For example, we have from the literature that, for a polymeric target, within 0.2 s, the

temperature in the center of the irradiated area increased to about 330K.⁵³ However, for the irradiation time of 0.2 s, the area in the center of the beam reaches a temperature that is high enough to evaporate the polymers.⁵³

The heat can be relevant depending on the mass of the ions, the density of the target, the milling pattern and, of course, and the incident energy.

In our case, the heat can cause bending of the membranes during milling, which may, in turn, influence the metal deposition. Anyhow, no major bending has been observed during milling.

The heat can also be a relevant issue for the graphene milling; therefore further analysis of this phenomenon will be necessary before a direct mill of graphene contacts.

- The contamination of the sample is of course a big issue in the FIB milling; Ga ions can be trapped in the structure, causing mismatch and changing the reticular structure. This once again is not a problem that has to be face in this section, in the sense that the internal structure of Si₃N₄ is not important, as long as the pattern shape is sharp and the membrane is milled trough.

However, it may be an issue once we come to the alignment and the contact deposition: the Ga can contaminate the metal contact and can end up in the graphene final device. Measurements of the contamination of the sample will be performed with EPS, and analyzed further.

In the pictures below, it is possible to see examples of breaking of the membranes. It is evident from the picture that the breaks happen on the stress points analyzed above.

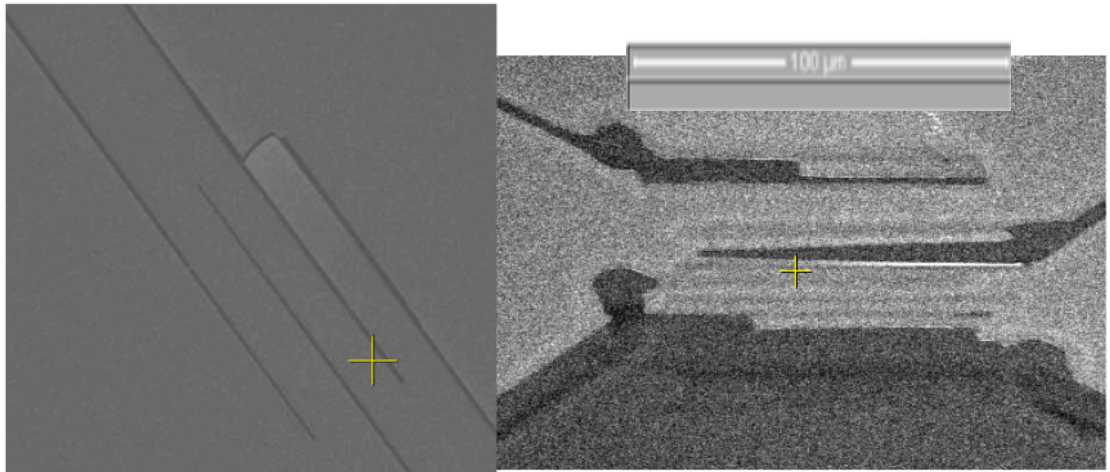


Figure 31 typical cracking of the Si₃N₄ membranes along the stress points.

Another possible breaking of the membrane is the one that cause the total collapse of the structure, probably due to a distributed internal stress when the membranes are stressed by too high current.

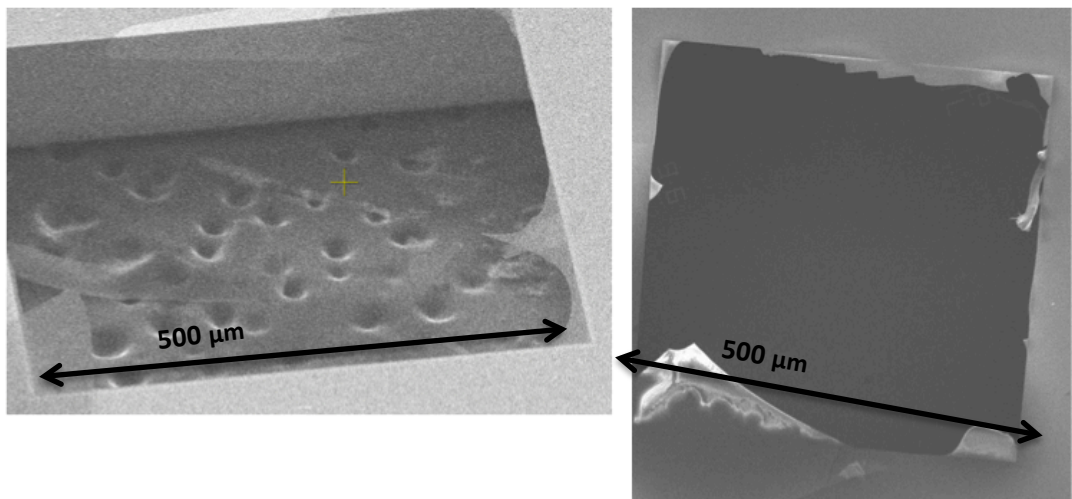


Figure 32 Two examples of total collapsing of membranes

4.2.2. Results and discussion

The final samples we obtained are respecting the specification, even if the percentage of success in milling the membranes without experiencing breaking or collapsing is around 50%.

The milled samples are shown below:

Old membranes:

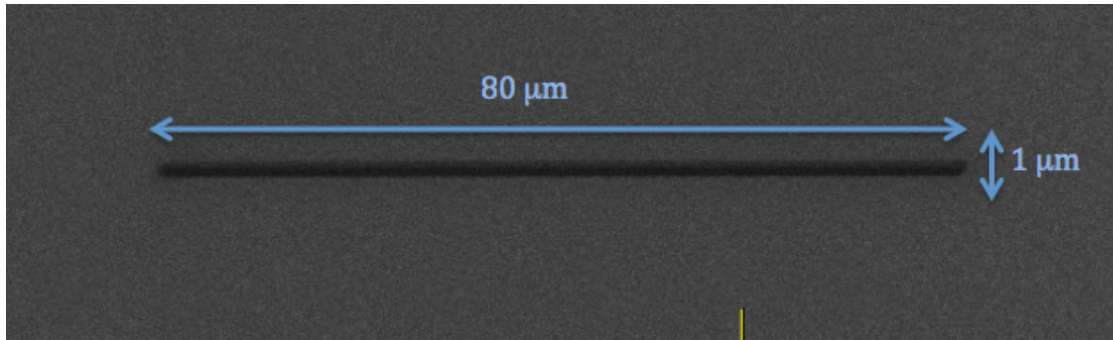


Figure 33 single milled lines of 80 μm

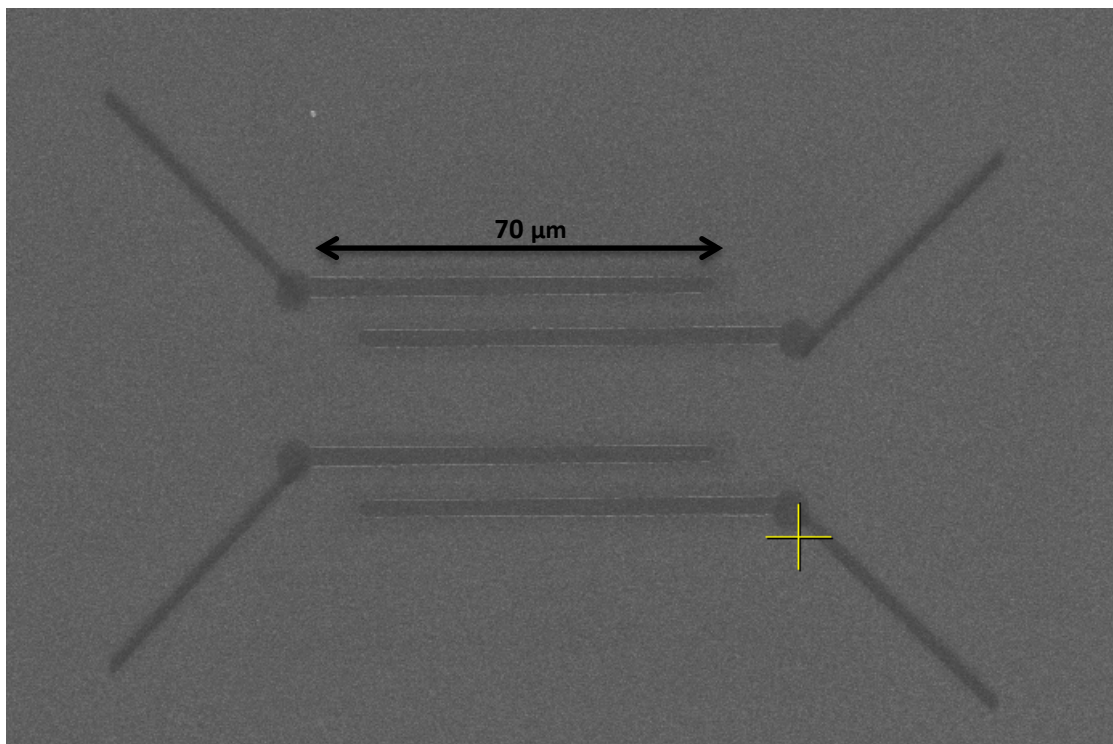


Figure 34 Comb finger lines pattern milled according to the specifications above

Membranes fabricated in Danchip:

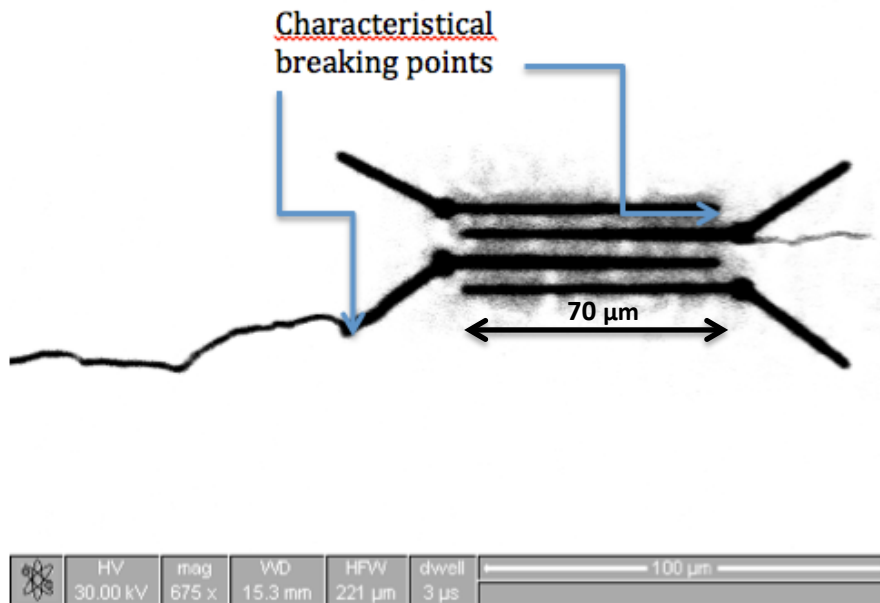


Figure 35 Comb finger pattern on a 150nm membrane fabricated in Danchip. We can see that the cracking is happening on the typical lines studied above; nevertheless the stencil mask is still working for our purpose.

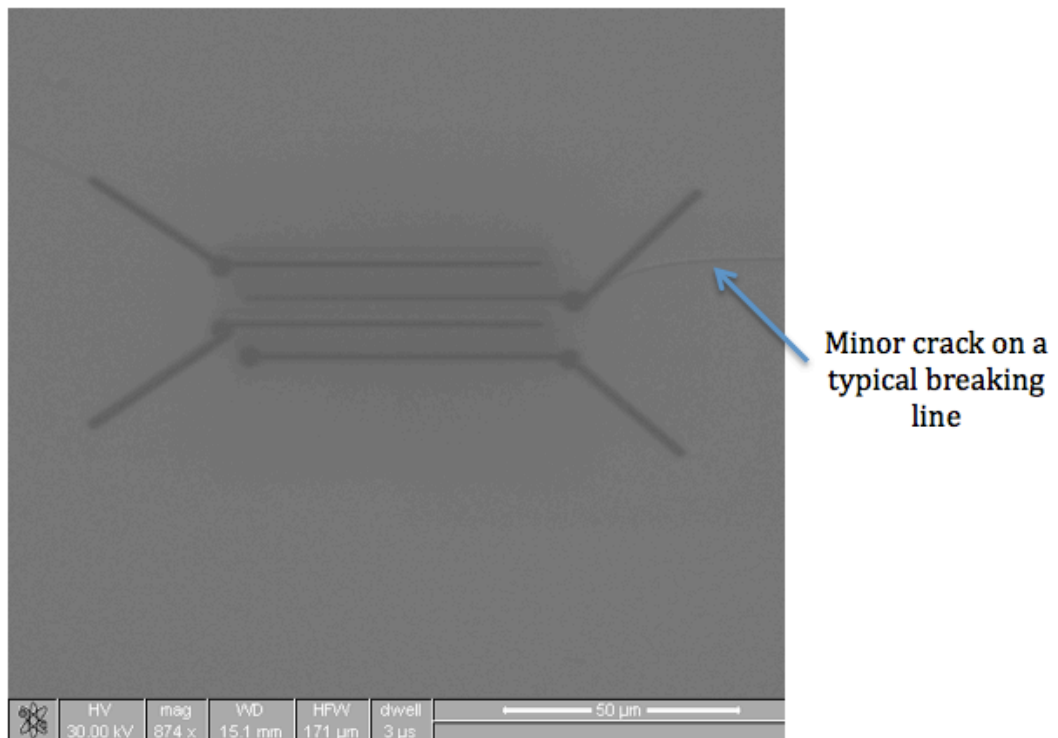


Figure 36 Comb finger pattern milled on 400 nm membranes. Also here a small crack is visible, but not influencing the contact deposition.

- At a first microscope observation, the lines seem sharp and neat, and the pattern is respecting the specification, since the dimensions are within 2% difference compared to the initial designed pattern.

- A first measurement obtained with XPS reveals no contamination from the Ga ions, and that could mean that the Ga percentage is so low that is below the resolution of the instrument. (Lower than 1%)
- Nevertheless, is visible from the milling tests how the membranes fabricated from us are stronger and with lower stress compared to the Protochips one: they can stand to be milled with higher current and they are less sensible to critical pattern (like sharp angles). Some of them are still fragile, and it can happen that they get broken as soon as the milling start, but the fact that this break happens normally with a partial or total collapse of the membrane prove the fact that it should be due to internal stress or defects in the fabricated batch.

In general, as I said above, I experienced a percentage of 90% of the fabricated membranes to be working properly and to stand the milling process better than the Protochips ones.

- Furthermore, some stenciling masks can be used anyway, even if some cracking appears during the milling. The stenciling masks in fig. 28 and 29, for example, present a small break, but this is not compromising the future deposition of contacts.

4.3. Milling of graphene and graphite

As presented in the introduction, the final goal of this project is to clear the way for the fabrication of graphene electrical contacts.

Although we didn't reach the complete fabrication of graphene contact in this project, some milling trials have been performed on graphene flakes.

The main issue in this procedure is, for sure, the alignment of the graphene flake with the membrane. Due to the small dimension of the flake, is crucial to know the position of the flake in respect of the membrane with good precision, so that the pattern can be centred on the flake. Even small misalignments can cause the failure of the procedure.

A good method can be picturing in the microscope the graphene flake under the membrane, and then calculate with a computer program the number of pixel between the graphene flakes and the edges of the membranes. In this way it is possible to transfer the right measurements in the electron microscope, and centre the Hall bar pattern on the flake.

Another, more accurate, techniques is to mill some alignment marks, and align the flake under them. An example of this procedure is shown in Figure 37, where the corners of the

Hall bar pattern have been milled before in the Si₃N₄ membrane, and then the flake have been aligned above them.

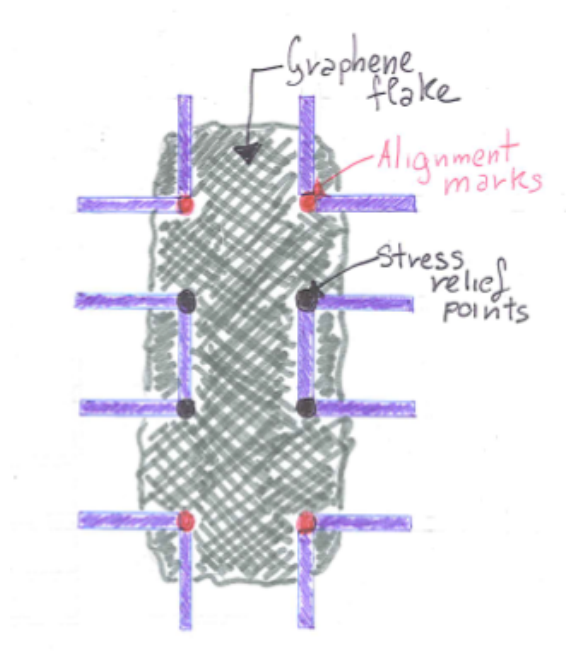


Figure 37 scheme of alignment technique using alignment marks (Red) for the milling of Hall bar patterns

In this way the pattern can easily be drawn starting from the 4 alignment points and knowing the sizes of the design.

Another fundamental issue found during the procedure was the gluing of the Si₃N₄ membrane to the graphene sample. This issue came up both in the fabrication of metal electrical contact on graphene flakes and on the milling of graphene itself.

A scheme of the possibilities for the attachment, with advantages and issues, is shown below:

Table 9 Overview of advantages and disadvantages of attaching methods

Attaching method	Advantages	Issues
Carbon tape	<p>Approved in alcatel</p> <p>Strong attachment, the sample is not falling off</p> <p>Easy to remove the stenciling mask</p>	<p>Difficult alignment</p> <p>Stenciling mask can be not in contact with the substrate</p>
Glue	<p>Approved in alcatel</p> <p>Hard contact between stenciling mask and sample</p> <p>The alignment is easier compared to carbon tape</p>	<p>Glue penetrates under the membrane, compromising the cleanliness</p> <p>Glue under membrane: hard contact not guarantee</p>

Isopropanol	Easier to handle the alignment	Not approved in alcatel
	Hard contact between stencil mask and substrate	Can crack the membrane
		Hard to remove the stenciling mask without breaking
		Risk of falling off

The membranes ordered from the external company have a too small holder, and is therefore difficult to use tape or glue without compromising the membrane area. With the glue especially, a leak under the membrane have been observed.

The best way to attach the membrane is the usage of isopropanol, to create a surface tension between the two wafers. This can nevertheless in some cases cause the cracking of the Si₃N₄ membrane, and it has to be reinforced with tape before the metal deposition, since this kind of gluing is not allowed in the deposition machine in Danchip, because of the danger of falling off.

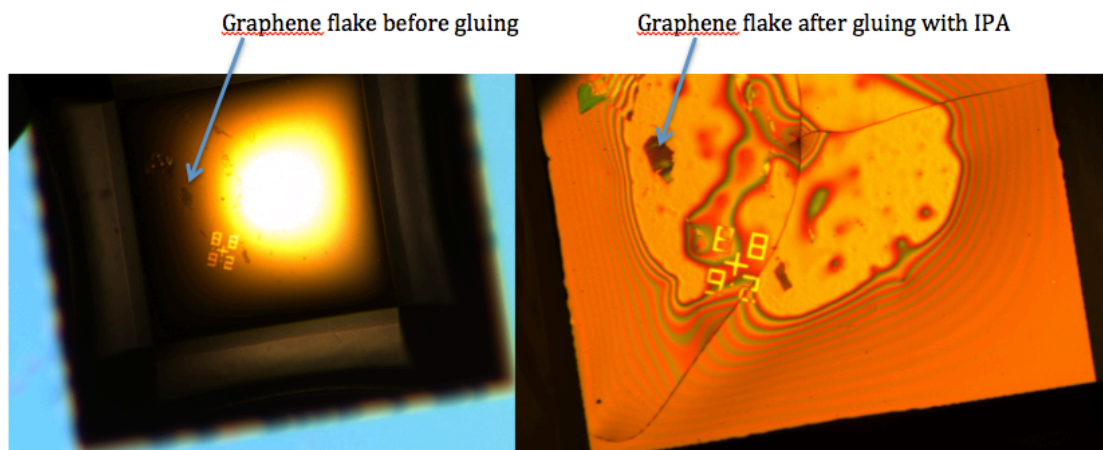


Figure 38 gluing of Si₃N₄ membrane with IPA. The cracking caused by the attachment is visible.

For the attachment procedure, the new membranes are way more suitable, since they offer a larger holder, that will allowed an easier handling and gluing, possibly with tape, that is safe and cleaner and will prevent breaking.

4.3.1. Design and requirements

The chosen pattern for milling of graphene flakes is shown below

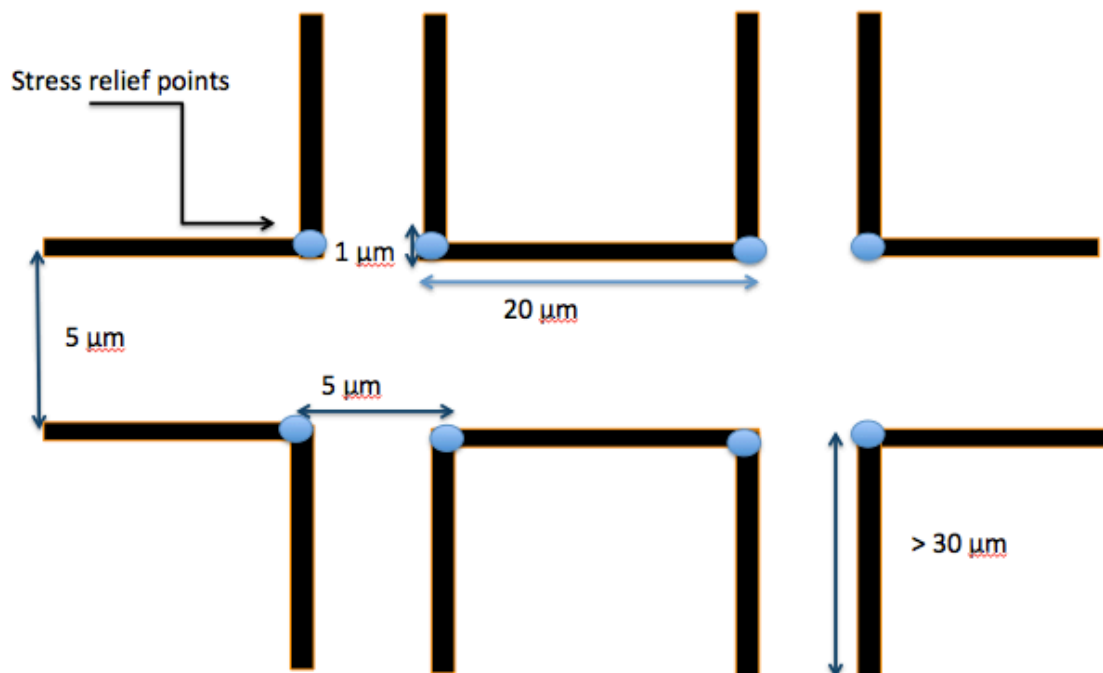


Figure 39 pattern design for graphene milling

The basic requirements are:

- Good alignment between the pattern and the graphene flake: the graphene has to be cut in a way such that the contact brakes will be separated, otherwise the contact is compromise. For this reason, the dimension of the flake is critical. An optimum flake for our device would require dimensions between 35 and $60\ \mu\text{m}$, and it is not so easy to find a single layer graphene big enough. Moreover, the calculation of the graphene position and the alignment has to be done with maximum precision, as well as the calibration of the microscope, in order to have alignment between electron beam and ion beam.
- It is desirable to have precise and sharp cut of the flake, especially if the graphene is not totally monolayer. This should not be a problem, since the FIB allows good milling of nanopatterns; nevertheless, the sharpness of the cut has to be checked after milling.
- The contamination should be as low as possible. Contamination of the flake with Ga ions may reduce the conductivity of the graphene and compromise its electrical properties. The contamination of the sample will be checked after milling, using XPS

measurements; nevertheless is already visible in fig.34 a lighted halo, which means there may be contamination on the milling borders.

- The redeposition and the side effects of the milling have to be minimized as well. Using the Si_3N_4 membranes, these effects should be reduced, but an inspection of the structure after the fabrication will allow us to discover eventual defects and structure alterations.
- The ideal contact we want to fabricate consists in a single layer graphene contact. In order to find a proper flake, Raman spectroscopy can be used. With this method is possible to inspect the graphene wafer, analysing the Raman emission from various flakes to distinguish the monolayers from the single layer.

4.3.2. *Results and discussion*

Trials of milling of single and monolayer graphene have been performed both with and without the Si_3N_4 membrane protection.

Despite the difficulties in the alignments, it has been possible to achieve some samples, even if we didn't reach a finite proper sample, with a perfect alignment and good pattern transfer.



Figure 40 pattern transfer on a graphene flake without a protective membrane. A small misalignment is visible. Furthermore an halo on the border of the milled area is indicating a possible local contamination

Anyway, the presence of the halo is more visible when the protective mask is not used. That may indicate that actually using a protective mask is a good way to reduce contamination from Ga ions.

4.4. Contact deposition on graphene

After the milling process, the next step is to deposit the contacts on the graphene flakes.

For the contact deposition, Alcatel equipment in the cleanroom has been used.

In this machine, different metal combinations are possible, and the combinations have been chosen by the cleanroom staff, and pre settled.

Since our goal is to test the quality of the contacts, the straightforward decision is to try different combinations, and measure the electrical properties on them to compare the results.

For the deposition of contact using the stencilling masks, the main issue is the alignment: as said before for the attachment of membranes to the graphene samples, aligning Si_3N_4 membrane on a graphene flake and glue that on it results quite tricky, for both the reduced dimension of the flake and the membrane holder.

Moreover, a gluing with IPA is not allowed in Alcatel, since the attachment may not hold during the deposition process, and the membrane may fall down in the vacuum chamber, so usage of glue or tape is necessary.

Deposition of contacts has been performed using gold and silver;

- The membranes fabricated in the cleanroom show better stability and strength. The handling is easier and they are not getting broken during the placing on the graphene sample.
- It is possible to use the membranes for more than a deposition. After a metal deposition, in fact, the stencilling mask is reinforced from the gold or silver layer deposited on top, and that may be an advantage for the reuse; nevertheless, multiple usage during deposition may cause
 - Redeposition along the border of the pattern, that will reduce the width of the lines (fig.)
 - Reduction of the transparency that will rend the next alignment more tricky.

In the images below it is possible to see some contacts deposited on the substrates.

4.5. Contact pad fabrication and alignment

For the contact pad fabrication, a nanodrill had been used to drill a PMMA film. According to the pattern shape milled with ion beam, a good contact pad has to have 4 holes placed at the corner of a rectangle, with the dimensions of $35 * 70 \mu m$

A scheme of the contact pad design is shown below

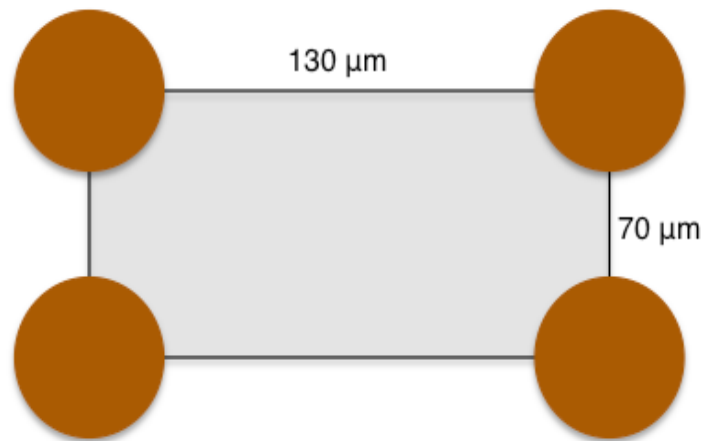


Figure 41 Scheme of the design for contact pads

The main issue with the contact pad is that they have to be fitting the initial pattern, so that each circle touch only one branch.

PMMA masks with different sizes and distances between the contact pads have been fabricated, so that it is possible to find a suitable mask for the contact pattern. To create the holes for the pads, a nano drill of 200 nm has been used.

Of course the alignment is not simple, but it can be done by previously placing some tape on the PMMA mask and glue it to the sample immediately during the alignment.

Some trials were needed to find the right dimensions of the pad, but once it is done correctly, it can be used for many depositions.

Obviously, another important requirement is that the contact pad doesn't bring any contamination to the graphene and the contact on it, since the two samples will be in direct contact. This should be straightforward with the PMMA, but contamination will be measured further on.

It has been proved that a layer of 200nm of metal is enough to obtain good electrical measurements with a four probe system.

Pictures of the final contact pad and the deposition of contact pads on sample is shown.

4.5.1. Devices for improvement of contacts and contact pads

In order to improve the contact pad, and facilitate the contacts, another stencilling mask have been fabricated. This will be a junction mask between the contact pad and the actual contacts. Once again, the mask will be fabricated with ion beam milling, on Si₃N₄ membranes.

The design of the mask will be the one in Figure 42:

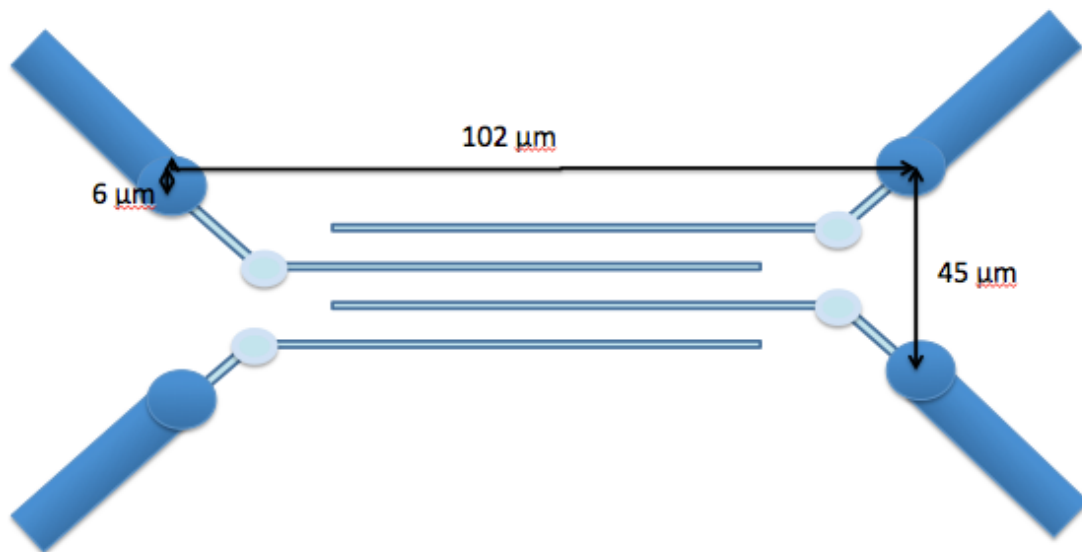


Figure 42 contact connection mask: the mask is the dark blue drawing. The dimensions are adapted to overlap the contact pattern of few micrometers

Aligning then the 3 masks, and performing the 3 depositions, it is possible to obtain a fair alignment of the contacts, with the possibility of performing electrical measurements with a 4-point probe system.

Furthermore, an attempt to simplify the process could be done by using a simpler contact pattern such as the one show in Figure 43:

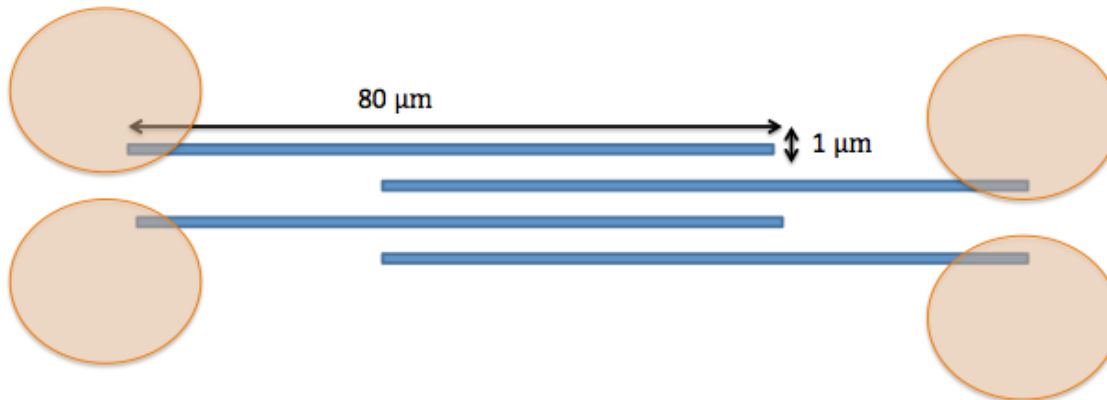


Figure 43 Blue pattern: simplified contact pattern; orange pattern: contact pads

Using this pattern, it may be possible to avoid the oblique lines, that are, as we have shown, critical in the fabrication process, since they create induced stress in the membrane risking cracking.

The only issue with this pattern, where the contact pads will be deposited directly on the horizontal lines, is that the spacing between the pads is very small, and it can get tricky to fabricate the pad mask with a nanodril. Furthermore, since the PMMA layer we are using for the contact pads have a thickness of 0.5mm, the deposition could be influenced by the thickness/spacing ratio of the holes, and the actual deposited pad may be smaller, so it may not be possible to achieve such a small spacing.

Anyway, other materials, such polymers, and other way of drilling the pad can be ideated to solve this problem and to achieve a faster fabrication process that is also safer for the Si₃N₄ membranes.

Chapter 5 Measurements and characterizations

5.1. Raman spectroscopy

5.1.1. *Measurements procedure and set up*

This kind of spectroscopy is based on the Raman effect, which basically consists in inelastic scattering of photons in the visible or UV spectra.

This effect was discovered by Raman, which won the Nobel price in 1930 for his studies of inelastic light scattering from molecules. By studying the dispersion of optical photons when hitting a sample, it is possible to see shifts of the peak around the Brillouin zone centre, and this gives information on the structure of the sample and on its vibrational modes.

Since the detected signal is relatively weak, and the frequency shift is really small, a specialized apparatus has to be used to overcome the difficulties. The light source should be intense, such as a laser, and an array of charged coupled device (CCD) sensor is normally used as a detector.

The sample is excited with a suitable source, and the scattered light is collected and focused onto the entrance slit of a scanning spectrometer. The number of photons emitted at a particular wavelength is registered on a photon counting detector and then the results are stored on a computer for analysis.

In our case, a blue laser (frequency ~ 400 nm) is used as a light source, and, by analysing the Raman shift, it is possible to determine if we are observing a single layer or multilayer graphene flake, or just graphite.

5.1.2. *Measurements with Raman spectroscopy technique*

Some measurements have been performed on our graphene samples, obtained by exfoliation and transfer on SiO₂ wafers.

In our case, Raman scattering spectroscopy has been used to characterize graphene.

It is in fact possible, with this technique, to distinguish the amount of layers on graphene flakes, as well of having information on its quality.

Raman spectrum of graphene consists of 3 main peaks or bands: G, D and 2D. The position and intensity of peaks is not fixed, but it varies for different excitation laser wavelengths, for intensity and other conditions.⁶¹

- G-peak appears around 1587 cm^{-1} . It can be called “graphite”-peak, because it corresponds to in-plane vibration mode of sp^2 hybridized atoms of graphite/graphene sheet.

- D-peak $1260\text{-}1370\text{ cm}^{-1}$ corresponds to defects or disorder in graphene. It is also called “defect peak”, and it has to be small for good quality graphite/graphene, since it identifies diamond sp^3 hybridization, so it comes from breathing mode of carbon rings and is activated only near the defects or borders of graphene sheet.⁶¹
- 2D-peak $2550\text{-}2800\text{ cm}^{-1}$ is a second order of D peak, but (unlike 2D) is not related to defects. It appears due to two-phonon lattice vibrational process.

A good single layer graphene flake can be identified basing on following criteria:

- 2D peak is twice higher than G ($I_{2D}/I_G=2$),
- Position of G peak should be centred at 1587.94 cm^{-1} (for 532 nm laser),
- 2D peak should be sharp (relatively narrow) and can be fitted to symmetrical bell-like curve (it is not exactly Gaussian).

Examples of acquired spectra for good SLG and MLG is given at Fig. 1. We can see appropriate I_{2D}/I_G ratio for SLG, that is close to 2. 2D peak is quite symmetrical, although it is not very narrow. D peak is relatively small and probably appears only due to borders of graphene flake. Multilayered graphene has characteristic non-symmetrical 2D peak and much higher G peak.⁶¹

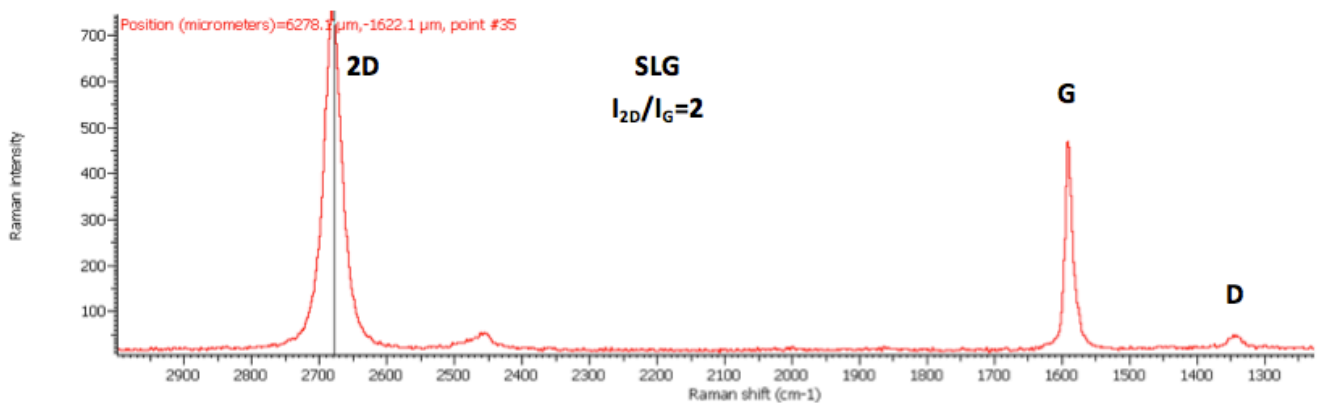


Figure 44 Raman spectra of good quality single layer graphene⁶¹

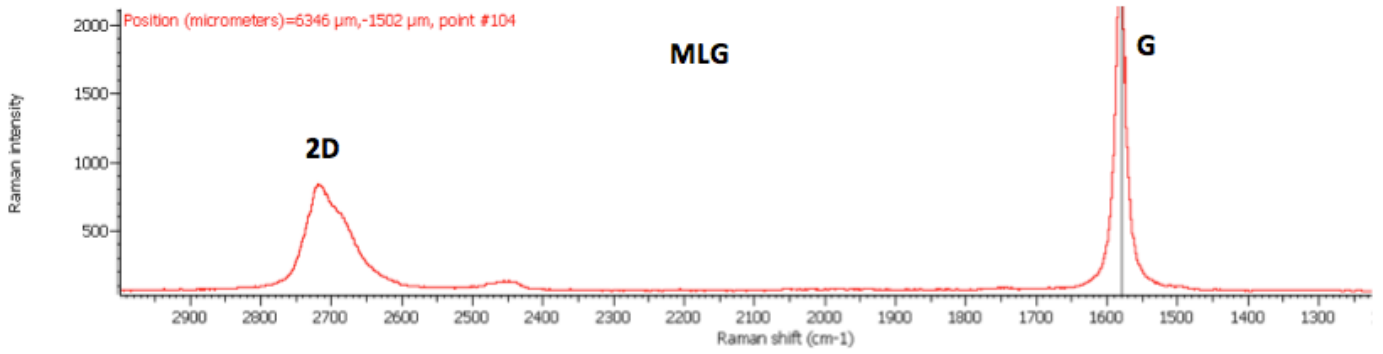


Figure 45 Raman spectra of multilayer graphene⁶¹

Maps of our graphene flakes are shown below:

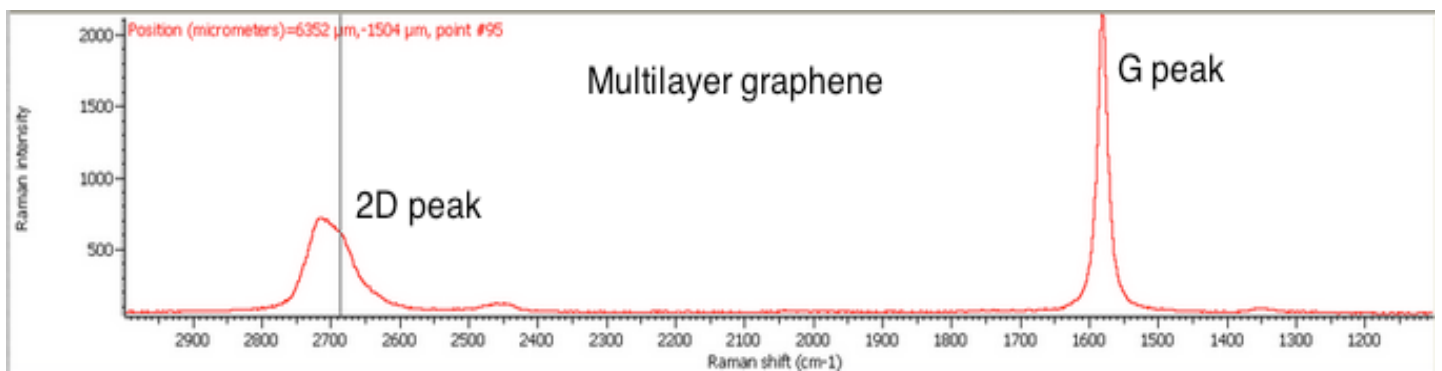
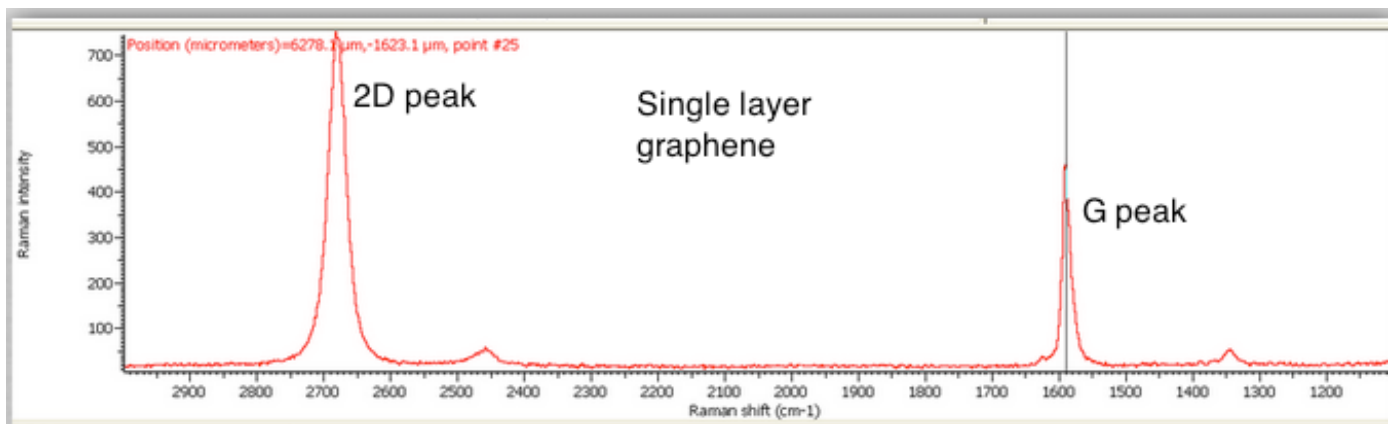


Figure 46 Raman spectroscopy of graphene from our laboratories

As is possible to see in the spectra, the 2D peak for the single layer graphene is 2 times higher than the G peak, and is way sharper than the 2D peak for the multilayer graphene. It can almost be approximated to a single Lorentzian, and these factors indicate without doubt that we are observing a single layer flake.

For the multilayer, in fact, just looking at the shape of the 2D peak we can clearly see that it is not sharp, and the intensity is lower than the G peak.

The D peak is practically absent, indicating the absence of defects.

5.2. Electrical measurements

5.2.2. Procedure and set up

In order to characterize the electrical properties of the fabricated various contacts, electrical measurements have been performed using a four point probe system.

The reason for using a four-probe system instead of a two point is obvious if we recall the basic Ohm law, $V = RI$.

Therefore, with a two point system, the intrinsic resistance of the points will enter in the circuits, since the voltage is measured with the same probes that injected current.

The total resistance will be then

$$R_{Meas} = R + 2 * R_i$$

So not only the final measured resistance R_{meas} will be altered from the intrinsic resistance R_i , but also, if the resistance we would like to measure (R) is very low, we will only see the intrinsic resistance of the points.⁹⁴

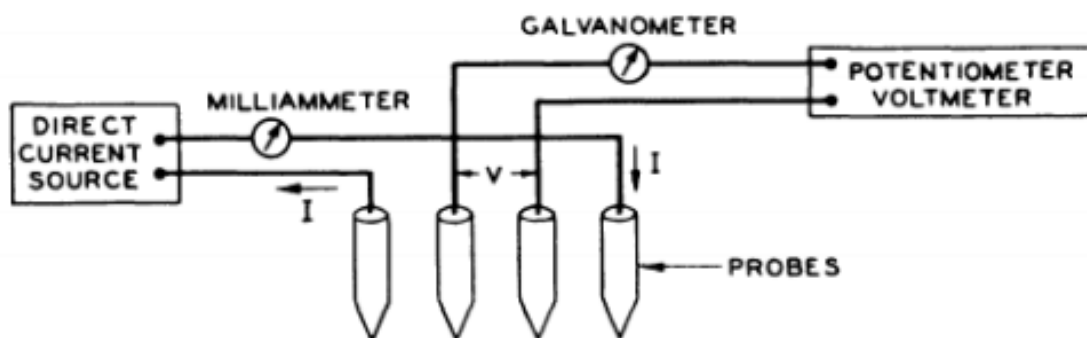


Figure 47 Scheme of a four probes system set up

With the four-probe system, instead, we can measure the voltage through the voltmeter that is behaving as an open circuit. No current is passing through it.

The current is instead injected through the current source points.

So if I is the injected current, and ΔV is the potential difference at the two voltmeter points,

we can directly calculate the resistance with $R = \frac{\Delta V}{I}$.

5.3. Contamination measurements

5.3.2. Overview of XPS techniques

To measure the contamination of our sample over the fabrication and the contact deposition procedures, one of the techniques that can be use is the X-ray photoelectron spectroscopy (XPS).

This is a quantitative spectroscopic technique that allows us to measures the elemental composition, together with the empirical formula, the chemical and electronic state of the elements present on the surface of a selected sample.⁵⁹

The procedure of XPS spectroscopy consists in irradiating a material with a beam of X-rays. At the same time the kinetic energy and number of electrons that escape from the top 1 to 10 nm of the material are detected and analyzed.⁵⁹

XPS techniques have to be performed in ultra high vacuum.

XPS is a surface chemical analysis technique, therefore is only analyzing the surface of the sample, and it is giving information about the state on which this material is when it is receiving the X rays.

There are some important informations about XPS spectroscopy that has to be taken in mind while working:

- XPS detects all elements that have atomic number of 3 (Lithium) and above. It is not detecting Hydrogen (Z=1) and Helium (Z=2), that have diameters of the orbitals so small that the probability of catching an electron there is almost zero. Therefore no contamination from Hydrogen and Helium will be detected on the samples.
- Elements are in the parts per thousand ranges. Detection limits of parts per million (ppm) are possible, but require special conditions: concentration at top surface or very long collection time (overnight).^{59 58}

Physical principle:

Since we know (and we set) the energy of X-rays send on the sample, or specifically we know their wavelength, the electron binding energy of each of the emitted electrons can be determined by using Rutherford equation:

$$E_{Binding} = E_{Photon} - (E_{Kinetic} + \phi)$$

Where:

$E_{binding}$ is the bonding energy of the scattered electron

E_{photon} is the incident energy of the X-ray

$E_{kinetic}$ is the kinetic energy of the outgoing electron

Φ is the work function of the material ⁵⁸

A typical XPS spectrum is a two dimensional plot of the number of electrons detected (sometimes per unit time) on the Y-axis versus the binding energy of the electrons detected on the X-axis. ⁵⁹

Each element produces a characteristic set of XPS peaks that have characteristic binding energy values that allows us to identify which elements are present on the surface of a sample. ^{59 58}

These characteristic peaks are due to the electron configuration of the electrons within the atoms, e.g., 1s, 2s, 2p, 3s, etc. The number of detected electrons in each of the characteristic peaks is directly related to the amount of element within the area (volume) irradiated

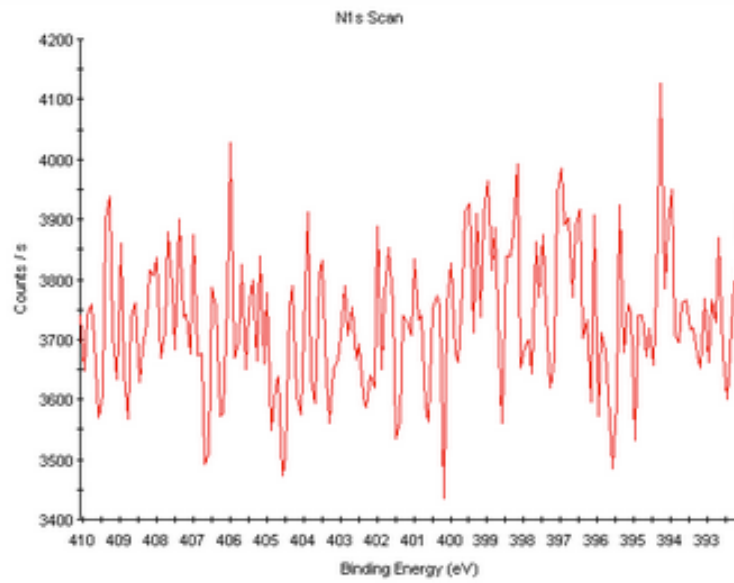
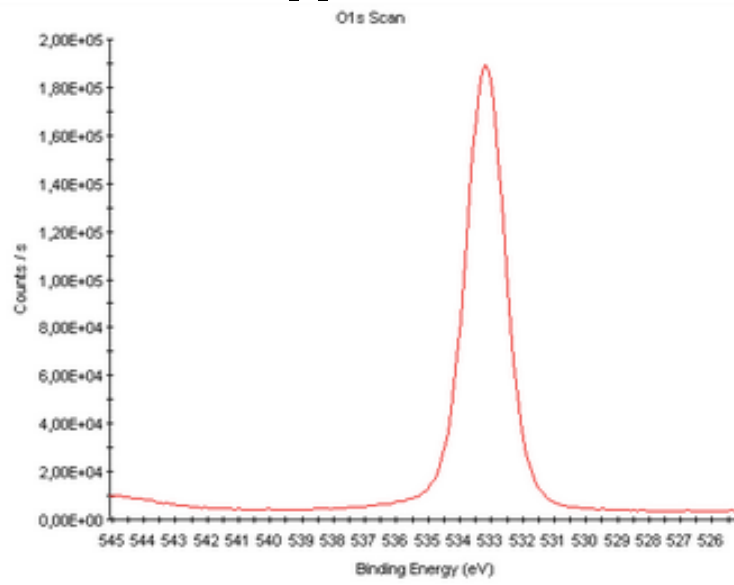
An important note is that only the electrons that gain enough kinetic energy to actually escape from the material are detected, and that means that the measure is not 100% precise, so probably some of the electrons coming from a certain element will have a kinetic energy that is lower than the work function, and therefore will not be seen. ^{59 58}

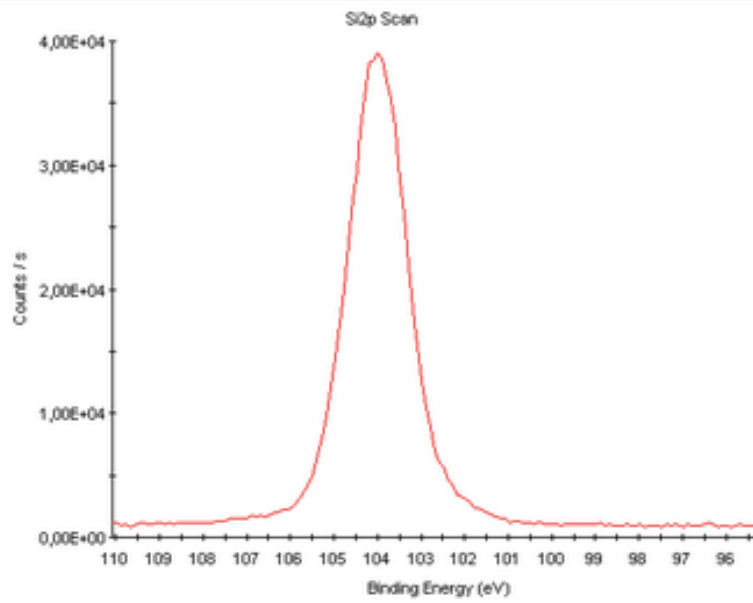
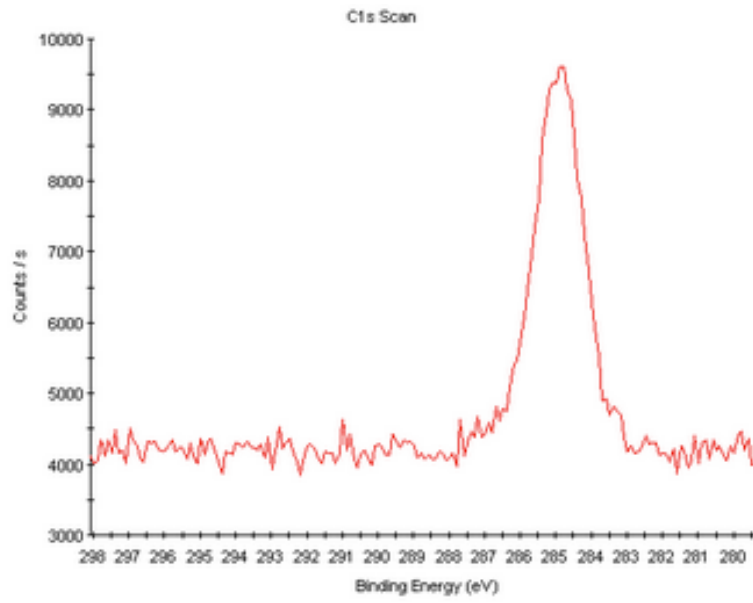
5.3.2. *Measurements with XPS technique*

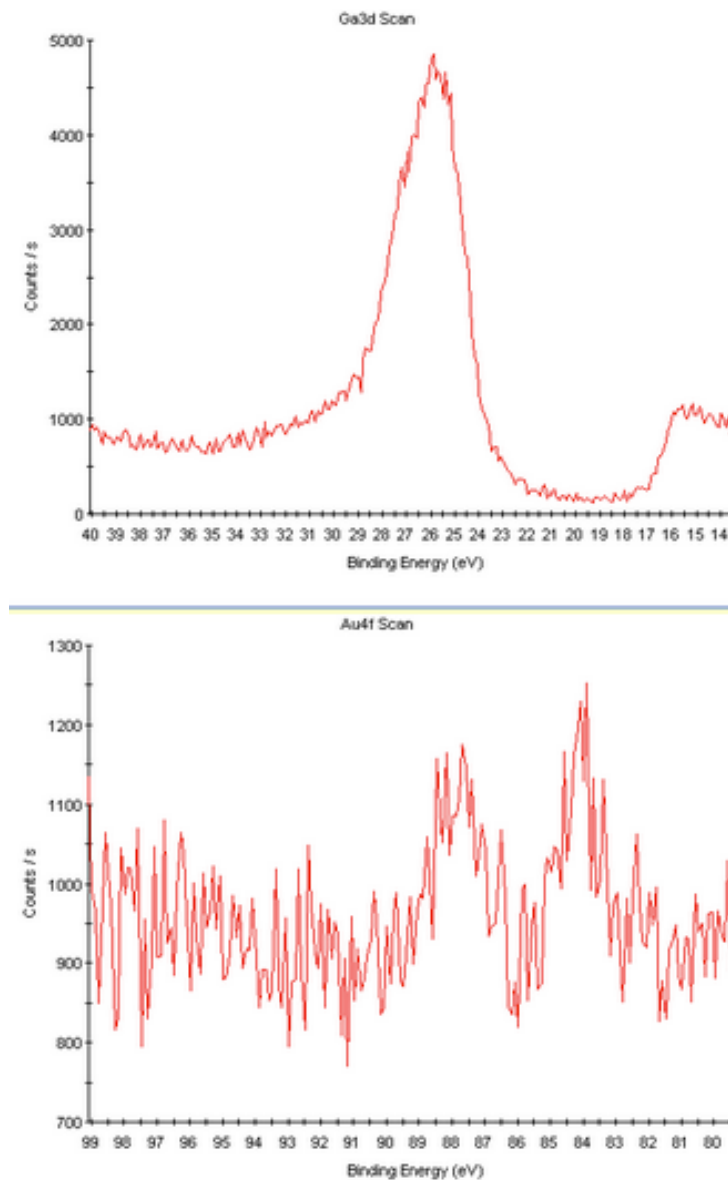
Tests with XPS spectroscopy have been run on 3 samples: 1 of them consisting in a gold contact deposited on a graphene flake, and 2 of them consisting on graphene flakes on which a cut using FIB have been performed.

The results are reported below.

Graphene contact deposited with Si_3N_4 stenciling mask







In the measurements, we have chosen to detect only the elements that we think are interesting regarding our scope.

It is possible to see from the graphs, that the SiO₂ of the substrate is very well detected, as well as the carbon of the graphene flake. Looking at the gold detected spectrum, it is possible to distinguish two peaks, but very weakly, since they are almost totally absorbed in the background noise.

This is due to the dimension of the contacts compare to the focus (?) of the XPS. The (?) is in fact 400 μm , compared to the contacts lines, that have a maximum length of 70 μm and a width of 1 μm .

The Gallium contamination is also practically absent, and also the nitride, indicating that the mask doesn't live any contamination trace on the samples during alignment and deposition of the contact.

The graphs showing the results of the XPS measurements on the graphene cut are shown in appendix. It is nevertheless possible to say for sure that the Ga spectra is practically totally background noise, and therefore the Ga contamination due to the FIB ions is less than 1%.

5.3.3. *Conclusions*

The FIB technique to fabricate contacts on graphene is valid, since it shown to leave practically no contaminations on samples.

Nevertheless, different depth of the cut and larger or thinner shapes has to be considered, since the Ga redeposition may depend on the shape of the milled pattern, and could therefore be a problem, for example, for deep and thin lines.

Another issue to keep into account is the very small size of the investigated pattern compared with the focus point of the XPS: since the scanned area is way bigger than the cut, it can also be that the contamination is way higher than expected around the area of interest, but it looks almost zero from the measurement, because is averaged with the rest of the scanned area.

Chapter 6 Conclusions and discussion

This project has been driven by the desire of find right parameters and process methods for the fabrication of grafene contacts using Focused Ion Beam milling to direct sharpened the flakes.

During the outgoing of the project, details on stress on Si₃N₄ membranes, both FIB induced and intrinsic, have been investigated, and a method of fabrication of Si₃N₄ membranes in cleanroom has been developed.

The main goals of the project have been:

- Fabricate Si₃N₄ membranes that are more suitable for our purpose, since they are easy to handle, thanks to a bigger holder, and more resistant to both FIB milling and handling during alignment and attachment, with thickness of nitride layer that can be defined during fabrication.
- Analyse the membrane stress, comparing the membranes from Protochips with the fabricated one, to have a clear overview of the reason of membrane breaking, milling parameters, data on stress point, critical patterns and limit currents.
- Perform contact deposition trough membranes, implementing a good way to align and attach the stencilling masks on the substrates, and characterizing the deposited contacts in terms of shape and dimensions transfer. Design, fabrication and alignment of suitable contact pads.

These individual goals have been successfully addressed:

With a standard lithographic method, and some optimizations of the parameters, it has been possible to fabricate Si₃N₄ membranes in Danchip that fulfil the requirements for this project.

Using empirical data from the FIB milling process, it has been possible to achieve a comparison between the membranes ordered from outside and the one we fabricated, and creation of suitable stencilling masks, for the deposition of contacts for two point probe measurements and four point probe measurements has been successfully performed.

Alignment and attachments trials have been performed with a variety of methods, and it was possible at the end to achieve pattern transfer on graphene and on SiO₂ substrate.

Contact pads have been fabricated on PMMA masks, with different dimensions, so that they will be suitable for different kind of contacts.

Measurements of contaminations, and analysis of pattern transfer quality on the substrate have been performed on the final samples.

6.1. Outlook

The final tasks to have working metal contacts on graphene flake and to create a graphene contact with direct FIB milling has not been completed. By improving the alignment of the contact pads, finding a method to fabricate this pad in smaller dimensions, would lead to a final sample of contacted graphene.

Regarding the milling of graphene flakes, trials has been performed, but the issue of the alignment of the flake with the pattern is a problem jet to be overcome. A step forward would be to use alignment marks on the membrane, but a way of aligning the marks to the flakes in a precise way has jet to be found. Once this problem is solved, the possibility of milling graphene trough membrane in an Hall bar shape has already been proved to be realistic.

Bibliography

1. Girolamo Di Francia, Ettore Massera, Mara Miglietta, Ivana Nasti, Tiziana Polichetti "Il grafene: proprietà tecniche di preparazione e applicazioni" studi e ricerche, review and assessment paper 1-3 (3/2011)
2. Gerasimos Konstantatos, Michela Badioli, Louis Gaudreau, Johann Osmond, Maria Bernechea, F. Pelayo Garcia de Arquer, Fabio Gatti and Frank H. L. Koppens "Hybrid graphene-quantum dot phototransistors with ultrahigh gain" nature nanotechnology letters (may 2012)
3. Cometox – grafene. At www.grafene.it (2011)
4. Eberhard Ulrich Stutzel, Marko Burghard, Klaus Kern, Floriano Travesi, Fabrizio Nichele, Roman Sordan "A graphene nanoribbon memory cell" Nanoletters (2010)
5. Lemme, M. C. *et al.* "A graphene field-effect device". *IEEE Electron Device Letters* **28** (4): (2007)
6. Bullis, K. "Graphene Transistors". Cambridge: MIT Technology Review, Inc. (2008-01-28).
7. Echtermeyer, Tim. J. *et al.* "Nonvolatile Switching in Graphene Field-Effect Devices". *IEEE Electron Device Letters* **29** (8): 952. (2008).
8. Sordan, R.; Traversi, F.; Russo, V. "Logic gates with a single graphene transistor". *Appl. Phys. Lett.* **94** (7): (2009).
9. Wang, H.; Nezich, D.; Kong, J.; Palacios, T. (2009). "Graphene Frequency Multipliers". *IEEE Electr. Device. L.* **30** (5): 547
10. Fiori G., Iannaccone G., "Ultralow-Voltage Bilayer graphene tunnel FET", *IEEE Electr. Dev. Lett.*, **30**, 1096 (2009)
11. Bourzac, Katherine (2010-02-05). "Graphene Transistors that Can Work at Blistering Speeds". *MIT Technology Review*.
12. IBM shows off 100GHz graphene transistor – Techworld.com News.techworld.com. Retrieved on 2010-12-10.
13. Lin *et al.*; Dimitrakopoulos, C; Jenkins, KA; Farmer, DB; Chiu, HY; Grill, A; Avouris, P (2010). "100-GHz Transistors from Wafer-Scale Epitaxial Graphene". *Science (Science)* **327** (5966):
14. "European collaboration breakthrough in developing graphene" NPL. 2010-01-19. Retrieved 2010-02-21.
15. "First graphene integrated circuit" *IEEE Spectrum*. 2011-06-09. Retrieved 2011-06-14.
16. Neil W. Ashcroft, N. David Mermin "Solid State Physic" Cornell university, Brooks/Cole
17. Adam H. R. Palser Interlayer interactions in graphite and carbon nanotubes Physical and Theoretical Chemistry Laboratory, South Parks Road, Oxford, UK OX1 3QZ 20th July 1999
18. Semenov, G.W. (1984). "condensed-Matter Simulation of a Three-Dimensional Anomaly". *Physical Review Letters* **53** (26): 2449
19. Avouris, P., Chen, Z., and Perebeinos, V. (2007). "Carbon-based electronics". *Nature Nanotechnology* **2** (10): 605–15.
20. Orloff, Jon (1996). "Fundamental limits to imaging resolution for focused ion beams" *Journal of Vacuum Science & Technology B: Microelectronics and Nanometer Structures* **14** (6): 3759.
21. "Introduction : Focused Ion Beam Systems" Retrieved 2009-08-06.
<<http://www.fibics.com/fib/tutorials/introduction-focused-ion-beam-systems/4>>
22. Lucille A. Giannuzzi, Brenda I. prenitzer, Brian W. kempshall "ION - SOLID INTERACTIONS" 'FEI Company, Hillsboro, OR 97124, Nanoselective Inc., Orlando FL
23. T. ishitani, Y. Taniguchi, S. Isakizwa *et al.* *J. Vac. Sci. Technol. B*, **16** (1998)
24. T. ishitani and H. Tsuboi. *Scanning* (1997)
25. E.J. Sternglass. *Phys. Rev.*, (1954)
26. M.W. Phaneuf. *Micron* (1999)
27. J. Schou. *Phys. Rev. B*, (1980)
28. Nan Yao, Focused Ion Beam System, basics and applications, Princeton university, (2007)
29. L. Reimer. *Image formation in low-voltage Scanning Electron Microscopy*, Washington DC, SPIE optical engineering press, (1993)
30. D.C.Joy. institute physic conference ser. No. 93 (1998)
31. K. Nikawa. *J. Vac. Sci. Technol. B* (1991)
32. M. Utlaut. *handbook of charged particle optics*, ed J. Orloff (new york press 1997)
33. Y. Sakai, T. Yamada, T. Suzuki *et al.*, *appl. Phys. Lett.* **73** (1998)
34. T. Ishitani, K. Ohya. *Scanning*, **25** (2003)
35. K. Edinger. *Direct-write Technologies for rapid prototyping applications: sensors, electronics, integrated power sources*, ed. A. Pique and D.B. Chrisey (San Diego, CA: academy press, 2002)
36. J.P.Biersack and L.G.Haggmark. *Nucl. Inst. Meth. Phys. Res. B* **174** (1980)
37. J.F.Zeigler, J.P.Bjersack and U.Littmark. *the stopping range of ions in solids* (New York Pergamon 1985)

38. L.Frey, C.Lehrer and H.Ryssel. Appl. Phys. A, 76 (2003)
39. A-Lugstein, B.Basnar, J.Smoliner and E.Bertagnolli. Appl. Phys. A, 76 (2003)
40. MICHAEL M. MARSHALL JIJIN YANG AND ADAM R. HALL "Direct and Transmission Milling of Suspended Silicon Nitride Membranes With a Focused Helium Ion Beam" Joint School of Nanoscience and Nanoengineering, University of North Carolina Greensboro, Greensboro, North Carolina Carl Zeiss NTS, LLC, Peabody, Massachusetts (2012)
41. Schmidt, C.; Mayer, M.; Vogel, H. Angew. Chem., Int. Ed. 2000,39, 3137-3140.
42. Li, J.; Stein, D.; McMullan, C.; Branton, D.; Azis, M. J.; Golovchenko, J. A. Nature 2001, 412, 166-169.
43. Hien D. Tong,* Henri V. Jansen, Vishwas J. Gadgil, Cazimir G. Bostan, Erwin Berenschot, Cees J. M. van Rijn, and Miko Elwenspoek "Silicon Nitride Nanosieve Membrane" MESA Research Institute, UniVersity of Twente, P.O. Box 217,7500 AE Enschede, The Netherlands (2003)
44. Y.-R. Kim, P. Chen, M. J. Aziz, D. Branton, J. J. Vlassak "Focused ion beam induced deflections of freestanding thin films" JOURNAL OF APPLIED PHYSICS 100, 104322 (2006)
45. Marek E. Schmidt, Zaharah Johari , Razali Ismail, Hiroshi Mizuta and Harold M. H. Chong "Focused Ion Beam Lithography and Deposition of Tungsten Contacts on Exfoliated Graphene for Electronic Device Applications" Nano Research Group, School of Electronics and Computer Science
46. D C Bell1,2, M C Lemme3, L A Stern4, J R Williams1,3 and C M Marcus "Precision cutting and patterning of graphene with helium ions" Nanotechnology 20 (2009)
47. N. Lei, Z. Chen, D. Kim, W. Xue, J. Xu "Mechanical fabrication of graphene devices using focused-ion beam: deposition and milling" Nanotech 2012 Vol. 2
48. G. Villanueva, J.A. Plaza, A. Sánchez-Amores, J. Bausells, E. Martínez, J. Samitier, A. Errachid "Deep reactive ion etching and focused ion beam combination for nanotip fabrication" Materials Science and Engineering C 26 (2006)
49. Univis – Graphene <<http://www.graphene.nat.uni-erlangen.de/grapheneng.htm>>
50. Raith – Innovative solutions for nanofabrication and semiconductor navigation <<http://www.raith.com/?xml=company%7CAbout+Raith%7CFocused-ion-beam>>
51. R. S. Averback and T. Diaz de la Rubia (1998). "Displacement damage in irradiated metals and semiconductors". In H. Ehrenfest and F. Spaepen. *Solid State Physics*. 51.Academic Press pp. 281–402.
52. R. Smith, ed. (1997). *Atomic & ion collisions in solids and at surfaces: theory simulation and applications* Cambridge University Press ISBN 0-521-44022-X
53. A. M. Ektessabi, T. Sano; "Sputtering and thermal effect during ion microbeam patterning of polymeric films" REVIEW OF SCIENTIFIC INSTRUMENTS VOLUME 71, NUMBER 2 FEBRUARY 2000
54. Han M Y, Ozyilmaz B, Zhang Y and Kim P 2007 Energy "band-gap engineering of graphene nanoribbons Phys. Rev. Lett. 98 206805
55. Ponomarenko L A, Schedin F, Katsnelson M I, Yang R, Hill E W, Novoselov K S and Geim A K 2008 Chaotic dirac billard in graphene quantum dots Science 320 356–8
56. Fischbein M D and Drndić M 2008 Electron beam nanosculpting of suspended graphene sheets Appl. Phys. Lett. 93 113107
57. Precision cutting and patterning of graphene with helium ions <http://pvcrom.pveducation.org/CHARACT/4pp.HTM>
58. Siegbahn, K.; Edvarson, K. I. Al (1956). "β-Ray spectroscopy in the precision range of 1 : 1e6". *Nuclear Physics* 1 (8): 137–159. Bibcode 1956NucPh...1..137S. doi:10.1016/S0029-5582(56)80022-9.
59. Electron Spectroscopy for Atoms, Molecules and Condensed Matter, Nobel Lecture, December 8, 1981
60. J.F. Dayen et al, "side gated transport in FIB fabricated multi-layered graphene nanoribbons. 2008, V4. I6. PP. 716-720
61. [Wall 2011] M. Wall, "The Raman spectroscopy of graphene and the determination of layer thickness." Thermo Scientific. Application Note 52252. 2011.
62. P. Delhaes (2001). *Graphite and Precursors*. CRC Press. ISBN 90-5699-228-7.
63. Kristóf Tahy, "Fabrication and characterization of 2D graphene and graphene nanoribbon field effect transistors", University of Notre Dame, april 2009
64. Jason P.G. Gao "Contamination Control in Photolithography of SAW Filter Wafers" controlled environment articles, 2012
65. W.R. McKenzie, E.A. Marquis and P.R. Munroe, "Focused ion beam sample preparation for atom probe tomography", Electron Microscope Unit, University of New South Wales, NSW 2052, Australia Department of Materials, Oxford University, Parks Road, Oxford OX1 3PH, UK
66. P. ekkels, R.W. Tjerkstra, G.J.M krijnen, J.W.Berenschot, J. Brugger, M.C. Elwenspoek, Fabrication of functional structure of thin silicon nitride membranes, transduction technology group, MESA+research institute, university of twente, P.O. box 217, 7500 AE Enschede, The Netherlands, Microelectronic engineering 67-68 (2003), 422-429
67. David Mackenzie researches on graphene devices, DTU 2012

68. A. Pirkle, J. Chan, A. Venugopal, D. Hinojos, C. W. Magnuson, S. McDonnell, L. Colombo, E. M. Vogel, R. S. Ruoff, and R. M. Wallace, "The effect of chemical residues on the physical and electrical properties of chemical vapor deposited graphene transferred to SiO₂", APPLIED PHYSICS LETTERS 99, 122108 (2011)

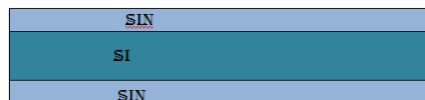
Appendix 1 Details of process for Si₃N₄ membranes fabrication


Process flow title					
Stenciling masks fabrication					
DTU Danchip National Center for Micro- and Nanofabrication			Contact email Eleonora.zamburlini@gmail.com	Contact person Eleonora Zamburlini	
			Created by Eleonora		
Lab manager group Nanointegration	Date of release Click here to enter a date.	Date of revision	Revision nr 1	Date of creation 20/03/2012	Batch nr 0

Objective
To create SiO ₂ membranes, and integrate them in a stenciling mask to be used with FIB technology for creation of, for example, grapheme contacts

Substrates								
Substrate	Orient.	Size	Doping/type	Polish	Thickness	Box	Purpose	# Sample ID
3xSilicon	<100>	4"	N doped	DSP	525 µm		Device wafers	
Dummy wafer (Si wafer from cleanroom)	<100>	4"	N doped	DSP	525 µm		Test wafer for LPCVD	

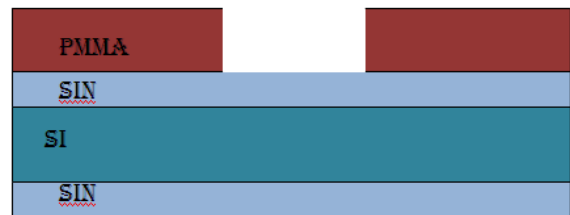
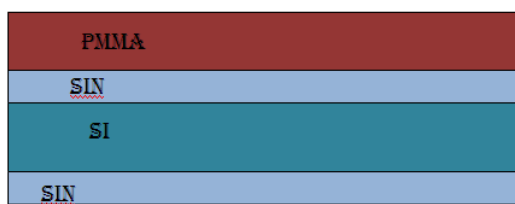
1 Growth of SiO ₂ layer					
Step Heading	Equipment	Procedure	Target	Comments	
1.1 Furnace	Nitride furnace for LPCVD	Place wafers and dummies in wafer holder for furnace.			
1.2 Recipe		Use the recipe 800 C, 150 mTorr	300 nm	Check SiN thickness (trial with dummy)	
1.3 Unload		Unload wafers			



2 Spinning of Photoresist					
Step Heading	Equipment	Procedure	Recipe/mask	Target	Comments
2.1 Cleaning	HMDS oven	Bake sample in HMDS	Recipe 4		
2.2 Spinning	KS spinner	Spinning of the PMMA	Resist AZ5214E positive standard resist Danchip_1.5um_4"and6"	1,5 µm thickness resist	Inspect resist thickness
2.3 Photo exposure	KS aligner	Mask alignment and Exposure (align the mask with the crystal orientation)		Back contact, topside alignment, exp time 10s	Inspect the resist in the microscope
2.4 Developing	Wet bench	Develop the resist	Use AZ3251B: Di water (1:5) Time: 65s		Check with microscope if the resist is gone, if not,

Process flow title					
Stenciling masks fabrication					
DTU Danchip National Center for Micro- and Nanofabrication			Contact email Eleonora.zamburlini@gmail.com		Contact person Eleonora Zamburlini
			Created by Eleonora		
Lab manager group Nanointegration	Date of release Click here to enter a date.	Date of revision	Revision nr 1	Date of creation 20/03/2012	Batch nr 0

Rinse (DI water) 3min Dry re exposure					
2.5 Descum	Ash plasma	Place the sample in the Ash plasma chamber and clean.	Time: 2 min Max power	Clean the residual of resist	Check structures in microscope



3 RIE of SiN					
Step Heading	Equipment	Procedure	Recipe/mask	Target	Comments
3.1 Etching	RIE2	Place the wafer in the RIE chamber	Recipe: CHF3 flux: 10sccm, C2F6 flux: 20 sccm P:35mTorr RFpower:60W Etch rate (estimate) 0,4 µm/min for Si	Etch the SiN	
3.2 Unload		Take the sample and analyze it			Check the structure with the microscope, trials may be needed
3.3 cleaning	Ash plasma	Place the sample in ash plasma chamber	Time: 20 min Max power	Remove the resist	Check structures in microscope, all the resist must be gone.



Process flow title					
Stenciling masks fabrication					
DTU Danchip National Center for Micro- and Nanofabrication			Contact email Eleonora.zamburlini@gmail.com		Contact person Eleonora Zamburlini
			Created by Eleonora		
Lab manager group Nanointegration	Date of release Click here to enter a date.	Date of revision	Revision nr 1	Date of creation 20/03/2012	Batch nr 0

4 KOH etching					
Step Heading	Equipment	Procedure	Recipe/mask	Target	Comments
4.1 Prepare the bench	KOH		Mask: the SiN on top		
4.2 Etching of Si	KOH	Bath of KOH solution	Recipe: Standard wt 28% KOH, T: 80C Time 2/3h Expected rate: 1,3 µm/min	Etch the Si until reaching the backstrate SiN	
4.3 Rinse and stop etching	Wet bench	Rinse with DI water and dry		Stop the etching and clean the sample	Observe the sample



Appendix 2 XPS measurments for cutted graphene

